TECHNISCHE UNIVERSITÄT MÜNCHEN

Fakultät für Chemie

Fachgebiet Analytische Chemie

Multielementanalyse von Rückständen aus der Müllverbrennung sowie Untersuchungen zur Extraktion von Metallen

Jasmin Bianca Haberl

Vollständiger Abdruck der von der Fakultät für Chemie der Technischen Universität München zur Erlangung des akademischen Grades eines

Doktors der Naturwissenschaften (Dr. rer. nat.)

genehmigten Dissertation.

Vorsitzender:	Prof. Dr. Klaus Köhler
Prüfer der Dissertation:	1. Prof. Dr. Michael Schuster
	2. Prof. Dr. Johann P. Plank

Die Dissertation wurde am 03.06.2019 bei der Technischen Universität München eingereicht und durch die Fakultät für Chemie am 12.11.2019 angenommen.

Die vorliegende Arbeit entstand in der Zeit von April 2016 bis Mai 2019 unter Anleitung von Herrn Prof. Dr. Michael Schuster in der Fachgruppe Analytische Chemie an der Fakultät für Chemie der Technischen Universität München.

Danksagung

Mein größter Dank gilt Herrn Prof. Dr. Michael Schuster für die freundliche Aufnahme in seinen Arbeitskreis und die wissenschaftliche Betreuung. Außerdem möchte ich mich für die interessante Aufgabenstellung, die wertvollen Ratschläge, die forscherische Freiheit und das mir entgegengebrachte Vertrauen bedanken.

Meinen Kolleginnen und Kollegen aus dem Arbeitskreis Stephan Fromm, Dominik Huber, Christine Hutterer, Alexander Urstöger, Florian Weigl und Andreas Wimmer danke ich für die gute Arbeitsatmosphäre und Zusammenarbeit. Insbesondere möchte ich Stephan Fromm für die technische Instandhaltung des TRFA-Spektrometers danken.

Ebenfalls danken möchte ich allen Arbeitsgruppen, deren Geräte ich für meine Arbeit nutzen konnte. Insbesondere Andrea Hartung (Lehrstuhl für Energiesysteme, TU München) danke ich für die Möglichkeit das Röntgenfluoreszenz-Spektrometer und das Lasergranulometer nutzen zu können sowie für die Hilfestellung bei deren Verwendung. Bei Katia Rodewald (Lehrstuhl für Makromolekulare Chemie, TU München) möchte ich mich für die Einweisung in das Lichtmikroskop bedanken und dafür, dass ich es nutzen konnte.

Dr. Marianne Hanzlik (Professur für Elektronenmikroskopie, TU München) danke ich für die REM/EDX-Messungen. Außerdem danke ich Wolfgang Zucha und Dr. Urs Eggenberger (Institut für Geologie, Universität Bern) für die kurzfristigen XRD Messungen.

Meinen Bachelorandinnen Lilla Koser und Patricia Grabler sowie allen Auszubildenden danke ich für ihre Unterstützung.

Ferner bedanke ich mich bei allen Beteiligten des Verbundprojekts *SESAM* für den interessanten Austausch auf den Projekttreffen. Ralf Koralewska und Stefan Schlumberger danke ich für die Organisation von Proben und den Betreibern der Müllverbrennungsanlagen für deren Bereitstellung. Bei der Bundesanstalt für Gewässerkunde bedanke ich mich für die Herstellung der Mischprobe, die als projektinterne Referenz diente.

Kurzfassung

Thema der vorliegenden Arbeit war die Multielementanalyse von Rückständen aus der Müllverbrennung, insbesondere von Flugaschen, sowie Untersuchungen zur Extrahierbarkeit einzelner Elemente mit Hilfe einer sequentiellen Extraktion.

Im ersten Teil dieser Arbeit wurden die Elementgehalte in Flugaschen aus mehreren verschiedenen Müllverbrennungsanlagen in Deutschland und der Schweiz umfassend analysiert, um deren Wertstoffpotential zu ermitteln. Außerdem wurde auf zeitliche Unterschiede in der Elementzusammensetzung innerhalb einzelner Anlagen eingegangen. Die Analysen erfolgten mit optischer Emissionsspektrometrie mit induktiv gekoppeltem Plasma (ICP–OES) und mit Massenspektrometrie mit induktiv gekoppeltem Plasma (ICP–MS) nach mikrowellenunterstütztem Aufschluss unter Einsatz von Flusssäure. Die Elementzusammensetzung in verschiedenen Anlagen war vergleichsweise ähnlich.

Kenntnisse über die Löslichkeit und Extrahierbarkeit einzelner Elemente aus den Verbrennungsrückständen sind in vielen Bereichen und Prozessen von Bedeutung. Dies wurde im zweiten Teil dieser Arbeit mit Hilfe einer sequentiellen Extraktion untersucht. Es wurde ein neues Konzept der sequentiellen Extraktion vorgeschlagen und das entwickelte Verfahren hinsichtlich verschiedener Einflussfaktoren und Fehlerquellen untersucht. Mit dem Verfahren wurden Flugascheproben aus zwei verschiedenen Anlagen und die Feinfraktion einer Schlackeprobe untersucht und verglichen. Die Elemente wiesen in den untersuchten Rückständen ein sehr ähnliches Extraktionsverhalten auf, lediglich die Alkalielemente in der Schlacke zeigten eine signifikant schlechtere Wasserlöslichkeit im Vergleich zu den Flugaschen.

Die Methodenkombination von ICP–OES und ICP–MS ermöglicht eine Analyse nahezu aller Elemente des Periodensystems. Nachteilig sind jedoch der notwendige Einsatz von Flusssäure für einen vollständigen Aufschluss sowie der hohe Zeitaufwand. Daher wurde im dritten Teil dieser Arbeit die Totalreflexions-Röntgenfluoreszenzanalyse (TRFA) als schnellere und routinefähigere Methode für die Analyse von Flugaschen getestet. Mittels TRFA können sowohl Aufschlusslösungen als auch Suspensionen gemessen werden. Beide Probenvorbereitungsmethoden wurden optimiert und hinsichtlich Genauigkeit und Präzision verglichen. Es wurden verschiedene Fehlerquellen aufgezeigt, die bei der Probenvorbereitung auftreten können, und Möglichkeiten zu deren Vermeidung aufgezeigt. Sowohl mit Aufschlüssen als auch mit Suspensionen konnte bei den Messungen eine Präzision im Bereich der Gerätepräzision erreicht werden. Ein aufwendiger Aufschluss mit Flusssäure erwies sich daher als nicht notwendig.

Abstract

The topic of the present work was the multielemental analysis of waste incineration residues, especially of fly ashes, as well as studies on the extractability of single elements using sequential extraction.

In the first part of this work, the elemental contents of fly ashes from several different waste incineration plants in Germany and Switzerland were comprehensively analyzed in order to determine their potential as a secondary raw material. Additionally, temporal differences in the elemental concentrations within some plants were discussed. The analyses were performed by inductively coupled plasma optical emission spectrometry (ICP–OES) and inductively coupled plasma mass spectrometry (ICP–MS) after microwave-assisted pressure digestion using hydrofluoric acid. The elemental composition was relatively similar in the different incineration plants.

Knowledge of the solubility and extractability of individual elements from incineration residues is important in many areas and processes. This was investigated in the second part of this work by means of a sequential extraction. A new concept of sequential extraction was proposed and the developed procedure was investigated with regard to various influencing factors and sources of error. The procedure was used to study and compare fly ash samples from two different plants and the fine fraction of a bottom ash sample. The elements showed a very similar extraction behavior in the investigated residues, only the alkali elements in the bottom ash showed a significantly lower water solubility compared to the fly ashes.

The combination of ICP–OES and ICP–MS enables an analysis of almost all elements of the periodic table. However, the necessary use of hydrofluoric acid for a complete digestion and the high expenditure of time are disadvantageous. In the third part of this work, total-reflection X-ray fluorescence analysis (TXRF) was therefore tested as a faster and more routine-capable method for the analysis of fly ash. By means of TXRF, digestion solutions as well as suspensions can be measured. Both sample preparation methods were optimized and compared with regard to accuracy and precision. Several sources of error have been identified, which may arise during sample preparation, and possibilities for avoidance are shown. A precision in the range of the instrument precision could be achieved with both digestions and suspensions. An elaborate digestion with hydrofluoric acid was therefore not necessary.

Abkürzungsverzeichnis

BCR	Referenzbüro der Europäischen Gemeinschaft (engl. *Community Bureau of Reference*)
EXAFS	*extended X-ray absorption fine structure* (engl.)
FE-Metalle	Eisenmetalle
FLUREC	Flugasche-Recycling
FLUWA	Flugaschen-Wäsche
ICP	induktiv gekoppeltes Plasma (engl. *inductively coupled plasma*)
MS	Massenspektrometrie (engl. *mass spectrometry*)
m/z-Verhältnis	Masse-zu-Ladung-Verhältnis
NE-Metalle	Nichteisenmetalle
OES	optische Emissionsspektrometrie (engl. *optical emission spectrometry*)
PVC	Polyvinylchlorid
RFA	Röntgenfluoreszenzanalyse
TRFA	Totalreflexions-Röntgenfluoreszenzanalyse
XANES	*X-ray absorption near edge structure* (engl.)
XAS	Röntgenabsorptionsspektrokopie (engl. *X-ray absorption spectroscopy*)
XRD	Röntgendiffraktometrie (engl. *X-ray diffraction*)

Inhaltsverzeichnis

1. Einleitung

Weltweit fallen tagtäglich riesige Abfallmengen an, die beseitigt werden müssen. Ein großer Teil davon wird ohne weitere Behandlung und ohne Recycling auf Deponien gebracht.[1] In manchen Ländern wie in Deutschland und in der Schweiz ist jedoch eine Behandlung der Abfälle vor der Deponierung gesetzlich vorgeschrieben. In Deutschland gilt das Deponierungsverbot für unbehandelte Abfälle seit dem 1. Juni 2005.[2-4] In der Schweiz besteht ein Deponierungsverbot für brennbare Abfälle bereits seit 1. Januar 2000.[5, 6] Die Behandlung kann beispielsweise thermisch durch Verbrennung erfolgen.[2, 7] In der Schweiz ist ausschließlich die thermische Behandlung der Siedlungsabfälle erlaubt.[7]

In Deutschland wurden im Jahr 2013 etwa 19 Millionen Tonnen Haus- und Gewerbeabfälle (ohne Sonderabfälle) in den insgesamt 68 Müllverbrennungsanlagen verbrannt.[8] In der Schweiz waren es im selben Jahr knapp 4 Millionen Tonnen Abfälle (Siedlungsabfälle, Abfälle aus Industrie und Gewerbe und Klärschlamm), die in 30 Anlagen verbrannt wurden.[9] Die Verbrennung soll Volumen und Masse dieser riesigen Abfallmengen reduzieren, indem die organischen Bestandteile in einfache natürliche Endprodukte, insbesondere zu Kohlenstoffdioxid und Wasser, umgewandelt werden. Außerdem sollen schädliche oder gefährliche Inhaltsstoffe zerstört, umgewandelt, abgetrennt, konzentriert oder immobilisiert werden. Rückstände sollen in eine ablagerungsfähige oder verwertbare Form gebracht werden. Die bei der Verbrennung frei werdende Energie wird zur Stromerzeugung oder als Fernwärme genutzt.[2, 4]

Bei der Verbrennung fällt Flugasche und Schlacke als Rückstand an. Metalle, darunter auch Wertmetalle, bleiben in den Verbrennungsrückständen zurück und werden im Falle einer Deponierung dem Rohstoffkreislauf entzogen. Insbesondere die Flugaschen werden seit einigen Jahren zunehmend als Sekundärrohstoff in verschiedensten Bereichen in Betracht gezogen.[10] Geforscht wird vor allem am Einsatz in der Produktherstellung (z.B. in Baumaterialien wie Zement [11] und Tonziegel [12]) und an praktischen Anwendungen (z.B. zur CO_2-Sequestierung [13]). Aber auch eine direkte Rückgewinnung von Elementen ist Gegenstand aktueller Forschung. Diese konzentriert sich insbesondere auf Zn [14-16] aber auch andere Elemente wie Cu [17, 18] oder P [19]. In der Schweiz wurde ein Verfahren zur Rückgewinnung von Zn, Pb, Cu und Cd aus Flugasche bereits großtechnisch umgesetzt.[10, 14] Die Rückgewinnung von Metallen aus Filterasche ist in der Schweiz ab dem 1. Januar 2021 sogar gesetzlich vorgeschrieben.[7] Ab diesem Datum dürfen Filteraschen ohne vorherige Metallrückgewinnung nicht mehr deponiert werden.

Für den Einsatz von Flugasche als Sekundärrohstoff ist eine genaue Kenntnis der Zusammensetzung Voraussetzung. Zu aktuellen Elementgehalten, insbesondere zu den

Gehalten an Spurenelementen und seltenen Erden, gibt es für Flugaschen aus deutschen Müllverbrennungsanlagen kaum Daten in der Literatur. Erstes Ziel dieser Arbeit war daher die Schaffung einer soliden Datengrundlage. Dazu wurden die Elementgehalte in Flugaschen aus verschiedenen deutschen und auch schweizerischen Anlagen bestimmt (Publikation 1). Im zweiten Teil dieser Arbeit wurde anschließend die Extrahierbarkeit einzelner Elemente mit Hilfe einer sequentiellen Extraktion untersucht (Publikation 2). Im letzten Teil der Arbeit wurde der Einsatz der Totalreflexions-Röntgenfluoreszenzanalyse (TRFA) zur Analyse von Flugaschen getestet und verschiedene Probenvorbereitungsmethoden untersucht (Publikation 3).

2. Thermische Abfallbehandlung

2.1. Technische Umsetzung der Müllverbrennung

Der genaue Aufbau und die technischen Details unterscheiden sich zwischen verschiedenen Müllverbrennungsanlagen, die wesentlichen Komponenten sind jedoch in der Regel in allen Anlagen zu finden (Abbildung 1). Dazu gehört der Feuerraum mit einem Rost, auf den der Abfall aufgegeben wird und auf dem die Verbrennung stattfindet. Der Rückstand auf dem Rost am Ende des Verbrennungsprozesses wird als Schlacke bezeichnet. Das Rauchgas besteht aus den Verbrennungsgasen und mitgetragenen feinen Aschepartikeln, den Flugaschen. Das Rauchgas strömt aus dem Feuerraum und zunächst an den Kesseln vorbei, die der Dampferzeugung für die Energienutzung dienen. Ein Teil der Flugaschen lagert sich dabei an den Rohren ab. Diese wird als Kesselasche bezeichnet. Das abgekühlte Rauchgas gelangt anschließend in die Rauchgasreinigung. Die Rauchgasreinigung lässt sich in die Abtrennung der partikelförmigen Schadstoffe (Flugaschen) und der gasförmigen Schadstoffe unterteilen. [4, 8]

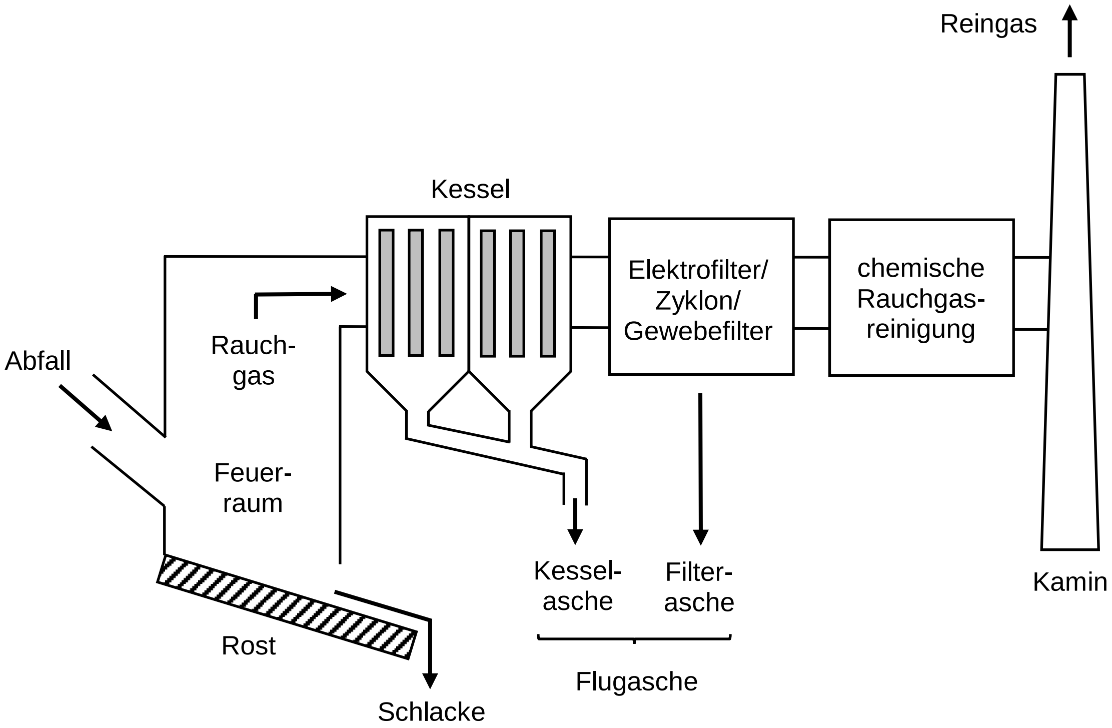

Abbildung 1: Schematischer Aufbau einer Müllverbrennungsanlage (eigene Darstellung, angelehnt an [20]).

Zur Abtrennung der Flugaschen existieren verschiedene Techniken, welche unterschiedliche physikalische Kräfte nutzen. Die in diesem Schritt abgetrennten Flugaschen werden oft auch als Filteraschen bezeichnet. Im Folgenden werden die gängigsten Techniken (Zyklone, Elektrofilter und Gewebefilter) kurz erläutert.

Zyklone: In Zyklonen wird das Rauchgas spiralförmig eingeleitet (Abbildung 2). Durch die spezielle Bauform werden die enthaltenen Partikel durch Fliehkräfte an die Wände des Zyklons gedrückt und nach unten in einen Sammelbehälter transportiert. Das entstaubte Rauchgas wird nach oben abgesaugt. Zyklone eignen sich nur für die Abtrennung gröberer Partikel, da Fliehkräfte proportional zur Masse der Partikel sind. Verglichen mit anderen Techniken ist die Staubabscheidung eher gering, weshalb Zyklone nur der Vorentstaubung dienen und eine Nachschaltung weiterer Techniken notwendig ist.[8]

Elektrofilter: In Elektrofiltern werden die Aschepartikel elektrostatisch aufgeladen und elektrische Anziehungskräfte für die Abscheidung genutzt (Abbildung 3). Das Rauchgas wird durch ein elektrisches Feld zwischen einer Elektronen emittierenden Sprühelektrode und einer Niederschlagselektrode geleitet. Durch Stoßionisation mit Gasmolekülen der umgebenden Luft bilden sich sekundäre Ionen, die sich an Gasmolekülen anlagern. Die negativ geladenen Gasionen wiederum lagern sich an den Aschepartikeln an, welche durch die negative Aufladung zur Niederschlagselektrode wandern und dort haften bleiben.[8]

Gewebefilter: Bei Gewebefiltern werden die Aschepartikel durch Filter aus faserigem Material aus dem Rauchgas abgetrennt. Im Vergleich zu anderen Entstaubungstechniken werden mit Gewebefiltern die höchsten Abscheidungsgrade erreicht.[8]

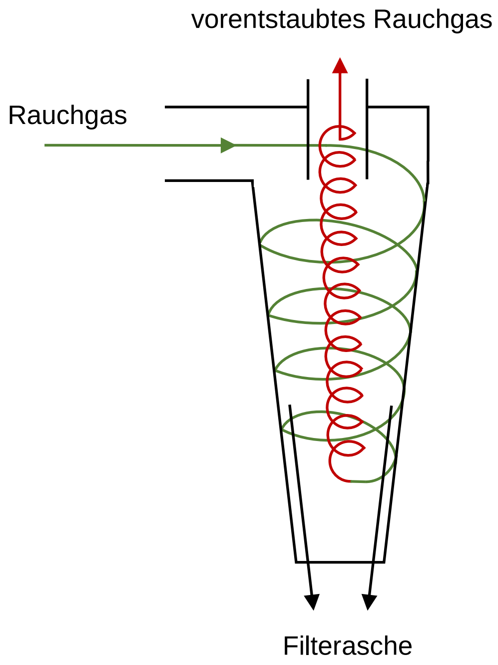

Abbildung 2: Funktionsprinzip eines Zyklons (eigene Darstellung, angelehnt an [8]).

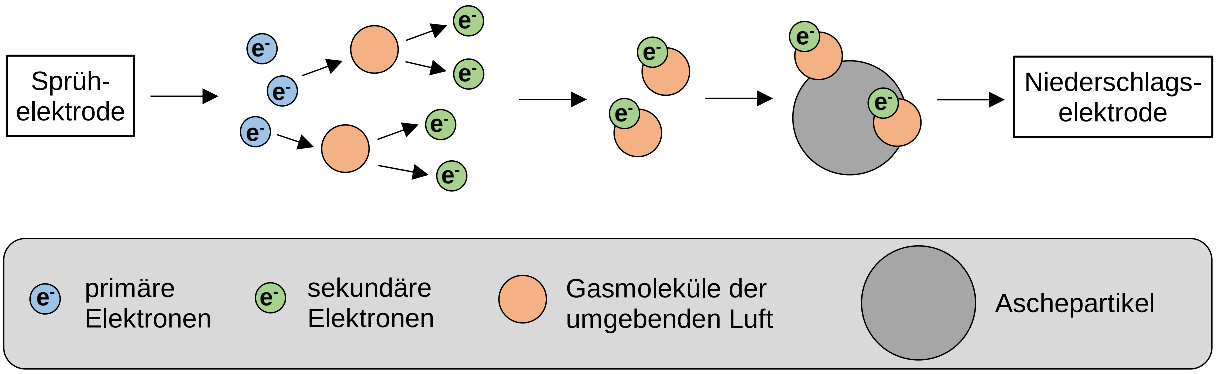

Abbildung 3: Funktionsprinzip eines Elektrofilter (eigene Darstellung, angelehnt an [8]).

In der anschließenden chemischen Rauchgasreinigung werden die gasförmigen Schadstoffe entfernt. Gasförmige Schadstoffe im Rauchgas sind leicht flüchtige Schwermetallverbindungen wie beispielsweise Quecksilberverbindungen, saure Gase wie Chlorwasserstoff, Fluorwasserstoff und Schwefeloxide, Stickoxide sowie organische Schadstoffe.[8]

Im Folgenden wird kurz auf die Reinigungsverfahren eingegangen, bei denen Rückstände bzw. Reaktionsprodukte anfallen, welche in dieser Arbeit relevant sind. Quecksilber und organische Verbindungen, die nicht bereits adsorbiert auf den Flugaschen abgeschieden wurden, werden mit Hilfe von Adsorptionsmitteln wie beispielsweise Aktivkohle entfernt und saure Gase können mit Wasser oder Natronlauge ausgewaschen werden (nasse Rauchgasreinigung). Alternativ können saure Gase in der trockenen oder quasitrockenen Rauchgasreinigung durch Reaktion mit Additiven wie beispielsweise $NaHCO_3$ oder $Ca(OH)_2$ entfernt werden. Dabei fallen feste Reaktionsprodukte in trockener Form als Rückstand an: $NaHCO_3$ reagiert mit den sauren Gasen zu NaCl, NaF und Na_2SO_3 bzw. Na_2SO_4. Bei der Verwendung von $Ca(OH)_2$ entstehen $CaCl_2$, CaF_2 und $CaSO_3$ bzw. $CaSO_4$. In manchen Müllverbrennungsanlagen mit trockener oder quasitrockener Rauchgasreinigung erfolgt dabei keine vorherige Entstaubung, sondern die Flugasche wird zusammen mit den Reaktionsprodukten der chemischen Rauchgasreinigung abgetrennt, wodurch diese vermischt werden.[8]

Neben dem Feuerungssystem und den Prozessbedingungen beeinflusst die Abfallart und -zusammensetzung wesentlich die Bestandteile des Rauchgases.[8] Bedingt durch die unterschiedliche Herkunft des Abfalls und die unterschiedlichen Anteile verschiedener Abfallarten, sind Abfälle eine sehr heterogene Mischung und haben je nach Anlage eine unterschiedliche Zusammensetzung.[21] Abfall kann z.B. aus Haus-, Gewerbe- und Sperrmüll, Bauabfällen und/oder Klärschlamm bestehen.[4] Daher kann die Abfallzusammensetzung auch innerhalb einer Anlage zeitlich stark variieren.[21]

Pro Tonne Abfall entstehen etwa 250-350 kg Schlacke (einschließlich Kesselasche) und etwa 20-40 kg Filterasche (ohne Reaktionsprodukte aus der Rauchgasreinigung).[4, 22] Die Menge an Flugasche wird unter anderem vom Feuerungssystem, von der Abgasgeschwindigkeit und vom Aschegehalt des Abfalls beeinflusst. Wieviel Asche sich an den Kesseln ablagert ist von der Bauart des Kessels abhängig.[8]

2.2. Zusammensetzung und Eigenschaften der Verbrennungsrückstände

2.2.1. Schlacke

Die Schlacke ist ein heterogenes Gemisch, in dem man bereits visuell verschiedene Bestandteile wie FE-Metalle (Eisenmetalle), NE-Metalle (Nichteisenmetalle), Glas und Keramik erkennen kann.[23] Pfrang-Stotz und Schneider [21] untersuchten die Mineralogie von Schlacken aus verschiedenen Müllverbrennungsanlagen. Die Studie zeigte, dass die kristallinen Phasen der Schlacke überwiegend aus Silikaten wie $Ca_2Al[AlSiO_7]$ (Gehlenit) und Oxiden wie Fe_3O_4 (Magnetit) oder SiO_2 (Quarz) besteht. Darüber hinaus wurden größere Mengen $CaCO_3$ (Calcit) und Mineralien aus der Gruppe der Feldspate ($K[AlSi_3O_8]$, $Na[AlSi_3O_8]$, $Ca[Al_2Si_2O_8]$) in einigen Proben nachgewiesen. Weitere Mineralien wurden nur in einzelnen Proben in geringen Mengen gefunden. Andere Studien [24-27] berichten von einer ähnlichen Hauptmineralogie und berichten zudem häufig auch von Fe_2O_3 (Hämatit) [24-26]. Schlacken reagieren in Wasser alkalisch.[28-30]

Die Korngröße erstreckt sich von Schlackestaub mit <100 µm bis zu mehrere Zentimeter großen Stücken.[23, 25, 31, 32] Elementar vorliegende Metalle sind nahezu vollständig in der gröberen Fraktion (>1 mm) enthalten, die Feinfraktion (≤1 mm) ist dagegen überwiegend mineralisch.[31] Loginova et al. [30] zeigten, dass die Chlorid- und Sulfatkonzentration mit zunehmender Partikelgröße sinkt.

In der Regel erfolgt ein Nassaustrag der Schlacke aus dem Verbrennungsraum. Dabei fällt die Schlacke in ein Wasserbad und wird dort abgekühlt, wodurch Staubaufwirbelungen unterbunden werden.[33] Der Trockenaustrag, bei dem die Schlacke nicht mit Wasser in Kontakt kommt, hat in den letzten Jahren jedoch zunehmend an Bedeutung gewonnen. Beim Trockenaustrag bilden sich keine mineralischen Ablagerungen auf den Metallen und die Metallstücke verklumpen nicht mit den mineralischen Bestandteilen. Dadurch ist eine bessere Separierung der einzelnen Metallbestandteile von der Schlacke möglich (siehe Kapitel 2.3) und die Metalle haben eine höhere Reinheit. Dies ist von Vorteil bei der Rückgewinnung von Rohstoffen aus der Schlacke und der Hauptgrund für die Anwendung des Trockenaustrags.[31, 33]

Die Schlacke ist weniger schadstoffbelastet als die Flugaschen, da flüchtige Schwermetalle größtenteils in die Flugaschen übergehen.[34, 35] In Tabelle 1 sind mehrere verschiedene Literaturangaben zu Elementkonzentrationen in Schlacken und Flugaschen gegenübergestellt.

2.2.2. Flugasche

Flugaschen sind ein feinkörniges Material, in dem visuell keine verschiedenen Bestandteile identifiziert werden können. Die Farbe kann von hellbraun über grau zu fast schwarz reichen. Eine dunklere Farbe weist allgemein auf eine schlechtere Verbrennungseffizient hin.[23]

Die Partikelgrößen von Flugaschen liegen überwiegend im Bereich zwischen 1 und 100 µm. In einer Studie von Buchholz und Landsberger [36] wiesen etwa 73 Gew.-% der untersuchten Flugasche eine Partikelgröße zwischen 20 und 250 µm auf. Den größten Anteil bildete dabei die Fraktion 20-38 µm, gefolgt von der Fraktion 38-63 µm. In einer Studien von Van Herck et al. [37] war der größte Anteil mit 45-63 µm in einem ähnlichen Größenbereich. Nur 7 Gew.-% hatten eine Partikelgröße >200 µm. Weitere Studien berichten von einer maximalen Partikelgröße von etwa 300 µm [12] und 150 µm [38].

Die gröberen Flugaschepartikel bleiben vorwiegend an den Kesselrohren hängen. Die feineren Partikel werden im Rauchgas weiter transportiert und erst durch die Filter abgetrennt.[39] Auf dem Weg vom Feuerraum zum Kamin kühlt das Rauchgas ab, wodurch gasförmige Verbindungen wie flüchtige Schwermetalle auf den Flugaschepartikeln kondensieren.[40] Es wurde häufig beobachtet, dass die Kondensation zum Großteil erst auf der Filterasche und noch nicht auf der Kesselasche stattfindet. Belevi und Moench [39] fanden beispielsweise das im Abfall enthaltene Hg nahezu vollständig in der Filterasche und im Abgas nach den Filtern wieder. In einer Studie von Morf et al. [35] waren die Konzentrationen der Elemente Cd, Pb, Se, Tl, Sn und Zn in der Elektrofilterasche signifikant höher im Vergleich zur Kesselasche, während Elemente wie beispielsweise Al, Cr, Fe, Ni und Sr nur geringe Unterschiede aufwiesen (vgl. Tabelle 1). Die Kesselasche ist dadurch weniger schadstoffbelastet als die Filterasche.

Welche Elemente sich in den Flugaschen anreichern und welche Elemente überwiegend in der Schlacke zurückbleiben, wurde in zahlreichen Studien untersucht.[32, 35, 39, 41, 42] Es reichern sich vor allem flüchtige Elemente in den Flugaschen an. Funari et al. [32] berichteten von einer starken Anreicherung von insbesondere Sb, Zn, Sn, Ag, Cd, Bi und Tl in der Flugasche. Der Transfer von Sb, Cd und Bi in die Flugasche war in der betrachteten Anlage sogar so hoch, dass von dem gesamten Input dieser Elemente der größere Masseanteil in die Flugasche gelangte, obwohl der Massestrom an Flugasche mit nur ca. einem Zehntel des

Tabelle 1: Vergleich verschiedener Literaturangaben zu Elementkonzentrationen in Schlacke und Flugasche. Die hier betrachteten Flugaschen enthielten keine Reaktionsprodukte aus der chemischen Rauchgasreinigung. Die Konzentrationen sind in mg/kg angegeben.

	Schlacken				**Flugaschen**						
Quelle	Funari et al., 2015 [32]	Allegrini et al., 2014 [43]	Chung et al., 2007 [44]	Kida et al., 1996 [45]	Weibel et al., 2016 [46]			Funari et al., 2015 [32]	Kida et al., 1996 [45]	Morf et al., 2013 ** [35]	
Standort der beprobten Anlage	Italien	Dänemark	Korea	Japan	Schweiz	Schweiz	Schweiz	Italien	Japan	Schweiz	Schweiz
Anmerkung zum beprobten Rückstand		Analyse nach Abtrennung der Fe- und NFe-Metalle	Analyse nach Siebung (5 mm Sieb)	Durchschnitt aus 14 Anlagen	Kesselasche und Elektrofilterasche	Kesselasche und Elektrofilterasche	Kesselasche und Elektrofilterasche		Elektrofilterasche	Kesselasche	Elektrofilterasche
Ag	5.51		11.2	4.9				19.5	11	36	71
Al	* 47 058		37 900	73 000	36 300	37 900	31 750	* 29 537	31 000	43 676	39 138
As	11.9	25	22.2	2.1				21.1	0.7		
Au	0.44	0.14	0.48	2.2				0.58	2.2	0.3	1.1
Ba	1404	1400	1700	69	1711	2901	1856	970	12	1186	2169
Bi	2.28			0				51.2	44	20	97
Br			37.5		3563	2798	3700				
Ca	* 167 254		199 000	200 000	191 500	168 900	151 150	* 275 897	53 000		
Cd	5.62	8.2			227	264	355	114		34	451
Ce	31.8	44	34.6					20.0			
Cl			28200	13000	106 900	97 050	103 010		140 000		
Co	35.4	39	76.5	17				21.0	12		
Cr	367	650	729	260	650	676	486	635	270	747	776
Cu	3490	4700	3100	800	3901	2573	2544	952	930	870	2597
Dy	1.87	2.3						0.96			
Er	1.26	1.95						0.60			
Eu	0.92	0.67	0.74					0.71			
Fe	* 76 493		48 500	26 000	19 120	21 610	20 635	* 15 470	10 000	31 126	24 174
Ga	14.5	10		10				7.88	8.6	8.7	15.6
Gd	2.43	2.8						1.29		1.9	1.7
Ge		0.53								0.9	2.3
Hf	2.70		2.67					1.44		32	46
Ho	0.39	0.43						0.26			
In		0.04								1.4	6.8

K	* 12 370		12 200	13 000	45 250	45 940	46 930	* 39 185	100 000		
La	18.8	21	23.8	6.0				11.6	1.9		
Li	26.6							23.7		34	51
Lu	0.17	0.17						0.08			
Mg	* 15 259	11 000	18 400	24 000	14 025	15 090	13 598	* 22 074	16 000		
Mn	* 1472		2700	470	761	806	762	* 852	360		
Mo	16.5	12		5.0				20.4	9.0	34	41
Na	* 23 074		21 100	19 000	43 100	46 300	48 800	* 51 118	77 000		
Nb	14.8	12						10.5		13	10
Nd	12.1	20						7.15		13	11
Ni	224	1100		65				85.9	34	332	383
Pb	1517	2500		410	9540	9108	12 055	2987	2700	1413	13 214
Pr	3.35	5.5						1.95		3.0	2.8
Rb			32.3							60	137
Sb	119	60	116	26	3037	2428	2935	1022	230		
Sc	10.2	4.6	2.11	1.3				4.59	0.6	4.5	4.7
Se		1.45								1.1	14
Si	* 151 944			120 000	83 100	83 090	69 490	* 64 985	35 000		
Sm	2.26	3.05	1.74					1.29			
Sn	201	170		220	1463	1334	1644	713	730	311	1762
Sr	440			310	542	425	346	429	150	565	460
Ta	1.12	6.8	5.29					1.19		5.7	6.4
Tb	0.41	0.43	0.64					0.29			
Ti	* 7433		10 200	12 000	10 120	10 010	8908	* 8512	7200		
Tl		0.26								0.03	2.3
Tm	0.16	0.18						0.08			
V	196	48	19.4	75				19.7	44	43	40
W	20.8	9.7	21.8					8.77		54	49
Y	14.3			3.1				9.88	0.9	119	182
Yb	1.10	1.25	0.65					0.52			
Zn	3562	3400	7700	2500	26 770	48 190	65 170	13 417	10 000	14 229	35 702
Zr	108			110				71.4	41	1341	2023

* In der Quelle sind die Konzentrationen dieser Elemente in Form ihrer Oxide angegeben. Zur besseren Vergleichbarkeit wurden die in der Tabelle angegebenen reinen Metallgehalte berechnet.

** In der Quelle sind die Konzentrationen der Elemente in den Rückständen nicht direkt angegeben. Die Elementkonzentrationen wurden daher aus den in der Quelle angegebenen Transferkoeffizienten und Rückstandsmengen berechnet.

Massestroms der Schlacke deutlich geringer war. Der jährliche Massestrom an Cd beispielsweise wurde zu 122 ± 24 kg/a in der Schlacke und zu 291 ± 6.1 kg/a in der Flugasche berechnet. Li et al. [40] beobachteten ebenfalls eine Anreicherung der flüchtigen Elemente Cd, Pb, Hg und As in der Flugasche.

Nach Belevi und Moench [39] haben folgende Faktoren einen Einfluss auf die Verteilung der Elemente:

1) in welcher Form ein Element im Abfall vorliegt und wie es verteilt ist, z.B. ob das Element in größeren Abfallstücken eingeschlossen ist oder ob sich Partikel bilden, die leicht mit dem Rauchgas aus dem Verbrennungsraum ausgetragen werden können
2) die physikalischen und chemischen Bedingungen während der Verbrennung: Temperatur, Redoxbedingungen, Chloridgehalt
3) Verweilzeit und Durchmischung des Abfalls auf dem Rost

Insbesondere die Chloride wurden in diesem Zusammenhang in mehreren Studien untersucht. Chlorid in den Verbrennungsrückständen stammt hauptsächlich aus der Verbrennung von PVC-Kunststoffen.[46, 47] In Anwesenheit von Chlorid reagieren einige Metalle wie beispielsweise Hg, Cd, Pb, Zn und Cu während des Verbrennungsprozesses zu Metallchloriden.[41, 48, 49] Metallchloride haben generell einen höheren Dampfdruck als die entsprechenden Oxide und reichern sich daher in der Flugasche an.[47] Daher ist die Chloridkonzentration in den Flugaschen deutlich höher als in der Schlacke (vgl. Tabelle 1). Je höher die Chloridkonzentration während der Verbrennung, desto mehr Metallchloride werden gebildet, wodurch die Anreicherung der entsprechenden Metalle in der Flugasche zunimmt.[41, 49] Die Tatsache, dass die Flüchtigkeit von Schwermetallen durch Chloride erhöht wird, wurde in mehreren Studien zur Entfernung von Schwermetallen aus den Flugaschen durch hohe Temperaturen genutzt, indem den Flugaschen Chlorid zugesetzt wurde.[50-52]

Die mineralogische Zusammensetzung von Flugaschen ist relativ komplex, da es sich um eine Mischung vieler verschiedener Mineralien und Elemente handelt. Daher war es bislang nur möglich, die Bindungsformen der Elemente zu bestimmen, die in höheren Konzentrationen vorliegen. Über die Mineralogie der Spurenelemente ist nur wenig bekannt. In einer umfangreichen Studie von Weibel et al. [46] wurde die Mineralogie von Flugaschen aus mehreren schweizerischen Anlagen untersucht. Mit 13-14% war $Ca_2Al[AlSiO_7]$ das am meisten vorliegende Mineral. Sulfat ist überwiegend in Form von $CaSO_4$ enthalten. Darüber hinaus waren größere Mengen Eisenoxide (Fe_2O_3 und Fe_3O_4) und Chloride (NaCl, KCl und K_2ZnCl_4) enthalten. Aluminium lag überwiegend als Al^0 in Form größerer metallischer Partikel vor. Außerdem konnte $CaCO_3$ und CaO nachgewiesen werden, das für die alkalische Reaktion von

Flugaschen in Wasser verantwortlich ist. Neben einigen der genannten Mineralien wurden in anderen Studien außerdem z.B. SiO_2, $K_3Na(SO_4)_2$ und $Ca(OH)_2$ gefunden.[53, 54] Chloride und Sulfate sind im Allgemeinen in hoher Konzentration in Flugaschen enthalten [55] und gut wasserlöslich [56, 57].

Flugaschen enthalten darüber hinaus auch organische Schadstoffe, insbesondere Dioxine und Furane. Im Abfall enthaltene Dioxine und Furane werden während der Verbrennung zerstört, im Rauchgas findet jedoch im Temperaturbereich von 200 bis 400 °C eine Neubildung (De-Novo-Synthese) aus organischen Verbindungen in Anwesenheit von Cl statt. Vorläuferverbindungen sind beispielsweise Chlorphenole. Übergangsmetalle in der Flugasche wie z.B. Cu wirken als Katalysator.[8, 58, 59] Dioxine und Furane sind daher größtenteils in der Flugasche zu finden während die Konzentration im Abfall und in der Schlacke gering ist.[60, 61]

2.3. Verbrennungsrückstände als Sekundärrohstoffe

Hinsichtlich der zunehmenden Rohstoffverknappung ist es notwendig, mögliche Sekundärrohstoffquellen zu identifizieren und zu nutzen. Da in den Abfällen enthaltene Wertmetalle nach der Verbrennung in den festen Rückständen zurück bleiben, werden diese zunehmend als Sekundärrohstoffquelle in Betracht gezogen und teilweise auch schon genutzt.[10, 14-16, 32, 35, 43, 62]

Sowohl für die Schlacke als auch für die Flugasche existieren großtechnische Rückgewinnungsverfahren, damit Wertstoffe wieder in den Stoffkreislauf zurückgeführt werden können. Der Stand der Technik zur Wertstoffrückgewinnung aus den Schlacken und Flugaschen wird im Folgenden erläutert.

Die Aufbereitung der Schlacke erfolgt durch physikalisch-mechanische Techniken und wird in einigen Anlagen erfolgreich betrieben.[63] Die Schlacke wird in mehrere Größenfraktionen getrennt, die anschließend verschiedene Trennschritte durchlaufen. Größere Metallteile werden händisch an einem Sortierband aussortiert. FE-Metalle werden mit Hilfe von Magneten separiert. Die Abtrennung der NE-Metalle erfolgt durch Wirbelstromabscheider.[33] Die NE-Metalle in den Schlacken schweizerischer Anlagen bestehen zu ca. 70% aus Al, zu 15% aus Cu und zu 15% aus anderen Metallen.[64] Die separierten Metalle werden vermarktet und die übrige Schlacke wird in der Regel als Baustoff verwendet, hauptsächlich im Straßenbau.[33, 65] Wie in Kapitel 2.2.1 beschrieben, können die Metalle bei Trockenaustragung besser und in größerer Reinheit aus der Schlacke separiert werden. Ein Trockenaustrag der Schlacke erfolgt beispielsweise in der KEZO Müllverbrennungsanlage in Hinwil (Schweiz) mit anschließender Schlackeaufbereitung. Neben den oben beschriebenen Trenntechniken ist hier außerdem ein Glasabscheider zur Abtrennung von Glasscherben installiert. Diese werden von einem Sensor anhand ihrer Transparenz erkannt und mit Hilfe einer Druckluftdüse von der restlichen Schlacke getrennt.[66]

Mit der Aufbereitung der Schlacken hat man bereits Anfang der sechziger Jahre begonnen. Dabei ging es zunächst vorrangig darum, die Schlacken so aufzubereiten, dass sie als Baustoff verwendet werden können. Mit der Zeit gewann die Metallrückgewinnung aus den Schlacken zunehmend an Bedeutung und die Aufbereitungstechniken und das Recycling entwickelten sich bis heute weiter.[33] Die Flugaschen dagegen fanden lange Zeit wenig Beachtung hinsichtlich Rohstoffrückgewinnung. Zur Behandlung der Flugaschen wurden thermochemische und nasschemische Verfahren entwickelt, von denen sich in Europa jedoch nur nasschemische Verfahren wie das FLUWA-Verfahren (saure Flugaschenwäsche) durchsetzen konnten.[63]

Im FLUWA-Verfahren wird die Flugasche mit dem sauren Waschwasser aus der nassen Abgasreinigung extrahiert. Die Suspension wird anschließend durch einen Vakuumbandfilter filtriert. Da Schwermetalle bei der Extraktion aus der Flugasche gelöst werden, enthält der Filterkuchen nur noch geringe Mengen Schwermetalle und erfüllt dadurch in der Schweiz die Kriterien zur Ablagerung auf einer Reststoffdeponie. Aus dem schwermetallhaltigen Filtrat werden die gelösten Schwermetalle durch Zugabe von Kalkmilch als Hydroxide ausgefällt und abfiltriert. Der schwermetallhaltige Hydroxidschlamm besteht hauptsächlich aus Zinkhydroxid und wird daher an Zinkhütten abgegeben. Verbliebene Schwermetallspuren im Filtrat werden durch Ionenaustauscher entfernt. Das gereinigte Filtrat kann anschließend ins Abwasser eingeleitet werden.[63]

In der Schweiz begann man Mitte der neunziger Jahre Flugaschen mit diesem Verfahren zu behandeln.[63] Inzwischen werden über 60% der Flugaschen in der Schweiz mit dem FLUWA-Verfahren behandelt.[10] Außerhalb der Schweiz gibt es das FLUWA-Verfahren nur in zwei weiteren Müllverbrennungsanlagen: seit 1998 in Liberec (Tschechien) und seit 2010 in Ingolstadt (Deutschland).[67]

Das FLUREC-Verfahren (Flugasche-Recycling) stellt eine Alternative zur Hydroxidfällung dar und wurde von Schlumberger et al. [14] entwickelt. Mit dem FLUREC-Verfahren können die Elemente Zn, Pb, Cu und Cd aus dem schwermetallhaltigen FLUWA-Filtrat zurückgewonnen werden. Der erste Schritt ist dabei die Zementierung. Dabei wird Zinkpulver als Reduktionmittel zu dem FLUWA-Filtrat gegeben, wodurch sich Cd, Pb und Cu auf dem Zink abscheiden. Ein Teil des Zinkpulvers geht dadurch in Lösung:[63]

$$Cd^{2+}, Pb^{2+}, Cu^{2+} + Zn \rightarrow Cd, Pb, Cu + Zn^{2+} \qquad [68]$$

Das Zementat wird abfiltriert und an Bleihütten abgegeben, da es überwiegend aus Pb besteht. Das in der Lösung verbliebene Zn wird anschließend durch Solventextraktion abgetrennt, gereinigt und aufkonzentriert. Dabei wird das Zn durch einen Komplexbildner selektiv in eine organische Phase überführt. Die organische Phase wird gewaschen und das Zn mit verdünnter Schwefelsäure reextrahiert. Da der Komplexbildner dabei regeneriert wird, handelt es sich bei der Solventextraktion um einen geschlossenen Stoffkreislauf. Durch Elektrolyse wird anschließend hochreines Zink gewonnen.[63]

Das FLUREC-Verfahren wurde 2012 in der Müllverbrennungsanlage Zuchwil in der Schweiz großtechnisch umgesetzt (Abbildung 4). Dort werden jährlich 300 t Zink mit einer Reinheit von >99.995% zurückgewonnen.[10] Das FLUREC-Verfahren erweckte in den letzten Jahren auch das Interesse von Wissenschaftlern außerhalb der Schweiz. Fellner et al. [16] untersuchten die ökonomische Rentabilität des Verfahrens und kamen zu dem Ergebnis, dass die Einsparung an Deponierungskosten einen wesentlich höheren Einfluss auf die Rentabilität hat als der Verkaufserlös des Zn. Insgesamt bewerteten sie die Rückgewinnung bei dem aktuellen Marktpreis von Zn als ökonomisch unrentabel. Purgar et al. [15] kamen zu einem ähnlichen Ergebnis.

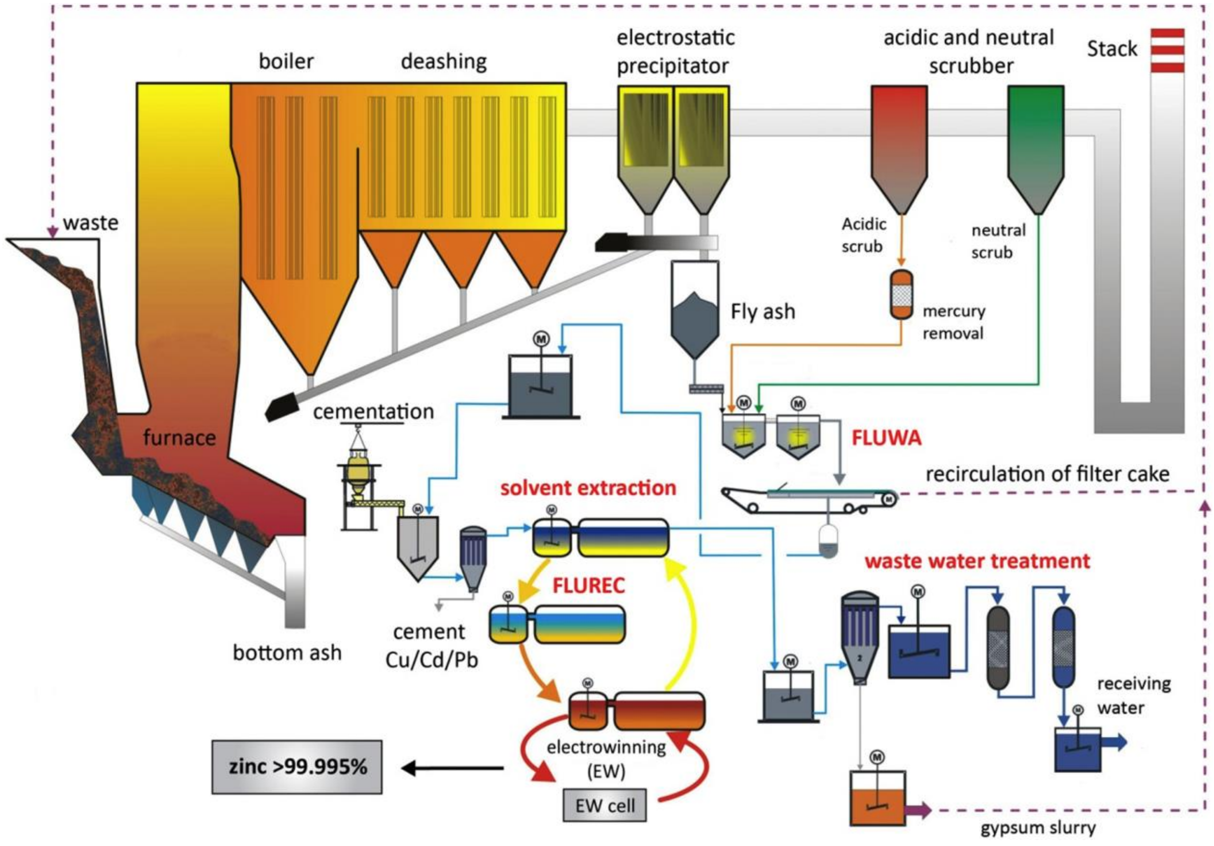

Abbildung 4: Großtechnisches FLUWA- und FLUREC-Verfahren. Abbildung aus Ref. [10]. Abdruck mit Genehmigung (siehe Kapitel 7.4).

Neben dem FLUWA- und FLUREC-Verfahren gibt es aktuell kein weiteres großtechnisch umgesetztes Verfahren, mit dem Wertmetalle aus Flugaschen zurückgewonnen werden. Wie in Tabelle 1 ersichtlich, enthalten Flugaschen neben Zn, Pb, Cu und Cd noch eine Vielzahl weiterer Wertmetalle, für die in der Zukunft eine Rückgewinnung lohnenswert und auch notwendig werden könnte. Die europäische Kommission hat 2011 eine Liste kritischer Rohstoffe für die Europäische Union erstellt.[69] Die Liste umfasste 14 Elemente und wurde 2014 auf 20 und 2017 auf 27 Elemente erweitert.[70, 71] Die Liste führt unter anderem Sb, Bi, Co, Ga, Ge, Hf, In, Mg, Nb, W, V und seltene Erden als kritische Rohstoffe auf, welche ebenfalls in den Ascherückständen enthalten sind (siehe Tabelle 1).

3. Sequentielle Extraktion

Für viele Verfahren zur selektiven Abtrennung und Rückgewinnung von Metallen müssen diese gelöst vorliegen. Beispiele hierfür sind Fällungsreaktionen wie beispielsweise die Hydroxidfällung im FLUWA-Verfahren und die Solventextraktion im FLUREC-Verfahren (siehe Kapitel 2.3). Ein weiteres Beispiel ist die polymergestützte Ultrafiltration, welche zur Metallrückgewinnung aus wässrigen Lösungen angewendet werden kann.[72-74] Für die Entwicklung von Metallrückgewinnungsverfahren aus Rückständen der Müllverbrennung ist es daher notwendig das Löslichkeitsverhalten der einzelnen Elemente in den Rückständen zu kennen. Kenntnisse über das Löslichkeitsverhalten können zum Beispiel durch sequentielle Extraktion erlangt werden.

3.1. Verfahrensprinzip

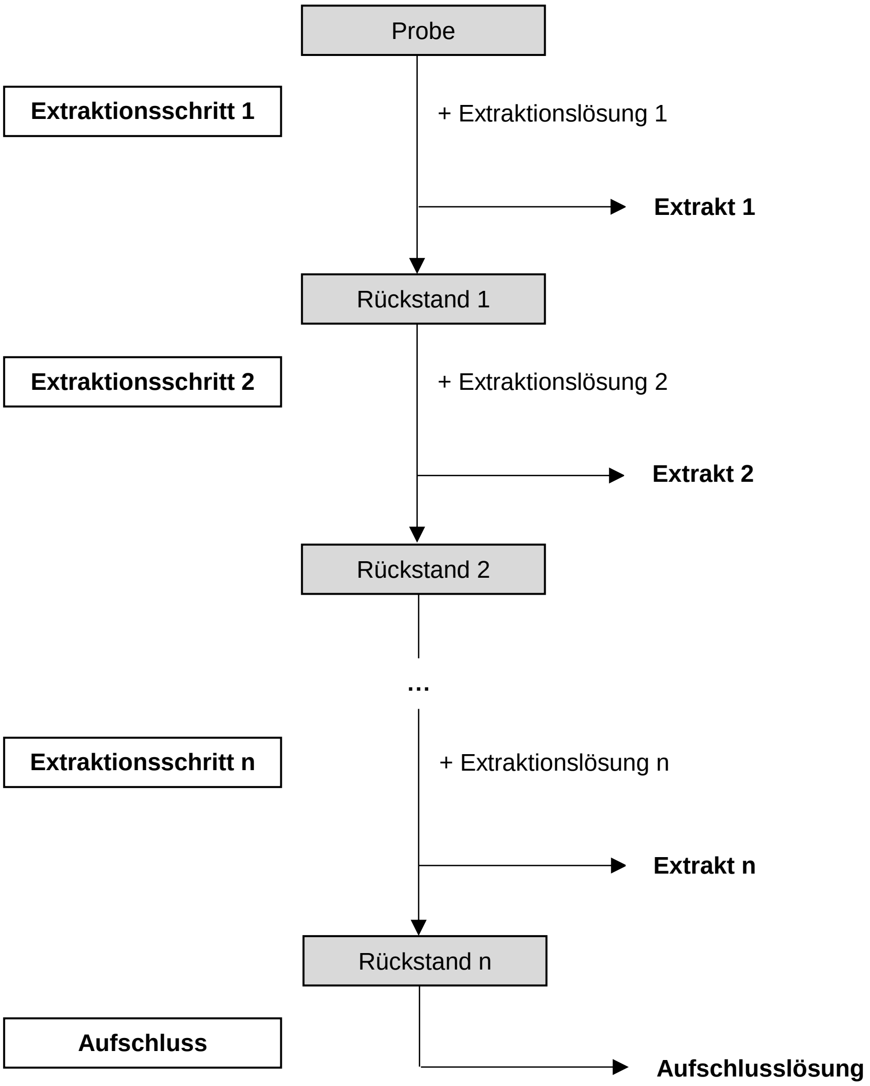

Abbildung 5: Allgemeines Schema einer sequentiellen Extraktion (eigene Darstellung, angelehnt an [75]).

Bei einer sequentiellen Extraktion wird eine Probe mehrmals nacheinander mit verschiedenen Extraktionslösungen extrahiert. Das allgemeine Schema einer sequentiellen Extraktion ist in Abbildung 5 dargestellt. Die Stärke der Extraktionslösung nimmt mit jedem Extraktionsschritt zu, wodurch eine Fraktionierung der einzelnen Elemente entsprechend ihrer Löslichkeit erzielt wird. Der Rückstand nach dem letzten Extraktionsschritt wird mit starken Säuren aufgeschlossen. Die Extrakte und die Aufschlusslösung werden mit analytischen Methoden analysiert.[75]

3.2. Geschichtliche Entwicklung und Zweck

Das Prinzip der sequentiellen Extraktion geht zurück auf ein Konzept von Viets [76]. Er schlug eine Einteilung von Kationen in Gruppen vor, abhängig von ihrer Löslichkeit, von Austauschreaktionen und der chemischen Form, um Aussagen über die Pflanzenverfügbarkeit von Mikronährstoffen in Böden treffen zu können. Ähnlich wie in den sich später daraus abgeleiteten sequentiellen Extraktionsverfahren wurden die Kationen durch Extraktion mit zunehmend stärkeren Extraktionslösungen in Gruppen abnehmender Löslichkeit eingeteilt.

Die sequentielle Extraktion wurde in den 1970er Jahren entwickelt, um Informationen über das Verhalten von Spurenelementen und potentiell toxischen Elementen in Böden und Sedimenten zu erhalten.[77] Durch die Bestimmung des Gesamtgehalts der Elemente erhält man zwar Informationen über die Schadstoffbelastung, darüber hinaus können aber keine Aussagen über die Mobilität und Bioverfügbarkeit getroffen werden.[78] Die Mobilität eines Elements hängt stark von dessen Bindungsform ab.[79] Durch die Bestimmung der Bindungsform können Mobilität, Verfügbarkeit und Toxizität abgeschätzt werden.[80] Durch Änderungen der Umweltbedingungen wie Veränderungen des pH Werts, der Temperatur, des Redoxpotentials, durch Zersetzung von organischer Substanz, Auswaschung, Ionenaustauschprozesse und mikrobielle Aktivität können Elemente aus der Festphase gelöst werden.[81] Mit sequentiellen Extraktionen werden verschiedene Umweltbedingungen sowie natürliche und anthropogene Veränderungen dieser Bedingungen simuliert.[79, 80] Spurenelemente liegen in Sedimenten in verschiedenen Bindungsformen vor, beispielsweise adsorbiert an Partikeloberflächen, gebunden an Carbonate, Fe- und Mn-Oxide, organischem Material oder Sulfide oder eingeschlossen in Silikaten oder schwerlöslichen Oxiden.[82, 83] Die Extraktionslösungen bzw. Reagenzien in sequentiellen Extraktionen wurden daher so entwickelt, dass diese mineralischen Phasen Schritt für Schritt möglichst selektiv gelöst werden, sodass über die Fraktionierung die Bindungsformen der Spurenelemente identifiziert werden können.[84]

3.3. Betrachtung der einzelnen Extraktionsschritte

Die Anzahl der Extraktionsschritte liegt meist zwischen 3 und 8.[84] Oft beinhalten die Verfahren einen Teil oder alle der folgenden Fraktionen: wasserlösliche Fraktion, austauschbare Fraktion, säurelösliche Fraktion, reduzierbare Fraktion, oxidierbare Fraktion, Residualfraktion.[57, 84, 85] Häufig erfolgt die Benennung der Fraktionen nach der jeweiligen Phase, die in dem jeweiligen Extraktionsschritt gelöst werden soll. Die säurelösliche Fraktion wird daher auch als „gebunden an Carbonate“, die reduzierbare Fraktion als „gebunden an Fe/Mn-Oxide“ und die oxidierbare Fraktion als „gebunden an organisches Material und Sulfide“ oder ähnlich bezeichnet.[80, 83] Im Folgenden werden die verschiedenen Fraktionen und die gängigen Reagenzien in den einzelnen Extraktionsschritten kurz erläutert.

Die wasserlösliche Fraktion wird meistens zusammen mit der austauschbaren Fraktion bestimmt und ist daher in den meisten Verfahren kein eigener Extraktionsschritt.[84]

Die austauschbare Fraktion beinhaltet Metalle, die durch elektrostatische Wechselwirkungen schwach auf der Feststoffoberfläche adsorbiert sind und durch Ionenaustausch gelöst werden.[79, 84] Die Desorption wird durch Veränderung der Ionenstärke erreicht.[83, 84] Daher werden für die Extraktion Salzlösungen verwendet, üblicherweise mit einer Konzentration von 1 mol/L [84] bei einem pH Wert von 7 [80]. Die verwendeten Salze sind meistens Chlorid-, Nitrat- oder Acetatsalze von Magnesium, Calcium oder Ammonium.[79, 84]

In der säurelöslichen Fraktion finden sich Metalle, deren Löslichkeit vom pH abhängig ist.[79] In diesem Schritt lösen sich beispielsweise Carbonate, da diese empfindlich auf pH Änderungen reagieren.[83] Meistens wird Essigsäure verwendet oder eine Pufferlösung aus Essigsäure und Natriumacetat bei pH 5.[79, 80, 83]

Unter reduzierenden Bedingungen lösen sich Fe- und Mn-Oxide, wodurch daran gebundene Metalle freigesetzt werden.[86] Gängige Reduktionsmittel in sequentiellen Extraktionen sind Hydroxylamin, Oxalsäure und Dithionit.[79] Die reduzierbare Fraktion wird in manchen Verfahren noch weiter in leicht und moderat reduzierbare Oxide aufgeteilt.[57, 87, 88]

Unter oxidierenden Bedingungen wird organisches Material zersetzt, wodurch gebundene Metalle freigesetzt werden.[79] Gängige Oxidationsmittel in sequentiellen Extraktionen sind H_2O_2, NaOCl, $Na_4P_2O_7$ und $K_4P_2O_7$.[84] H_2O_2 löst neben organischem Material auch Sulfide.[83]

Die Residualfraktion wird mit Mischungen starker Säuren wie HF, $HClO_4$, HCl und HNO_3 aufgeschlossen.[79] Zum Aufschluss von Silikaten und der Freisetzung der darin eingeschlossenen Metalle ist HF notwendig, da Silikate von anderen Säuren nicht gelöst werden.[89]

In der Literatur gibt es eine Vielzahl verschiedener Durchführungsvarianten der sequentiellen Extraktion. Am bekanntesten und am weitesten verbreitet sind das Tessier-Verfahren [83], das in Tabelle 2 zusammengefasst ist, und das BCR-Verfahren. Die vielen verschiedenen Varianten waren der Anlass für die Entwicklung des BCR-Verfahrens, mit dem Ziel ein einheitliches Standardverfahren zur Verfügung zu stellen um vergleichbare Ergebnisse zwischen verschiedenen Laboren zu erreichen.[90, 91] Da sich jedoch herausstellte, dass das Verfahren eine schlechte Reproduzierbarkeit zwischen verschiedenen Laboren aufwies, wurde der Verfahren nochmal überarbeitet. Das überarbeitet BCR-Verfahren ist in Tabelle 3 zusammengefasst.[92] Im Tessier-Verfahren sind die einzelnen Fraktionen nach spezifischen Mineralien benannt, die in dem jeweiligen Extraktionsschritt gelöst werden sollen. Da die Spezifität der Extraktionsreagenzien aber zunehmend angezweifelt wurde (siehe Kapitel 3.5) [77], wurden diese Bezeichnungen im BCR-Verfahren nicht mehr verwendet.[92]

Viele sequentielle Extraktionen in der aktuellen Literatur wurden nach dem Tessier- oder dem BCR-Verfahren oder Abwandlungen von diesen durchgeführt (siehe z.B. [93-97]).

Tabelle 2: Sequentielle Extraktion nach dem Tessier-Verfahren.[83]

Schritt	Bezeichnung der Fraktion	Extraktionslösung
1	austauschbar	1 mol/L $MgCl_2$ bei pH=7
2	gebunden an Carbonate	1 mol/L NaOAc, mit HOAc auf pH=5 eingestellt
3	gebunden an Fe- und Mn-Oxide	0.04 mol/L $NH_2OH{\cdot}HCl$ in 25% HOAc, 96 °C
4	gebunden an organisches Material	1. 8.8 mol/L H_2O_2, mit HNO_3 auf pH=2 eingestellt, 85 °C 2. 3.2 mol/L NH_4OAc in 20% HNO_3
5	Residual	$HClO_4$ und HF

Tabelle 3: Sequentielle Extraktion nach dem überarbeiteten BCR-Verfahren.[92]

Schritt	Extraktionslösung
1	0.11 mol/L HOAc
2	0.5 mol/L $NH_2OH{\cdot}HCl$ in verdünnter HNO_3
3	1. 8.8 mol/L H_2O_2, 85 °C 2. 1 mol/L NH_4OAc, mit HNO_3 auf pH=2 eingestellt
4	Königswasser

In der bestehenden Literatur wurden die Extraktionsschritte mit nur wenigen Ausnahmen in der in diesem Kapitel vorgestellten Reihenfolge durchgeführt. Eine Studie von Miller et al. [98] ist eine der wenigen Studien, in der untersucht wurde, welche Auswirkung eine Veränderung der Reihenfolge der Extraktionsschritte auf das Ergebnis hat. In dieser Studie wurde sowohl die Änderung der Reihenfolge der austauschbaren und der säurelöslichen Fraktion, als auch die Änderung der Reihenfolge der reduzierbaren und der oxidierbaren Fraktion untersucht. Es stellte sich heraus, dass die Reihenfolge der Extraktionsschritte einen signifikanten Einfluss auf die Elementkonzentrationen in den einzelnen Fraktionen hat. Da Partikel in Böden und Sedimenten häufig mit einer Schicht organischen Materials überzogen sind, vermuteten Schultz et al. [99], dass diese Schicht die Auflösung der darunter liegenden Mineralien verhindern könnte. Schultz et al. veränderten das Tessier-Verfahren daher dahingehend, dass die Oxidation des organischen Materials bereits nach der austauschbaren Fraktion durchgeführt wurde. Nur in wenigen anderen Studien wurde die Position des oxidativen Extraktionsschritts ebenfalls geändert und schon vor dem reduktiven Extraktionsschritt durchgeführt (siehe z.B. [100-102]). Nach Filgueiras et al. [84] sollte H_2O_2 erst nach der Auflösung der reduzierbaren Fraktion eingesetzt werden, da dieses Reagenz Fe-/Mn-Oxide angreifen kann. Diese Reihenfolge hat sich bis auf wenige Ausnahmen durchgesetzt.

3.4. Sequentielle Extraktion als Methode zur Speziesbestimmung

Die sequentielle Extraktion wird als eine Methode zur Bestimmung chemischer Spezies betrachtet. Ure [103] definiert Speziierung als *“the active process of identification and quantification of the different defined species, forms or phases in which an element occurs in a material”* oder *“the description of the amounts and kinds of species, forms or phases present in the material”*. Die Speziierung kann in drei Kategorien eingeteilt werden:[77, 103]

a) Die **funktionelle Speziierung** bezieht sich auf die Funktion des Elements wie z.B. pflanzenverfügbare Spezies.

b) Die **klassische Speziierung** bezieht sich auf konkrete chemische Verbindungen oder Oxidationsstufen wie z.B. $PbCO_3$ vs. $Pb_5(PO_4)_3Cl$ oder Cr^{III} vs. Cr^{VI}.

c) Die **operative Speziierung** bezieht sich auf das Verfahren, das zur Extraktion eines Elements verwendet wird wie z.B. die Bestimmung der „in Essigsäure löslichen“ Spezies. Das erhaltene Ergebnis hängt vor allem von den Reagenzien und experimentellen Bedingungen ab, unter denen die Extraktion durchgeführt wird.[78] Die Spezies werden über die extrahierbaren Elemente mit einem gegebenen Verfahren definiert und die Aussagekraft ist mit dem verwendeten Extraktionsschema verbunden.[91] Die Spezies können, müssen aber nicht, die tatsächlich vorliegende Bindungsform wiedergeben.[104]

Die sequentielle Extraktion ist ein Beispiel für eine operative Speziierung.[77] Die sequentielle Extraktion als eine Form der Speziierung zu bezeichnen wird in der Literatur jedoch kritisiert. Nach Quevauviller et al. [91] kann der Begriff Speziierung streng genommen nicht für operativ definierte Verfahren angewendet werden, sondern nur für die klassische Speziierung. Auch nach Schultz et al. [99] ist der Begriff Speziierung nur auf die klassische Form der Speziierung anzuwenden und bei sequentiellen Extraktionen handle es sich stattdessen um eine Fraktionierung.

Trotz dieser Kritik fand die sequentielle Extraktion zur indirekten Speziesbestimmung weite Verbreitung, da eine direkte Speziesbestimmung in Feststoffen bei geringer Spezieskonzentration und einer komplexen Matrix mit anderen Methoden relativ schwierig und durch hohe Nachweisgrenzen limitiert ist.[77, 105] Zur direkten Speziesbestimmung in Müllverbrennungsflugaschen werden beispielsweise häufig Röntgenabsorptionsspektrokopie (XAS, engl. *X-ray absorption spectroscopy*) wie EXAFS (engl. *extended X-ray absorption fine structure*) und XANES (engl. *X-ray absorption near edge structure*) [106-108] oder Röntgendiffraktometrie (XRD, engl. *X-ray diffraction*) [46, 53] angewendet. Funatsuki et al. [106] bestimmten die Bleispezies in Müllverbrennungsflugasche sowohl mit sequentieller Extraktion als auch mit XANES und EXAFS und kamen zu den Ergebnis, dass die Ergebnisse der sequentiellen Extraktion nicht die chemischen Spezies wiedergeben.

Darüber hinaus werden in der Literatur weitere Nachteile und Limitierungen genannt, auf welche im folgenden Kapitel näher eingegangen wird.

3.5. Kritik, Nachteile und Limitierungen

Die Extraktionsreagenzien sind oft nicht ausreichend selektiv, wodurch nicht nur die gewünschten Mineralphasen gelöst werden.[99] Da die angewendeten Prozeduren in der Literatur nicht einheitlich sind, sind die Ergebnisse verschiedener Studien darüber hinaus häufig nicht vergleichbar.[92] Die Bindungsformen der Elemente dürfen sich während der Extraktion nicht verändern. Die Bindungsformen können sich durch Übergang eines Elements von einer Phase in eine andere oder durch die Bildung neuer Phasen durch Fällungsreaktionen verändern.[77] Auch können Elemente, die während der Extraktion freigesetzt werden, wieder an dem verbleibenden Feststoff adsorbieren.[99] Außerdem dürfen sich die Bindungsformen während der Probenvorbereitung nicht verändern. Ein vorheriges Trocknen der Probe beispielsweise kann zu einer Veränderung der Verteilung auf die einzelnen Fraktionen führen.[109, 110] Bei einer unvollständigen Extraktion wird die entsprechende Fraktion nicht quantitativ bestimmt.[77] Sequentielle Extraktionen sind zudem sehr zeitaufwendig.[84]

3.6. Sequentielle Extraktion von Rückständen aus der Müllverbrennung

Obwohl sequentielle Extraktionen ursprünglich für Böden und Sedimente entwickelt worden waren, wurde das Verfahren später auch auf andere Proben angewendet, unter anderem auch auf Rückstände aus der Müllverbrennung. In der Literatur finden sich sowohl einige Studien zu Flugaschen [36, 57, 89, 111-115] als auch zu Schlacken [36, 116, 117]. Dabei wurde häufig eine Modifikation des Tessier-Verfahrens [83] angewendet.

4. Analytische Methoden

Im Folgenden sind die wichtigsten analytischen Methoden beschrieben, die in der vorliegenden Arbeit verwendet wurden.

4.1. Spektrometrie mit induktiv gekoppeltem Plasma

Optische Emissionsspektrometrie mit induktiv gekoppeltem Plasma (ICP–OES, engl. *inductively coupled plasma optical emission spectrometry*) [15, 25, 46, 112, 118, 119] und Massenspektrometrie mit induktiv gekoppeltem Plasma (ICP–MS, engl. *inductively coupled plasma mass spectrometry*) [32, 53, 118] sind zwei der gängigsten Methoden zur Multielementanalyse von Müllverbrennungsrückständen. Da Proben bei beiden Methoden zu einem Aerosol zerstäubt und über einen Argon-Gasstrom in ein Argon-Plasma eingebracht werden, müssen die Proben gelöst vorliegen. Müllverbrennungsrückstände werden dazu meist mikrowellengestützt mit Säure aufgeschlossen.[25, 46, 53, 118, 119] Dabei werden oft verschiedene Säuremischungen wie z.B. HNO_3 und HF [46, 119], HNO_3, H_2O_2 und HCl [118] oder HNO_3, HCl und HF [53] verwendet. Durch die hohe Temperatur des Plasmas wird die Probe atomisiert und ionisiert.[120, 121]

4.1.1. Optische Emissionsspektrometrie mit induktiv gekoppeltem Plasma

Die Atome und Ionen werden im Plasma in einen angeregten Zustand überführt und emittieren beim Zurückfallen in den Grundzustand charakteristische Strahlung, welche in der optischen Emissionsspektrometrie detektiert wird.[120, 121]

Die Energie der bei der Relaxation emittierten Photonen entspricht der Differenz der beteiligten Energiezustände. Da Energieniveaus und damit die Energie der Photonen spezifisch für jedes Element sind, können Elemente über die Wellenlänge der emittierten Strahlung identifiziert werden (qualitative Analyse). Die Emissionsintensität ist proportional zur Anzahl der Atome, wodurch eine quantitative Analyse möglich ist.[122] Die Detektion der Strahlung kann entweder an der Spitze der Plasmafackel (axiale Plasmabeobachtung) oder seitlich der Plasmafackel (radiale Plasmabeobachtung) erfolgen.[121]

Da die Übergänge zwischen verschiedenen Energieniveaus stattfinden können, haben einige Elemente im Plasma sehr viele Emissionslinien. Für die Analyse muss eine Emissionslinie mit geeigneter Empfindlichkeit und ohne spektrale Störungen durch Emissionslinien anderer Elemente ausgewählt werden.[121]

In dieser Arbeit wurde ein iCAP 7600 Duo ICP–OES Spektrometer von Thermo Fisher Scientific verwendet, welches mit einem Echelle-Spektrometer und einem CID–Detektor ausgestattet ist. Es ist sowohl eine axiale als auch eine radiale Plasmabetrachtung möglich.

4.1.2. Massenspektrometrie mit induktiv gekoppeltem Plasma

In der Massenspektrometrie werden die im Plasma gebildeten Ionen detektiert. In dieser Arbeit wurde ein Agilent 7900 ICP–MS Gerät verwendet, dessen Aufbau im Folgenden kurz beschrieben ist. Die im Plasma erzeugten Ionen werden über das Interface in ein Hochvakuum überführt.[123] In der Ionenoptik werden die Ionen durch sogenannte Ionenlinsen durch elektrostatische Felder fokussiert [124] und in eine Kollisionszelle mit Oktopol geleitet, welche der Beseitigung von Störungen (siehe unten) dient.[123] Im darauf folgenden Quadrupol, der als Massenanalysator dient, werden die Ionen nach ihrem Masse-zu-Ladung-Verhältnis (m/z) getrennt. Ionen mit dem zu analysierenden m/z-Verhältnis werden selektiert und gelangen zum Detektor.[123]

In der ICP–MS können verschiedene Interferenzen auftreten. Dazu gehören isobare Überlappungen, doppelt geladene Ionen und polyatomare Störungen.

Die meisten Elemente haben mehrere natürlich vorkommende Isotope.[125] Wenn zwei Isotope von unterschiedlichen Elementen eine so ähnliche Masse aufweisen, dass die Auflösung des Quadrupols nicht mehr ausreicht um diese voneinander zu trennen, spricht man von einer isobaren Überlappung.[126] Das zur Bestimmung des Analyten herangezogene Isotop kann daher durch ein Isotop eines anderen Elements gestört sein.[125] Mögliche Lösungswege zur Vermeidung dieser Störungen sind:

- Verwendung eines Geräts mit einer höheren Auflösung.[126]
- Messung eines anderen Isotops des Analyten.[125, 126]
- Anwendung einer mathematischen Korrekturgleichung. Dazu wird von dem störenden Element zusätzlich ein weiteres, ungestörtes Isotop gemessen. Über das Verhältnis der natürlichen Häufigkeit dieser zwei Isotope kann der störende Signalanteil berechnet und subtrahiert werden.[125]

Neben einfach geladenen Ionen können sich im Plasma auch doppelt geladene Ionen bilden. Da die Trennung im Quadrupol nach dem m/z-Verhältnis erfolgt, verhalten sich diese Ionen bei der Trennung wie ein einfach geladenes Ion mit der halben Masse.[126] Die Bildung doppelt geladener Ionen kann durch Optimierung der Plasmabedingungen minimiert werden.[125]

Im Plasma können Plasmagas, Bestandteile der Probe und Lösemittel miteinander reagieren und polyatomare Ionen bilden. Bei gleicher Ladung verhält sich ein polyatomares Ion bei der

Trennung im Quadrupol wie ein einatomiges Ion, das eine Masse wie die Gesamtmasse des polyatomaren Ions aufweist. Dies führt zu einer Interferenz auf dem Signal des einatomigen Ions.[126] Zur Beseitigung dieser Störungen wurde die Kollisions-/Reaktionszelle entwickelt, in der sich ein Oktopol befindet, der unter anderem zur Fokussierung der Ionen dient.[127] In die Zelle wird eine geringe Menge eines Gases eingeleitet, welches mit den polyatomaren Ionen interagiert. Reaktive Gase reagieren mit den polyatomaren Ionen, z.B. durch Neutralisation der Ladung durch Ladungsaustausch (H_2, NH_3), Oxidation (O_2, N_2O) oder Anlagerung (CH_4), wodurch jeweils eine Veränderung des m/z-Verhältnisses erreicht wird.[128] Aber auch mit nicht reaktiven Gasen wie z.B. He können Störungen beseitigt werden. Dabei wird der Effekt der kinetischen Energiediskriminierung durch Kollisionen genutzt. Ein polyatomares Ion erfährt durch seinen größeren Wirkungsquerschnitt mehr Kollisionen mit dem zugeführten Gas als ein einatomiges Ion mit der gleichen Masse. Dadurch nimmt die kinetische Energie des polyatomaren Ions stärker ab. Am Ende der Kollisionszelle befindet sich eine Potentialbarriere, die durch das Einstellen unterschiedlicher Vorspannungen an Oktopol und dem darauf folgenden Quadrupol erreicht wird. Die Barriere kann nur von den schnelleren einatomigen Ionen überquert werden, nicht jedoch von den langsameren polyatomaren Ionen.[127, 129]

4.2. Röntgenfluoreszenzanalyse

Neben der ICP–OES und der ICP–MS wird auch die Röntgenfluoreszenzanalyse (RFA) häufig zur Multielementanalyse von Müllverbrennungsrückständen eingesetzt.[24, 32, 112, 119] Eine spezielle Variante der RFA ist die Totalreflexions-Röntgenfluoreszenzanalyse (TRFA), die gegenüber der klassischen RFA mehrere Vorteile bietet, jedoch nur selten zur Analyse von Müllverbrennungsrückständen angewendet wird.[130-134]

Beiden Verfahren liegt das gleiche physikalische Prinzip zugrunde. Die Probe wird mit Röntgenstrahlung bestrahlt, wodurch kernnahe Elektronen aus den Atomen herausgeschlagen werden. Dabei muss die Energie der Röntgenstrahlung größer sein als die Bindungsenergie des Elektrons, da sowohl die Bindungsenergie als auch kinetische Energie zum Verlassen des Atoms aufgewendet werden muss. Die entstehenden Lücken werden von Elektronen aus höheren Schalen aufgefüllt und die Energiedifferenz zwischen den beteiligten Energieniveaus wird als elementcharakteristische Röntgenstrahlung freigesetzt. Die charakteristischen Linien im Röntgenspektrum werden in Serien eingeteilt, welche nach der Schale bezeichnet werden, in die das Elektron übergeht (K-, L- oder M-Serie). Ein tiefgestellter griechischer Buchstabe gibt über die Differenz der Hauptquantenzahlen der beteiligten Schalen an, aus welcher Schale das nachrückende Elektron stammt. Die K_α-Linie entsteht beispielsweise durch den Übergang eines Elektrons von der L- in die K-Schale, die K_β-Linie durch einen Übergang von der M- in die K-Schale. Jede Serie besteht daher aus mehreren

Linien, welche durch unterschiedliche Übergangswahrscheinlichkeiten unterschiedlich intensiv sind. Die α-Linien haben die stärkste Intensität, da dieser Übergang am häufigsten auftritt. Röntgenfluoreszenzanalyse eignet sich nicht für leichte Elemente, da bei diesen der Auger-Effekt überwiegt. Dabei handelt es sich um einen strahlungslosen Übergang, der einen Konkurrenzvorgang zur Fluoreszenzemission darstellt.[135]

Im Folgenden wird zunächst kurz auf die klassische RFA eingegangen und anschließend genauer auf die Besonderheiten der TRFA.

4.2.1. Klassische Röntgenfluoreszenzanalyse

Bei der klassischen Röntgenfluoreszenzanalyse wird aus der Probe z.B. eine Press- oder Schmelztablette hergestellt, eine Analyse von Flüssigkeiten ist jedoch auch möglich.[135] Die Probe wird mit Röntgenstrahlung unter einem Einfallswinkel von etwa 45° bestrahlt und die emittierte Röntgenfluoreszenz in einem Winkel von etwa 45° detektiert.[136] In Abbildung 6a ist der Aufbau eines RFA-Spektrometers schematisch gezeigt. Bei der energiedispersiven RFA (ED-RFA) wird die Energie der emittierten Röntgenphotonen gemessen, beispielsweise mit einem Halbleiterdetektor. Bei der wellenlängendispersiven RFA (WD-RFA) wird die emittierte Röntgenfluoreszenz durch Beugung an einem Kristall in die einzelnen Wellenlängen aufgespalten und anschließend z.B. mit einem Gasdurchfluss- oder Szintillationszähler detektiert.[135]

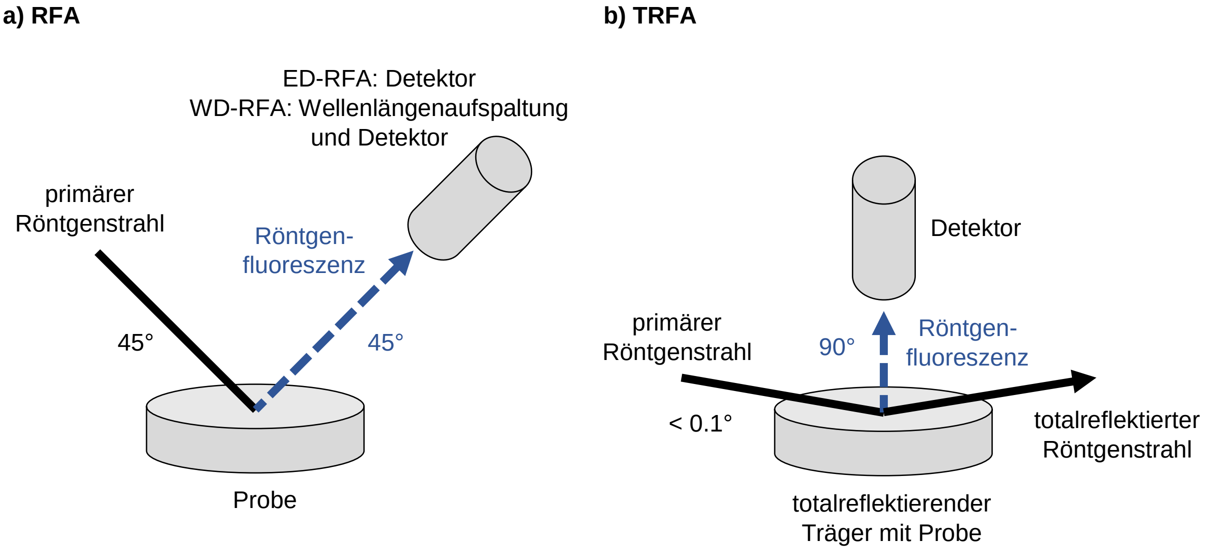

Abbildung 6: Messgeometrie bei der RFA (a) und der TRFA (b) (eigene Darstellung, angelehnt an [136], [135] und [137]).

Bei der quantitativen Auswertung von RFA-Spektren stellen Matrixeffekte eine der Hauptschwierigkeiten dar. Matrixelemente können sowohl die Anregungsstrahlung als auch die Fluoreszenzstrahlung absorbieren oder streuen. Dies hat eine Abschwächung der Fluoreszenzintensität des Analyten zur Folge. Die Fluoreszenzstrahlung von Matrixelementen kann außerdem zusätzlich zur Anregungsstrahlung den Analyten anregen, wodurch es zu einer Verstärkung des Analytsignals kommt. Um Fehler durch Matrixeffekte zu vermeiden, können beispielsweise Standardproben verwendet werden, die eine möglichst ähnliche Zusammensetzung wie die Realprobe haben.[135]

4.2.2. Totalreflexions-Röntgenfluoreszenzanalyse

Die TRFA ist eine Variante der ED-RFA und unterscheidet sich von dieser hauptsächlich in der Probenvorbereitung und der Anregungs- und Messgeometrie. Die Probe wird als dünne Schicht auf einen totalreflektierenden Probenträger aufgebracht. Der anregende Röntgenstrahl trifft in einem sehr flachen Winkel auf die Probe, sodass dieser am Probenträger totalreflektiert wird (Abbildung 6b). Der Einfallswinkel entspricht dabei dem Ausfallswinkel. Die emittierte Röntgenfluoreszenz wird in einem Winkel von 90° detektiert.[135, 137]

Durch Interferenz der ein- und ausfallenden Röntgenstrahlen bildet sich ein Feld stehender Wellen über der Oberfläche des Probenträgers oder innerhalb einer darauf befindlichen dünnen Schicht. Knoten und Wellenlänge dieser stehenden Wellen sind dabei vom Einfallswinkel abhängig. Dieser Zusammenhang ist in Abbildung 7 schematisch dargestellt. An den Knoten ist die Amplitude der Welle Null und damit die Feldstärke Null. An den Schwingungsbäuchen ist die Amplitude der Welle maximal und damit auch die Feldstärke maximal. Das Feld der stehenden Wellen ist somit inhomogen und die Anregung und damit die Intensität der emittierten Röntgenfluoreszenz von der Lage der Knoten und Schwingungsbäuche abhängig, was durch den Einfallswinkel verändert werden kann.[137]

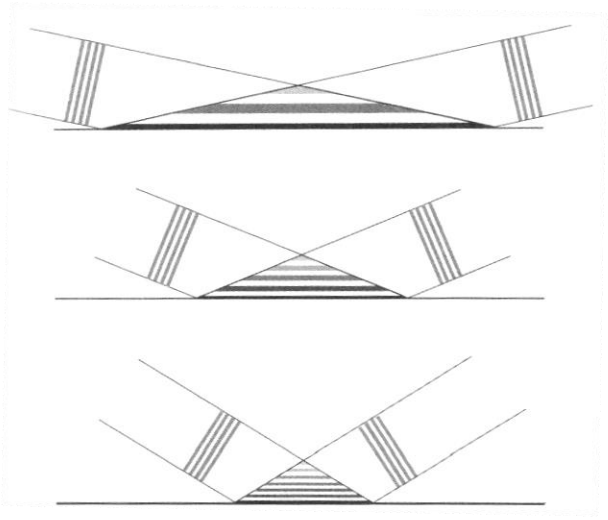

Abbildung 7: Schematische Darstellung des Felds stehender Wellen über einer Oberfläche und Veränderung mit dem Einfallswinkel. Die Schwingungsknoten sind in weiß und die Schwingungsbäuche in schwarz dargestellt. Abbildung aus Ref. [137]. Abdruck mit Genehmigung (siehe Kapitel 7.5).

Im Bereich der Totalreflexion ist die Eindringtiefe der Röntgenstrahlung in die Oberfläche nur gering und klingt unterhalb der Oberfläche als evaneszente Welle exponentiell ab.[135, 137] Dadurch sind die Compton- und Rayleigh-Streuung und Matrixeffekte reduziert. Im Vergleich zur RFA ist dadurch der spektrale Untergrund geringer, das Signal-Rausch-Verhältnis besser und die Nachweisgrenzen sind kleiner.[135]

Die Fluoreszenzausbeute ist von der Kernladungszahl abhängig und nimmt mit dieser zu. Auch bei gleicher Konzentration unterscheidet sich folglich die Intensität der emittierten Röntgenfluoreszenz bei verschiedenen Elementen. Für eine quantitative Auswertung müssen die Sensitivitäten der einzelnen Elemente relativ zueinander bekannt sein. Die relativen Sensitivitäten sind neben der Kernladungszahl auch von der Anregungsart und dem genauen Geräteaufbau abhängig. Werden Veränderungen z.B. an Röntgenröhre, Spannung, Filter oder Monochromator vorgenommen, müssen die relativen Sensitivitäten wieder neu bestimmt werden. Die relativen Sensitivitäten werden mit Standardlösungen der Elemente bestimmt. Um Elemente in einer Probe quantitativ zu bestimmen, muss außerdem ein interner Standard mit bekannter Konzentration zugegeben werden, über den die Konzentration eines Analyten mit nachfolgender Formel berechnet werden kann:[137]

$$c_x = \frac{N_x/S_x}{N_{is}/S_{is}} c_{is}$$

Dabei sind c, N und S Konzentration, Nettointensität und relative Sensitivität des Analyten x bzw. des internen Standards is.

Mittels TRFA können sowohl Feststoffe als auch Flüssigkeiten gemessen werden. In der Literatur sind zahlreiche verschiedene Probenvorbereitungsmethoden beschrieben. Je nach Art der Probe kann die Probenvorbereitung auf sehr unterschiedliche Weise erfolgen. Eine umfangreiche Übersicht hierzu wurde von De La Calle et al. [138] erstellt. Im Folgenden werden gängige Probenvorbereitungsmethoden für Feststoffe beschrieben.

Lösliche Feststoffe können in einem geeigneten Lösungsmittel gelöst und auf den Probenträger aufgebracht werden.[139-141] Feststoffe wie Lippenstift [142] oder Farbpigmente von antiken Gemälden [143] können auch direkt auf den Probenträger aufgebracht werden. Häufig werden Proben jedoch mineralisiert, meist durch Säureaufschluss [144, 145] oder mikrowellenunterstützten Säureaufschluss [146, 147]. Alternativ können Feststoffe auch als Suspension aufgetragen werden.[148-150] Die Probe wird dazu in der Regel gemahlen und als Suspensionsmedium wird häufig Wasser [148-152] oder auch verdünnte Säure [153] eingesetzt. Zusätzlich werden häufig Tenside oder Stabilisierungsreagenzien wie Triton X-100 [151, 154], Polyethylenimin [155] oder Polyvinylalkohol [156] zugesetzt. Um Sedimentierung zu vermeiden und eine homogene Suspension zu erhalten, werden die Suspensionen häufig mit Ultraschall behandelt [150-152, 155] oder anderweitig homogenisiert, z.B. durch Rühren [153] oder mit einem Vortexmischer [154]. Die auf den Probenträger aufgebrachten Tropfen werden anschließend eingetrocknet, z.B. auf einer Heizplatte [153]. Müllverbrennungsflugaschen werden für die Analyse mittels TRFA meist aufgeschlossen [130-133], seltener suspendiert [134].

5. Zusammenfassungen der Publikationen

5.1. Publikation 1: *„Quantification of main and trace metal components in the fly ash of waste-to-energy plants located in Germany and Switzerland: An overview and comparison of concentration fluctuations within and between several plants with particular focus on valuable metals“*

In dieser Publikation wurden die Konzentrationen an Haupt- und Spurenelementen in Flugaschen umfassend untersucht. Anhand von Monatsmischproben, die jeweils aus mindestens einer Tagesstichprobe hergestellt worden waren, wurden 61 Elemente in Flugaschen aus 2 schweizerischen Anlagen (A und B) sowie aus 6 deutschen Anlagen (C–H) bestimmt. Für die Anlagen A und B wurden jeweils 2 bzw. 3 Mischproben von verschiedenen Monaten untersucht, um Unterschiede in der Elementzusammensetzung zwischen verschiedenen Monaten zu sehen.

Die Proben wurden mikrowellengestützt mit HNO_3, HCl und HF druckaufgeschlossen und mittels ICP–OES und ICP–MS analysiert. Für einen Großteil der Elemente konnten die Ergebnisse anhand von Referenzmaterialien oder durch die Bestimmung mit zwei unabhängigen Methoden validiert werden.

Die Elementkonzentrationen in den verschiedenen Flugascheproben waren relativ ähnlich. Auch die Unterschiede zwischen den verschiedenen Monatsmischproben der Anlagen A und B waren vergleichsweise gering.

Um einen genaueren Einblick in die zeitlichen Schwankungen der Gehalte an Zn, Pb, Cu, Cd, Sb und Sn in den Anlagen A und B zu erhalten, sind die Konzentrationen in Wochenmischproben über den Zeitraum von knapp 3 Jahren gezeigt. Diese Analysen werden routinemäßig in den Müllverbrennungsanlagen mit ED–XRF durchgeführt. Die Daten wurden für die Publikation bereitgestellt. Die Konzentrationen der betrachteten Elemente wiesen im betrachteten Zeitraum nur geringe Schwankungen auf.

Ein Teil der in dieser Publikation beschriebenen Flugascheproben wurden für die weitergehenden Studien in den Publikationen 2 und 3 verwendet.

Eigener Beitrag:

- *Durchführung und Auswertung der in den Kapiteln 2.2, 2.3 und 2.4 der Publikation beschriebenen Experimente (ausgenommen der REM/EDX-Messungen)*
- *Schreiben der Publikation*

5.2. Publikation 2: *„Solubility of elements in waste incineration fly ash and bottom ash under various leaching conditions studied by a sequential extraction procedure“*

In dieser Publikation wurde mit einer 7-stufigen sequentiellen Extraktion das Löslichkeitsverhalten von 37 Elementen in zwei Flugascheproben aus Anlagen A und C und in einer Schlackeprobe (Feinfraktion <0.3 mm) aus Anlage B untersucht und verglichen. Eine Flugascheprobe aus Anlage B wurde darüber hinaus für ein ergänzendes Experiment verwendet. Ziel der sequentiellen Extraktion war dabei nicht die Bestimmung der Bindungsformen der Elemente, sondern einen detaillierten Einblick in die zum Lösen eines Elements notwendigen Extraktionsbedingungen zu bekommen. Das angewendete Extraktionsverfahren ist hinsichtlich dieses Ziels entwickelt worden. Eine Übersicht über die einzelnen Extraktionsschritte ist in Tabelle 4 gegeben.

Tabelle 4: Übersicht über die 7 Extraktionsschritte der sequentiellen Extraktion.

Extraktionsschritt	Gelöste Fraktion	Verwendete Extraktionsreagenzien
1	Wasserlöslich bei alkalischem pH	Wasser
2	Wasserlöslich bei neutralem pH	Wasser, Neutralisation auf pH=7 mit Essigsäure
3	Ionenaustausch	$MgCl_2$
4	Säurelöslich	Essigsäure, pH=3
5	Reduzierbar	$NH_2OH \cdot HCl$, pH=3 mit Essigsäure
6	Oxidierbar	H_2O_2, pH=3 mit HNO_3
7	Rückstand	Aufschluss mit HNO_3, HCl und HF

Es wurde festgestellt, dass das Extraktionsmuster von allen drei Proben sehr ähnlich war. Sogar Elemente wie Zn, Cd, Sb, Pb und Bi, die in deutlich niedrigerer Konzentration in der Schlacke vorhanden waren, zeigten ein vergleichbares Löslichkeitsverhalten wie in den Flugaschen. Auffällig war zudem das sehr ähnliche Löslichkeitsverhalten der seltenen Erden untereinander. Nur die Alkalielemente Li, Na, K und Rb waren in der Schlacke lediglich zu 10–25% wasserlöslich, während sie in den Flugaschen eine sehr hohe Wasserlöslichkeit zeigten (Li ca. 60–80%; Na, K, und Rb ca. 90%).

Während Schritt 1 war bei Suspensionen mancher Flugaschen ein pH-Anstieg von neutral zu alkalisch (pH ca. 10–11) über mehrere Stunden zu beobachten. Ein Monitoring der Elementkonzentrationen während des Anstiegs zeigte, dass die Elemente Cd, Tl, Zn, Pb und Ba zum Großteil oder vollständig bei alkalischem pH ausfallen. Der gelöste Anteil an Cd und Tl beispielsweise beträgt anfangs bei noch neutralem pH je nach Probe 69%/57% (Cd) bzw. 87%/94% (Tl) und fällt im Alkalischen auf 0%/0% (Cd) bzw. 23%/31% (Tl) ab. Nur für Mo wurde ein signifikanter Konzentrationsanstieg mit steigendem pH beobachtet.

In Schritt 2 wurden die immer noch stark alkalischen Suspensionen auf pH=7 neutralisiert. Die ausgefallenen Tl-Verbindungen konnten nur in vernachlässigbaren Mengen wieder gelöst werden und auch von den ausgefallenen Cd-Verbindungen war nur ein geringer Teil im Neutralen löslich. Schritt 2 diente außerdem dazu sicherzustellen, dass sich in Schritt 3 keine Elemente aufgrund von pH-Unterschieden zum vorangegangen Schritt lösen und dadurch eine Aussage über Ionenaustauschprozesse verhindern.

Der Ionenaustausch in Schritt 3 wurde mit $MgCl_2$ durchgeführt. Ein Vergleich mit $MgNO_3$ ergab, dass das Lösen von Cd und Ag in diesem Schritt ausschließlich auf die Chloride in $MgCl_2$ zurückzuführen war und nicht auf Ionenaustausch durch Mg^{2+}. Neben Cd und Ag lösten sich in diesem Schritt hauptsächlich andere Erdalkalielemente, was auf Ionenaustausch zurückgeführt wurde.

In den Schritten 4–6 wurde stets der gleiche pH eingestellt, um die in Schritt 5 und 6 gelösten Mengen eindeutig auf Reduktions-/Oxidationsprozesse zurückführen zu können. Durch den Vergleich von $NH_2OH{\cdot}HCl$ mit NaCl in Schritt 5 wurde festgestellt, dass nur wenige Elemente wie z.B. Fe und V tatsächlich durch Reduktion gelöst wurden und auch in diesem Schritt die Chloride in $NH_2OH{\cdot}HCl$ einen starken Einfluss haben. Weiterhin wurde gezeigt, dass die Reihenfolge von Schritt 5 und 6 vertauschbar ist.

Durch Trocknen zwischen den einzelnen Extraktionsschritten wurde die Gesamtmasse bestimmt, die sich in den einzelnen Schritten löst. Bei den zwei Flugaschen wurde hier ebenfalls eine sehr große Übereinstimmung beobachtet. Der wasserlösliche Anteil der Schlacke war mit nur 7% deutlich geringer als der von den Flugaschen (ca. 45%).

Die Summe über alle Extraktionsschritte stimmte sehr gut mit den Analyseergebnissen (siehe Publikation 1 für die Analysenergebnisse der Flugaschen) der Proben überein.

Eigener Beitrag:

- *Entwurf des Versuchskonzepts und Planung der Experimente*
- *Entwicklung des angewendeten sequentiellen Extraktionsverfahrens aus bestehenden Verfahren in der Literatur sowie Optimierung der einzelnen Extraktionsschritte*
- *Durchführung eines Teils der Experimente*
- *Interpretation der Ergebnisse*
- *Schreiben der Publikation*

5.3. Publikation 3: *„Digestions vs. suspensions: The influence of sample preparation on precision and accuracy in total-reflection X-ray fluorescence analysis by the example of waste incineration fly ash“*

In dieser Publikation wurden verschiedene Probenvorbereitungsmethoden zur TRFA Analyse von Flugaschen untersucht und hinsichtlich Präzision und Richtigkeit verglichen. Für die Experimente wurde exemplarisch die Flugascheprobe aus Anlage C verwendet. Gegenstand der Studie waren die Elemente K, Ca, Ti, Mn, Fe, Cu, Zn, Rb, Sr, Pb und Br.

Es wurden die Ergebnisse von Aufschlusslösungen (siehe Publikation 1) und Suspensionen verglichen. Bei den Aufschlusslösungen wurden unter anderem verschiedene interne Standards verwendet und der Einfluss eines Tensids getestet. Bei den Suspensionen wurden unter anderem die Ergebnisse ungemahlener und gemahlener Flugasche sowie verschiedene Suspendiermedien (Wasser und 1% HNO_3) verglichen. Von jeder Lösung bzw. Suspension wurden stets 10 Aliquote gemessen. Die Streuung der Ergebnisse diente als Maß für die Präzision und anhand der Übereinstimmung des Median mit den ICP–OES bzw. ICP–MS Analysenergebnissen (siehe Publikation 1) wurde die Richtigkeit beurteilt. Eine Übersicht des experimentellen Vorgehens ist in Abbildung 8 dargestellt.

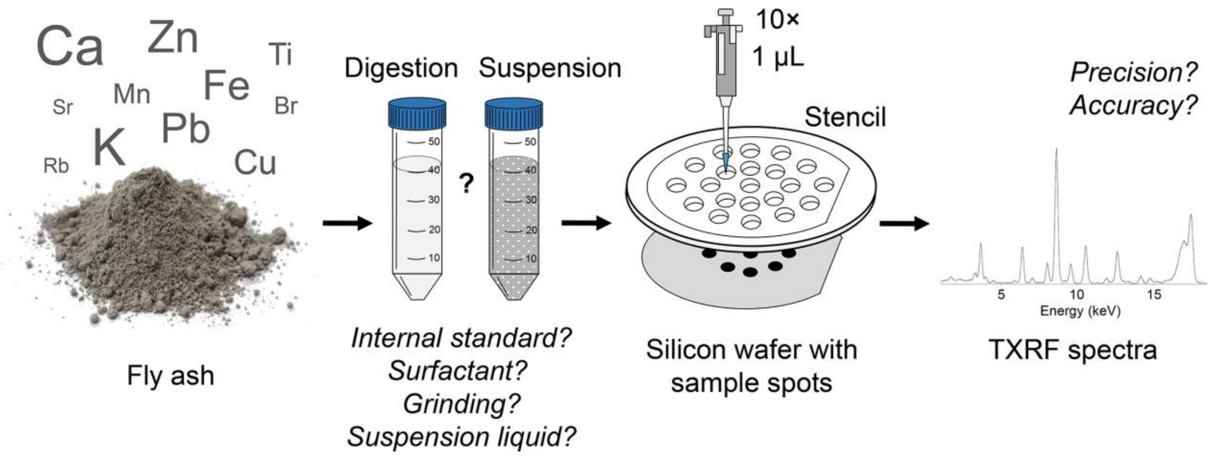

Abbildung 8: Grafische Zusammenfassung der Experimente (Graphical abstract der Publikation). Abdruck mit Genehmigung (siehe Kapitel 7.3).

Es wurde festgestellt, dass die Probenvorbereitung die Präzision und Richtigkeit der Messung stark beeinflusst. Die Ursachen für geringe Präzision und Abweichungen von den ICP–OES bzw. ICP–MS Analysenergebnissen wurden identifiziert und eingehend untersucht.

Bei der Messung der Aufschlusslösungen wurde eine inhomogene Tiefenverteilung der Elemente innerhalb der Probenspots als Ursache für geringe Präzision und/oder Richtigkeit identifiziert. Dies konnte durch Winkelscans nachgewiesen werden und konnten je nach Analyt durch die Zugabe eines Tensids und/oder durch Verwendung eines anderen internen Standards vermieden werden. Das Auftreten einer inhomogenen Tiefenverteilung von Elementen in einem Probenfleck erwies sich als schwer vorhersagbar, weshalb stets Winkelscans zur Validierung von Messergebnissen in der Methodenentwicklung angewendet werden sollten.

Bei wässrigen Suspensionen aus ungemahlener Flugasche wurde eine Unterbestimmung für manche Analyten beobachtet, insbesondere für Ca, Ti, Mn, Fe und Sr. Dies konnte zum Großteil auf Absorptionsverluste der Röntgenstrahlung in größeren Partikeln zurückgeführt werden. Durch ein vorheriges Mahlen der Flugasche konnte dieser Fehler für alle Elemente behoben werden. Es wurde gezeigt, dass alternativ zum Mahlen der Flugasche 1% HNO_3 anstelle von Wasser als Suspensionsmedium verwendet werden kann, um große Partikel durch Auflösung zu vermeiden. Nur für die Elemente Ti und Fe war diese Methode nicht ausreichend und ein Mahlen der Flugasche notwendig, um präzise und richtige Ergebnisse für diese Analyten zu erhalten.

Mit einer optimierten Probenvorbereitung für Suspension und Aufschluss konnte mit beiden Methoden eine vergleichbare Präzision erreicht werden, welche mit der Gerätepräzision, die durch 10-malige Messung eines Probenflecks bestimmt wurde, vergleichbar war. Folglich sind aufwendige Aufschlüsse der Flugaschen nicht notwendig.

Auf die Bestimmung von Br wurde gesondert eingegangen. Bromid verflüchtigt sich in Anwesenheit von Säure als HBr, weshalb die Bestimmung von Br in neutralem Medium erfolgen muss.

Ergänzend wurden ausgewählte Probenflecken mit einem Lichtmikroskop aufgenommen, um die deutlichen optischen Unterschiede zu zeigen, welche sich aus den verschiedenen Probenvorbereitungsmethoden ergeben.

Eigener Beitrag:

- *Entwurf des Versuchskonzepts*
- *Planung und Durchführung der Experimente*
- *Auswertung und Interpretation der Ergebnisse*
- *Schreiben der Publikation*

Vorarbeiten zu dieser Publikation waren Teil meiner Masterarbeit [157]. Das Versuchskonzept und die durchgeführten Experimente in der Publikation bauen auf ersten grundlegenden Erkenntnissen aus der Masterarbeit auf.

6. Schlussfolgerungen und Ausblick

Diese Arbeit gibt einen umfassenden Einblick in die Elementgehalte in Flugaschen einschließlich enthaltener Spurenelemente und seltener Erden. Die Analysenergebnisse tragen zur Verbesserung der Datenlage insbesondere für Flugaschen aus deutschen Müllverbrennungsanlagen bei und zeigen deren Wertstoffpotential auf. Insbesondere im Hinblick auf die großen anfallenden Mengen an Flugasche sind die Konzentrationen einiger Wertmetalle nicht zu vernachlässigen. Daher ist eine Erweiterung und Intensivierung der Rückgewinnung mit bestehenden Verfahren sowie die Entwicklung neuer Verfahren in der Zukunft anzustreben.

Für die Entwicklung von Verfahren, die auf der Rückgewinnung von Elementen aus Lösungen beruhen, bieten die umfangreichen Daten der sequentiellen Extraktion in dieser Arbeit eine Hilfestellung. Die Daten geben einen detaillierten Einblick in die Löslichkeit der einzelnen Elemente und in die Bedingungen, die zur Extraktion notwendig sind.

Durch die zunehmende Rohstoffverknappung wird die Nutzung von Sekundärrohstoffquellen wie beispielsweise von Müllverbrennungsrückständen in den kommenden Jahrzehnten notwendig werden. Im Zuge dessen wird auch eine zuverlässige Elementanalytik an Bedeutung gewinnen. Wie in dieser Arbeit gezeigt, stellt die TRFA für einige Elemente eine geeignete Alternative zu den Standardmethoden RFA, ICP–OES und ICP–MS dar. Die Probenvorbereitung für die TRFA Analyse weist zwar einige mögliche Fehlerquellen auf, welche in dieser Arbeit aber umfassend aufgezeigt wurden und vermieden werden können. TRFA Geräte benötigen keine aufwendige Laborinfrastruktur wie eine Gasversorgung und moderne Geräte wie beispielsweise das Modell S4 T-STAR von Bruker [158] benötigen auch keinen flüssigen Stickstoff zur Kühlung des Detektors mehr und die Röntgenröhre kann mit Luft statt mit Wasser gekühlt werden. Auch die Probenvorbereitung ist mit wenig Aufwand verbunden und wie in dieser Arbeit gezeigt müssen keine Aufschlüsse mit Flusssäure durchgeführt werden, wodurch die dafür notwendigen Sicherheitsvorkehrungen entfallen. Dadurch wäre ein Einsatz der TRFA direkt vor Ort in den Müllverbrennungsanlagen zur Routineanalyse der Verbrennungsrückstände denkbar. Das analysierbare Elementspektrum könnte durch Anwendung einer anderen Anregungsstrahlung (z.B. W-Anregung) noch erweitert werden.

In Müllverbrennungsrückständen steckt noch ein großes Potential, für dessen Nutzung aber noch weitere Forschungsarbeit notwendig ist. Eine umfangreiche Elementanalytik wie in dieser Arbeit bildet dafür die Grundlage.

7. Abdruckgenehmigungen

7.1. Publikation 1

Title: Quantification of main and trace metal components in the fly ash of waste-to-energy plants located in Germany and Switzerland: An overview and comparison of concentration fluctuations within and between several plants with particular focus on valuable metals

Author: Jasmin Haberl,Ralf Koralewska,Stefan Schlumberger,Michael Schuster

Publication: Waste Management

Publisher: Elsevier

Date: May 2018

© 2018 Elsevier Ltd. All rights reserved.

If you're a copyright.com user, you can login to RightsLink using your copyright.com credentials.
Already **a RightsLink user** or want to learn more?

Quick Price Estimate

I would like to...	reuse in a thesis/dissertation
I would like to use...	full article
Circulation	11
My format is...	both print and electronic
I am the author of this Elsevier article...	Yes
I will be translating...	No
My currency is...	EUR - €
Quick Price	Click Quick Price

This service provides permission for reuse only. If you do not have a copy of the content, you may be able to purchase a copy using RightsLink as an additional transaction. Simply select 'I would like to.... 'Purchase this content'.

Unclear about who you are?

Exchange rates under license from XE.com.
To request permission for a type of use not listed, please contact Elsevier Global Rights Department.

Are you the author of this Elsevier journal article?

Copyright © 2019 Copyright Clearance Center, Inc. All Rights Reserved. Privacy statement. Terms and Conditions.
Comments? We would like to hear from you. E-mail us at customercare@copyright.com

Title:	Quantification of main and trace metal components in the fly ash of waste-to-energy plants located in Germany and Switzerland: An overview and comparison of concentration fluctuations within and between several plants with particular focus on valuable metals
Author:	Jasmin Haberl,Ralf Koralewska,Stefan Schlumberger,Michael Schuster
Publication:	Waste Management
Publisher:	Elsevier
Date:	May 2018

© 2018 Elsevier Ltd. All rights reserved.

If you're a copyright.com user, you can login to RightsLink using your copyright.com credentials.
Already **a RightsLink user** or want to learn more?

Please note that, as the author of this Elsevier article, you retain the right to include it in a thesis or dissertation, provided it is not published commercially. Permission is not required, but please ensure that you reference the journal as the original source. For more information on this and on your other retained rights, please visit: https://www.elsevier.com/about/our-business/policies/copyright#Author-rights

Copyright © 2019 Copyright Clearance Center, Inc. All Rights Reserved. Privacy statement. Terms and Conditions.
Comments? We would like to hear from you. E-mail us at customercare@copyright.com

7.2. Publikation 2

Title: Solubility of elements in waste incineration fly ash and bottom ash under various leaching conditions studied by a sequential extraction procedure
Author: Jasmin Haberl,Michael Schuster
Publication: Waste Management
Publisher: Elsevier
Date: 15 March 2019

© 2019 Elsevier Ltd. All rights reserved.

If you're a copyright.com user, you can login to RightsLink using your copyright.com credentials.
Already **a RightsLink user** or want to learn more?

Quick Price Estimate

I would like to...	reuse in a thesis/dissertation
I would like to use...	full article
Circulation	11
My format is...	both print and electronic
I am the author of this Elsevier article...	Yes
I will be translating...	No
My currency is...	EUR - €
Quick Price	Click Quick Price

This service provides permission for reuse only. If you do not have a copy of the content, you may be able to purchase a copy using RightsLink as an additional transaction. Simply select 'I would like to..... 'Purchase this content'.

Unclear about who you are?

Exchange rates under license from XE.com.
To request permission for a type of use not listed, please contact Elsevier Global Rights Department.

Are you the author of this Elsevier journal article?

Copyright © 2019 Copyright Clearance Center, Inc. All Rights Reserved. Privacy statement. Terms and Conditions.
Comments? We would like to hear from you. E-mail us at customercare@copyright.com

Title: Solubility of elements in waste incineration fly ash and bottom ash under various leaching conditions studied by a sequential extraction procedure
Author: Jasmin Haberl,Michael Schuster
Publication: Waste Management
Publisher: Elsevier
Date: 15 March 2019

© 2019 Elsevier Ltd. All rights reserved.

If you're a copyright.com user, you can login to RightsLink using your copyright.com credentials.
Already **a RightsLink user** or want to learn more?

Please note that, as the author of this Elsevier article, you retain the right to include it in a thesis or dissertation, provided it is not published commercially. Permission is not required, but please ensure that you reference the journal as the original source. For more information on this and on your other retained rights, please visit: https://www.elsevier.com/about/our-business/policies/copyright#Author-rights

Copyright © 2019 Copyright Clearance Center, Inc. All Rights Reserved. Privacy statement. Terms and Conditions.
Comments? We would like to hear from you. E-mail us at customercare@copyright.com

7.3. Publikation 3

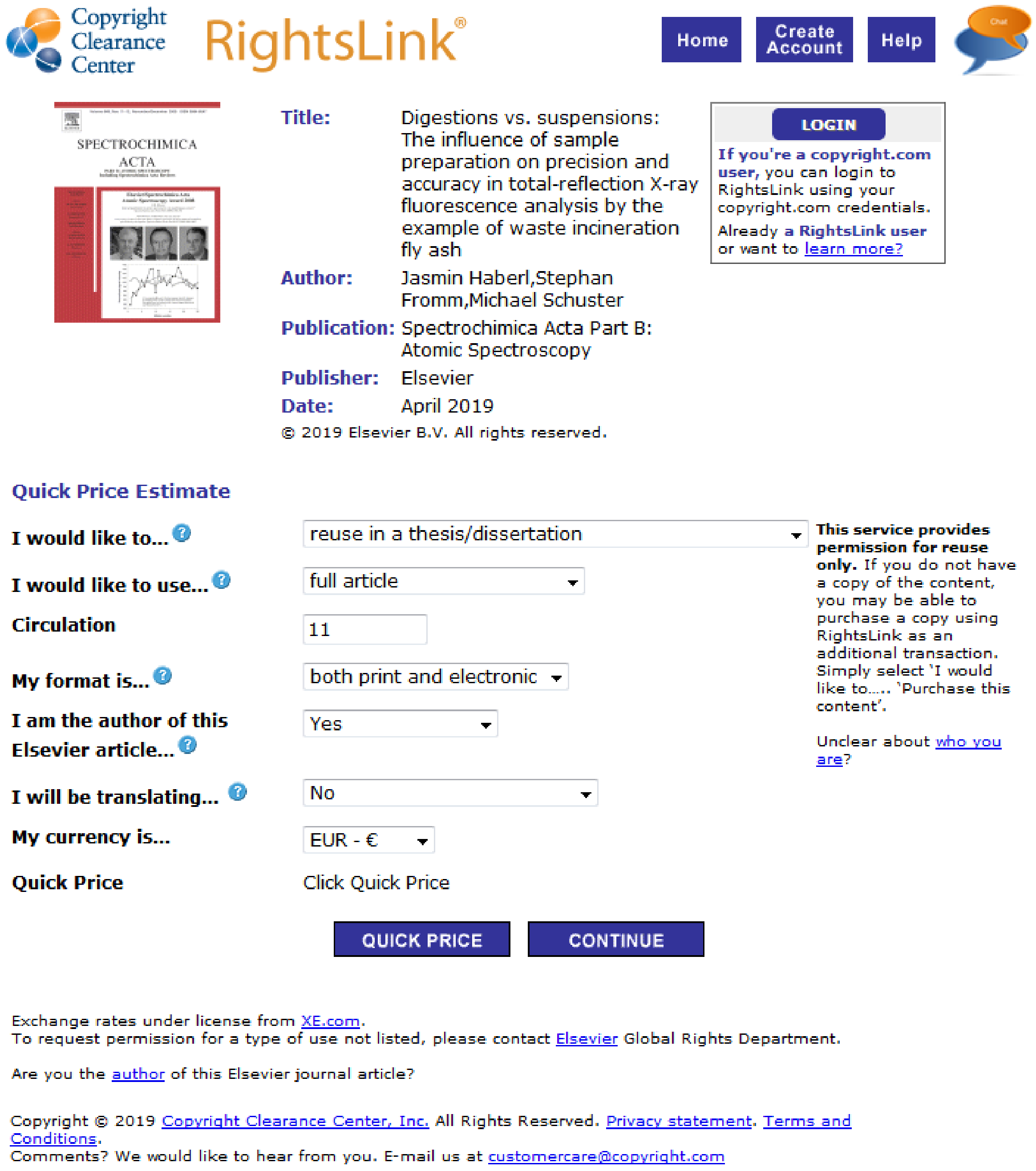

Title:	Digestions vs. suspensions: The influence of sample preparation on precision and accuracy in total-reflection X-ray fluorescence analysis by the example of waste incineration fly ash
Author:	Jasmin Haberl,Stephan Fromm,Michael Schuster
Publication:	Spectrochimica Acta Part B: Atomic Spectroscopy
Publisher:	Elsevier
Date:	April 2019

© 2019 Elsevier B.V. All rights reserved.

If you're a copyright.com user, you can login to RightsLink using your copyright.com credentials.
Already **a RightsLink user** or want to learn more?

Quick Price Estimate

I would like to...	reuse in a thesis/dissertation
I would like to use...	full article
Circulation	11
My format is...	both print and electronic
I am the author of this Elsevier article...	Yes
I will be translating...	No
My currency is...	EUR - €
Quick Price	Click Quick Price

This service provides permission for reuse only. If you do not have a copy of the content, you may be able to purchase a copy using RightsLink as an additional transaction. Simply select 'I would like to..... 'Purchase this content'.

Unclear about who you are?

Exchange rates under license from XE.com.
To request permission for a type of use not listed, please contact Elsevier Global Rights Department.

Are you the author of this Elsevier journal article?

Copyright © 2019 Copyright Clearance Center, Inc. All Rights Reserved. Privacy statement. Terms and Conditions.
Comments? We would like to hear from you. E-mail us at customercare@copyright.com

Title: Digestions vs. suspensions: The influence of sample preparation on precision and accuracy in total-reflection X-ray fluorescence analysis by the example of waste incineration fly ash

Author: Jasmin Haberl,Stephan Fromm,Michael Schuster

Publication: Spectrochimica Acta Part B: Atomic Spectroscopy

Publisher: Elsevier

Date: April 2019

© 2019 Elsevier B.V. All rights reserved.

If you're a copyright.com user, you can login to RightsLink using your copyright.com credentials.

Already **a RightsLink user** or want to learn more?

Please note that, as the author of this Elsevier article, you retain the right to include it in a thesis or dissertation, provided it is not published commercially. Permission is not required, but please ensure that you reference the journal as the original source. For more information on this and on your other retained rights, please visit: https://www.elsevier.com/about/our-business/policies/copyright#Author-rights

Copyright © 2019 Copyright Clearance Center, Inc. All Rights Reserved. Privacy statement. Terms and Conditions.
Comments? We would like to hear from you. E-mail us at customercare@copyright.com

7.4. Abbildung 4

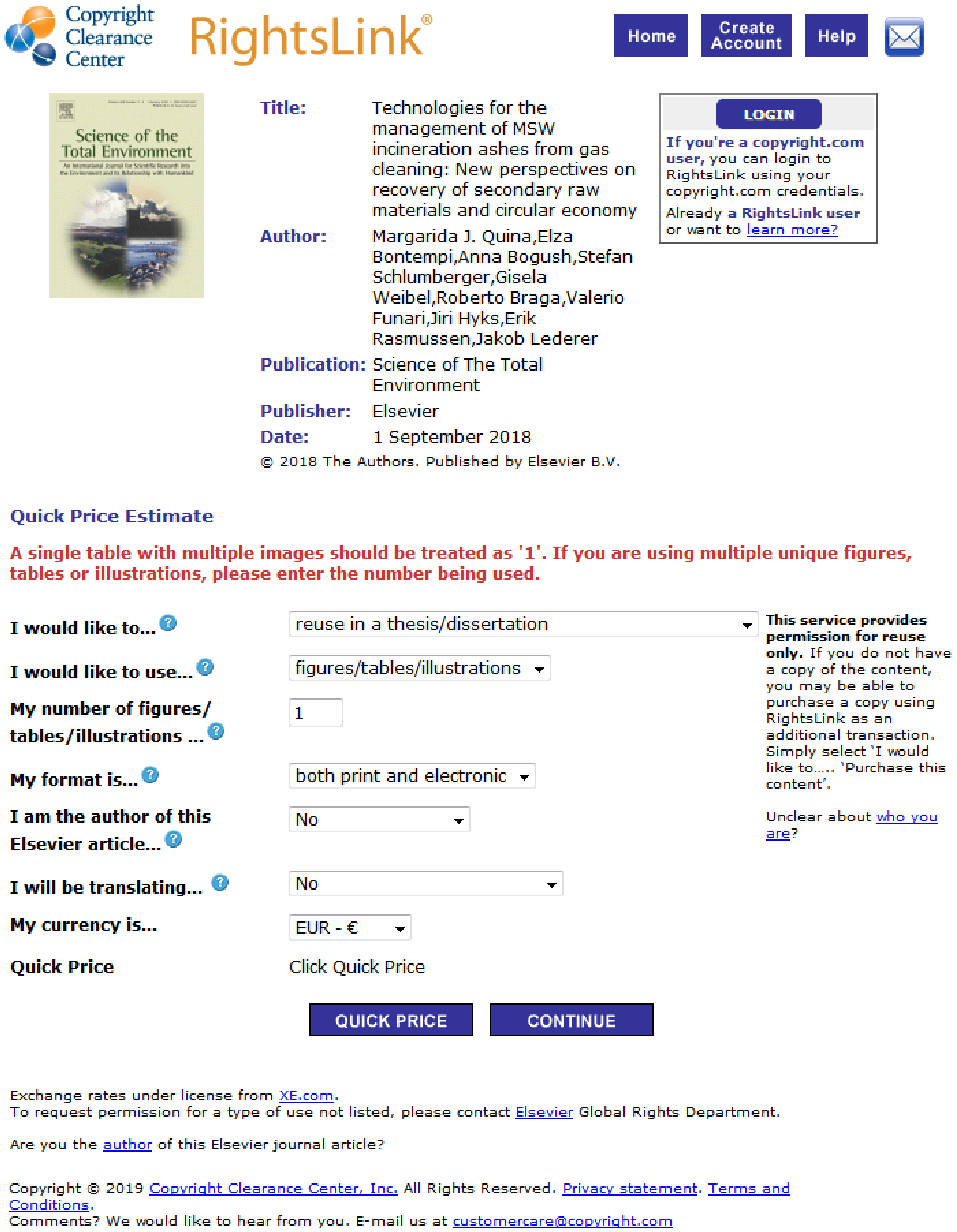

Title:	Technologies for the management of MSW incineration ashes from gas cleaning: New perspectives on recovery of secondary raw materials and circular economy
Author:	Margarida J. Quina,Elza Bontempi,Anna Bogush,Stefan Schlumberger,Gisela Weibel,Roberto Braga,Valerio Funari,Jiri Hyks,Erik Rasmussen,Jakob Lederer
Publication:	Science of The Total Environment
Publisher:	Elsevier
Date:	1 September 2018

© 2018 The Authors. Published by Elsevier B.V.

If you're a copyright.com user, you can login to RightsLink using your copyright.com credentials.
Already **a RightsLink user** or want to learn more?

Quick Price Estimate

A single table with multiple images should be treated as '1'. If you are using multiple unique figures, tables or illustrations, please enter the number being used.

I would like to...	reuse in a thesis/dissertation
I would like to use...	figures/tables/illustrations
My number of figures/ tables/illustrations ...	1
My format is...	both print and electronic
I am the author of this Elsevier article...	No
I will be translating...	No
My currency is...	EUR - €
Quick Price	Click Quick Price

This service provides permission for reuse only. If you do not have a copy of the content, you may be able to purchase a copy using RightsLink as an additional transaction. Simply select 'I would like to... 'Purchase this content'.

Unclear about who you are?

Exchange rates under license from XE.com.
To request permission for a type of use not listed, please contact Elsevier Global Rights Department.

Are you the author of this Elsevier journal article?

Copyright © 2019 Copyright Clearance Center, Inc. All Rights Reserved. Privacy statement. Terms and Conditions.
Comments? We would like to hear from you. E-mail us at customercare@copyright.com

Title: Technologies for the management of MSW incineration ashes from gas cleaning: New perspectives on recovery of secondary raw materials and circular economy

Author: Margarida J. Quina,Elza Bontempi,Anna Bogush,Stefan Schlumberger,Gisela Weibel,Roberto Braga,Valerio Funari,Jiri Hyks,Erik Rasmussen,Jakob Lederer

Publication: Science of The Total Environment

Publisher: Elsevier

Date: 1 September 2018

© 2018 The Authors. Published by Elsevier B.V.

If you're a copyright.com user, you can login to RightsLink using your copyright.com credentials. Already **a RightsLink user** or want to learn more?

Creative Commons Attribution-NonCommercial-No Derivatives License (CC BY NC ND)

This article is published under the terms of the Creative Commons Attribution-NonCommercial-No Derivatives License (CC BY NC ND).
For non-commercial purposes you may copy and distribute the article, use portions or extracts from the article in other works, and text or data mine the article, provided you do not alter or modify the article without permission from Elsevier. You may also create adaptations of the article for your own personal use only, but not distribute these to others. You must give appropriate credit to the original work, together with a link to the formal publication through the relevant DOI, and a link to the Creative Commons user license above. If changes are permitted, you must indicate if any changes are made but not in any way that suggests the licensor endorses you or your use of the work.

Permission is not required for this non-commercial use. For commercial use please continue to request permission via Rightslink.

Copyright © 2019 Copyright Clearance Center, Inc. All Rights Reserved. Privacy statement. Terms and Conditions.
Comments? We would like to hear from you. E-mail us at customercare@copyright.com

Link zur Originalarbeit: https://doi.org/10.1016/j.scitotenv.2018.04.150

Die Originalarbeit ist unter den Bedingungen der Creative Commons Attribution-NonCommercial-No Derivatives Lizenz (CC BY NC ND) veröffentlicht.

Link zur Lizenz: http://creativecommons.org/licenses/by-nc-nd/4.0/

Es wurden keine Änderungen an der Abbildung vorgenommen.

7.5. Abbildung 7

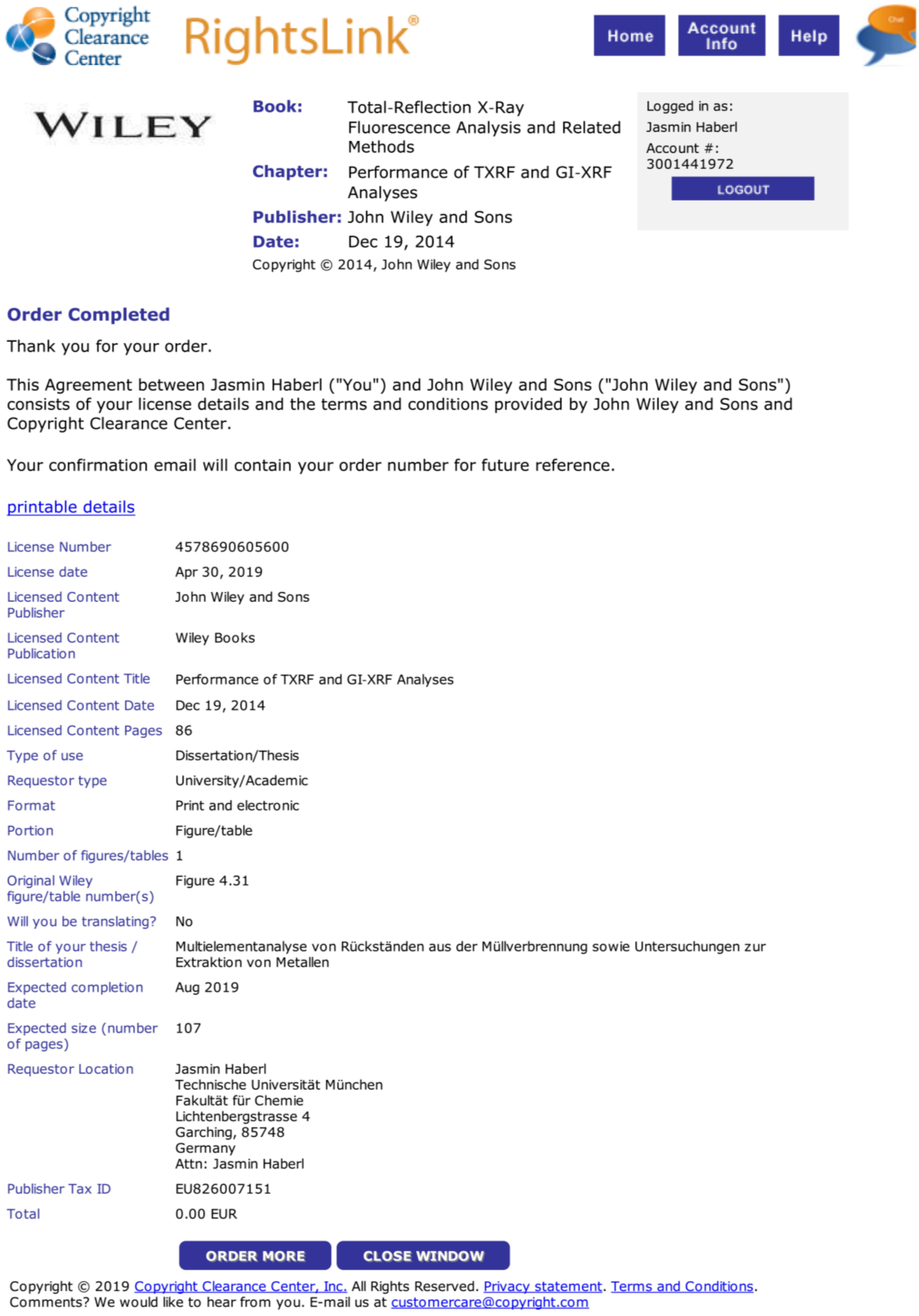

Book: Total-Reflection X-Ray Fluorescence Analysis and Related Methods

Chapter: Performance of TXRF and GI-XRF Analyses

Publisher: John Wiley and Sons

Date: Dec 19, 2014

Copyright © 2014, John Wiley and Sons

Logged in as:
Jasmin Haberl
Account #:
3001441972

Order Completed

Thank you for your order.

This Agreement between Jasmin Haberl ("You") and John Wiley and Sons ("John Wiley and Sons") consists of your license details and the terms and conditions provided by John Wiley and Sons and Copyright Clearance Center.

Your confirmation email will contain your order number for future reference.

printable details

License Number	4578690605600
License date	Apr 30, 2019
Licensed Content Publisher	John Wiley and Sons
Licensed Content Publication	Wiley Books
Licensed Content Title	Performance of TXRF and GI-XRF Analyses
Licensed Content Date	Dec 19, 2014
Licensed Content Pages	86
Type of use	Dissertation/Thesis
Requestor type	University/Academic
Format	Print and electronic
Portion	Figure/table
Number of figures/tables	1
Original Wiley figure/table number(s)	Figure 4.31
Will you be translating?	No
Title of your thesis / dissertation	Multielementanalyse von Rückständen aus der Müllverbrennung sowie Untersuchungen zur Extraktion von Metallen
Expected completion date	Aug 2019
Expected size (number of pages)	107
Requestor Location	Jasmin Haberl Technische Universität München Fakultät für Chemie Lichtenbergstrasse 4 Garching, 85748 Germany Attn: Jasmin Haberl
Publisher Tax ID	EU826007151
Total	0.00 EUR

8. Bibliographische Angaben und Abdruck der Publikationen

8.1. Publikation 1

Quantification of main and trace metal components in the fly ash of waste-to-energy plants located in Germany and Switzerland: An overview and comparison of concentration fluctuations within and between several plants with particular focus on valuable metals

Jasmin Haberl [a,*], Ralf Koralewska [b], Stefan Schlumberger [c], Michael Schuster [a]

[a] Division of Analytical Chemistry, Department of Chemistry, Technical University of Munich, 85748 Garching, Lichtenbergstrasse 4, Germany

[b] Martin GmbH für Umwelt- und Energietechnik, 80807 Munich, Leopoldstrasse 248, Germany

[c] Foundation Development Center for Sustainable Management of Recyclable Waste and Resources, ZAR, 8340 Hinwil, Wildbachstrasse 2, Switzerland

* Corresponding author.
E-Mail: jasmin.haberl@tum.de

Abdruck des Artikels mit allgemeiner Genehmigung von Elsevier (siehe Kapitel 7.1) aus

Waste Management, 2018, 75, 361–371

DOI: 10.1016/j.wasman.2018.02.015

Waste Management 75 (2018) 361–371

Contents lists available at ScienceDirect

Waste Management

journal homepage: www.elsevier.com/locate/wasman

Quantification of main and trace metal components in the fly ash of waste-to-energy plants located in Germany and Switzerland: An overview and comparison of concentration fluctuations within and between several plants with particular focus on valuable metals

Jasmin Haberl [a,*], Ralf Koralewska [b], Stefan Schlumberger [c], Michael Schuster [a]

[a] Division of Analytical Chemistry, Department of Chemistry, Technical University of Munich, 85748 Garching, Lichtenbergstrasse 4, Germany
[b] Martin GmbH für Umwelt- und Energietechnik, 80807 Munich, Leopoldstrasse 248, Germany
[c] Foundation Development Center for Sustainable Management of Recyclable Waste and Resources, ZAR, 8340 Hinwil, Wildbachstrasse 2, Switzerland

ARTICLE INFO

Article history:
Received 25 July 2017
Revised 1 February 2018
Accepted 8 February 2018
Available online 2 March 2018

Keywords:
Fly ash composition
Waste incineration
Multi-element analysis
Trace elements
Urban Mining

ABSTRACT

The elemental composition of fly ash from six waste-to-energy (WTE) plants in Germany and two WTE plants in Switzerland were analyzed. Samples were taken daily over a period of one month and mixed to a composite sample for each German plant. From two Swiss plants, two and three of these composite samples, respectively, were collected for different months in order to assess temporal differences between these months. In total, 61 elements, including rare earth elements, were analyzed using ICP-OES and ICP-MS. The analysis method was validated for 44 elements either by reference materials (BCR 176R and NIST 1633c) or analysis with both methods. Good recoveries, mostly ±10%, and high agreements between both methods were achieved. As long as no additives from flue gas cleaning were mixed with the fly ash, quite similar element contents were observed between all of the different incinerators. For most elements, the variations between the different months within the two Swiss plants were lower than differences between various plants. Especially main components show low variations between different months. To get a more detailed insight into temporal fluctuations within the mentioned Swiss plants, the concentrations of Zn, Pb, Cu, Cd, Sb, and Sn are presented over a period of three years (Jan. 2015 – Oct. 2017). The concentration profiles are based on weekly composite samples (consisting of daily taken samples) analyzed by the routine control of these plants using ED-XRF. The standard deviations of the average concentrations were around 20% over the three years for the regarded elements. The fluctuations were comparable at both plants. Due to the relatively low temporal concentration fluctuations observed within the plants, fly ash would be a continuous and constant source of secondary raw materials. Beside Zn, Pb, Cu, and Cd, which were already recovered on an industrial scale, Sb, Sn, and Bi also show a high potential as secondary raw material due to the high concentration of these elements in fly ash.

1. Introduction

Fly ash from grate-based waste-to-energy (WTE) plants has been the subject of many studies in the last few decades. Most of these studies address the toxic potential of this substance group, which results from its high contents of heavy metals and highly toxic organic compounds. In this context, e.g. the leaching behavior of harmful substances from fly ash into the environment has been extensively studied because landfilling is a common practice for the ultimate disposal of fly ash (Huang et al., 2007; Karlfeldt Fedje et al., 2010). Economic utilization is not found on a large scale, but a few possible applications, such as use in construction materials as an additive, are increasingly discussed (Ferreira et al., 2003; Lam et al., 2010).

At the Kebag WTE plant in Zuchwil, Switzerland, an industrial process for the recovery of Zn, Pb, Cu, and Cd from fly ash has been established, which was first described by Schlumberger et al. (2007). Within the now commercially offered Valuable Metal Recovery Process (FLUREC, BSH, Sursee, Switzerland), high-purity Zn (>99.995%) is recycled from fly ash in various separation stages. The FLUREC process also awaked interest from other countries,

---

[*] Corresponding author.
E-mail address: jasmin.haberl@tum.de (J. Haberl).

https://doi.org/10.1016/j.wasman.2018.02.015

Austria as an example (Fellner et al., 2015) to evaluate the potential and economic viability of Zn recovery from different waste incineration residues. Furthermore, Purgar et al. (2016) focused on the question of whether the FLUREC process is applicable to fly ashes from four WTE plants in Vienna. In addition to analysis of the contents of Zn, Pb, Cu, and Cd in fly ash from four WTE plants in Vienna from 2009 to 2012, the Zn flow was investigated by a material flow analysis.

Apart from this, little attention has been paid to precious metals that are also contained in fly ash. Morf et al. (2013) studied the resource potential of precious metals and rare earth elements in the waste input and their partitioning into recyclable fractions and residues at the Kezo WTE plant in Hinwil, Switzerland.

The utilization of fly ash as a source for secondary raw materials is not only desirable in terms of resource recovery, but also for environmental reasons. The volume of fly ash, and thus the volume of hazardous waste that needs to be stored in landfills, would be reduced and this reduces the amount of landfill space needed. Furthermore, the hazardousness is reduced by removal of heavy metals. Another aspect is the lower dependency on raw material imports because the main production of most critical raw materials, according to the European Commission (2017), is from China.

Data from the analytical composition of fly ash from WTE plants exists almost exclusively for toxic elements and some of the main components (Derie, 1996; Fermo et al., 1999; Hong et al., 2000a; Hong et al., 2000b; Li et al., 2004; Mangialardi et al., 1999; Wu and Ting, 2006). Very little information is available about the content of rare earth elements in fly ash. This insufficient and fragmentary data situation complicates a comprehensive evaluation and comparison of the true resource potential for fly ash from WTE plants. Especially for fly ash originating from German WTE plants, no data relating to detailed compositions is available. More detailed data on the fly ash from Swiss WTE plants can be found in a recent publication, which contains data for 18 metals from three different plants (Weibel et al., 2017).

In general, the representativeness of the analyzed fly ash sample is usually not specified for the entirety of fly ash arising from a specific WTE plant. Most of the available data is likely based on randomly acquired daily samples excluding deviations that might be caused by spatial and temporal fluctuations of the waste input streams, thereby affecting the elemental composition of the fly ash. To obtain representative results, the analyses in this work were carried out with composite samples consisting of daily taken samples. Furthermore, no detailed studies regarding temporal fluctuations in element concentrations in WTE plants are currently available. Under the aspect of a possible use of fly ash as secondary raw material, it is important to know, whether the respective elements arise in constant quantities and moreover whether the matrix is subject to strong fluctuations. Therefore, the concentrations of some selected elements (Zn, Pb, Cu, Cd, Sb, Sn) in the fly ash from two plants are presented over a period of three years.

Much of the available data was obtained several years ago; therefore, the data is now out of date. Combustion technologies and/or waste compositions may have changed over the years, which may result in changes to the elemental composition of the fly ash. Due to this fact, updated information is necessary to provide an overview of the current resource potential of fly ash obtained from current waste incineration practices.

2. Material and methods

For all of the experiments, ultrapure water (UPW), obtained from the Direct-Q® 5 UV (Merck Millipore, Darmstadt, Germany) water purification system, was used. For sample digestion and stabilization, the following acids were used: nitric acid (65% for analysis, Merck, Darmstadt, Germany), hydrochloric acid (30% suprapure, Merck, Darmstadt, Germany), hydrofluoric acid (47% ultrapure, VWR, Darmstadt, Germany), and boric acid (suprapure, Merck, Darmstadt, Germany). Nitric acid was purified by subboiling distillation prior to use. All solutions were prepared and stored in polypropylene centrifuge tubes. Digestion solutions were stored in the dark at 6 °C until measurement. The limit of quantitation (LOQ) was calculated according to DIN 32645 (calibration line method).

2.1. Sample collection

Fly ash was collected at six German and two Swiss grate-based WTE plants. All WTE plants were operated under normal combustion conditions. The anonymized WTE plants, sampling periods, daily sampling frequency, approximate waste composition, and further relevant information are listed in Table 1.

The flue gas cleaning processes and the combination of the flue gas cleaning components from the investigated WTE plants were different according to the technical requirements of each plant. From the Swiss WTE plants (A and B) and from plant C, fly ash samples were taken out of an intermediate storage silo that contained both boiler ash and ash sparated by an electrostatic precipitator (ESP). At plant C fabric filter ash was also part of the sampled mixture. At this plant coke and calcium hydroxide were added on the fabric filters whereby these substances also end up in the fabric filter ash. The fly ashes from plants D, E, and F were taken at the boiler end either at the ESP or the cyclone. Samples from plants G and H were taken downstream after a spray absorber injected additives, separated either by a fabric filter or a combination of cyclone and fabric filter. Therefore, the additives from the flue gas cleaning system were mixed with the fly ash at plants G and H. There were no additional mixtures with boiler ash or other residues.

At each plant, samples were taken one to four times during the working day over a period of one month and mixed to a composite sample that was stored in a sealed container. From each composite sample, a representative sample of 1–5 l was sent to the laboratory in plastic containers for analysis. At the two Swiss WTE plants, monthly composite samples were collected from several months (plant A: two months, plant B: three months) in order to obtain additional data about differences in elemental composition between these months.

2.2. Sample preparation

Triplicates of each composite sample were digested for subsequent analysis. Before taking samples out of the storage containers, the containers were rotated around different axis for several minutes so as to reverse possible sedimentation caused by differences in fly ash particle size and density. For each replicate, approximately 25 random aliquots (about 20 ml in total) were withdrawn from the composite fly ash sample and combined. The combined random aliquots were homogenized for 3 min at 350 rpm with a ball mill (PM 100, Retsch, Haan, Germany) using corundum grinding tools and a 50 ml grinding bowl. After drying on aluminum pans at 100 °C to constant weight (moisture analyzer HE53, Mettler-Toledo, Columbus, OH, USA), 300 mg of the homogenized subsample were digested as described below.

As the extractability of elements is different in different acids, a combination of nitric acid, hydrochloric acid, and hydrofluoric acid was used for a preferably complete digestion. Aluminosilicates form a major part of the fly ash matrix (Karstensen and Lund, 1989). Hydrofluoric acid is necessary to dissolve these aluminosilicates and elements trapped inside (Bogush et al., 2015). Chang et al. (2009) report significantly worse recovery rates for several elements (e.g. Al, Mg, Ba, Cr) for the BCR 176 reference material

Table 1
Overview of the fly ash samples (MSW = municipal solid waste, CW = commercial waste, SS = sewage sludge, SW = special waste).

WTE plant	Location of WTE plant	Sampling period: month/year	Daily sampling frequency	Waste composition	Remarks
A	Switzerland	3/2015 (A1) 7/2015 (A2)	Min. 3 Min. 3	48% MSW 50% CW 2% SS	Boiler + ESP ash
B	Switzerland	3/2015 (B1) 7/2015 (B2) 8/2015 (B3)	Min. 3 Min. 3 Min. 3	44% MSW 36% CW 10% SW 10% SS	Boiler + ESP ash
C	Germany	1/2015 – 2/2015	1	65% MSW 35% CW	Boiler + ESP + fabric filter ash
D	Germany	3/2016	3–4	70% MSW 30% CW	ESP ash
E	Germany	3/2016	3–4	75% MSW 25% CW	ESP ash
F	Germany	3/2016	3–4	99% MSW 1% CW	Cyclone ash
G	Germany	3/2016	3–4	No information	Fabric filter ash, additive: lime milk (spray absorber)
H	Germany	3/2016	3–4	No information	Cyclone + fabric filter ash, additives: $NaHCO_3$ and activated carbon (spray absorber)

if only nitric and hydrochloride acid are used. Instead of hydrochloric acid, perchloric acid is often used in combination with nitric and hydrofluoric acid (Chang et al., 2009; Li et al., 2004; Pan et al., 2013). Hydrochloric acid was used instead, because it is sufficient to digest the samples (apart from soot particles and formation of insoluble fluorides by hydrofluoric acid) and because hydrochloric acid is safer to handle. The microwave-assisted pressure digestion (Ethos.lab, MLS, Leutkirch, Germany) was conducted in two steps using PTFE vessels. The applied temperature programs for both steps are shown in Fig. 1. In the first step, 8 ml nitric acid, 1 ml hydrochloric acid, and 1.5 ml hydrofluoric acid were added to the 300 mg sample. In addition, a digestion blank was prepared. The mixtures were heated according to the schedule found in Fig. 1 (step 1). Subsequently, the mixtures were allowed to cool to room temperature. In the second step, 9 ml saturated boric acid solution was added and the mixtures were heated again (Fig. 1, step 2). Boric acid neutralizes the excess hydrofluoric acid to form fluoroboric acid, which does not attack glass.

After cooling to room temperature, the digestion solutions were topped up with UPW to a final volume of 50 ml. Minimal residues were removed by filtration through a syringe filter (pore size 0.45 µm, polyethersulfone membrane, VWR, Darmstadt, Germany). The digestion residue was characterized as described in Section 2.3.

The reference materials BCR 176R (fly ash collected in the electrostatic filters of a city waste incineration plant) and NIST 1633c (coal fly ash) were used for method validation and were subjected to the same digestion procedure as the authentic test samples.

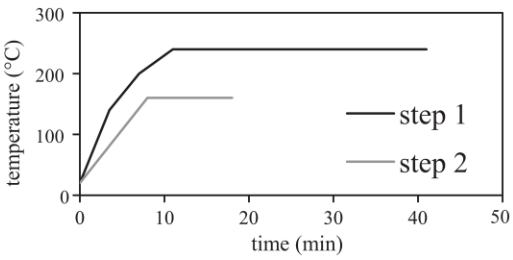

Fig. 1. Temperature program for the microwave-assisted pressure digestion (step 1) and the reaction with boric acid (step 2).

2.3. Characterization of the digestion residues

The digestion residues of two ashes (two different WTE plants) were investigated by SEM/EDX. For this purpose, three digestion solutions (including the residues) of each ash were combined. The residue was then isolated by centrifugation for 5 min at 6000 rpm (Z 206A, Hermle, Wehingen, Germany) and removing the supernatant. The residue was washed three times with 10–20 ml UPW and dried overnight in a drying cabinet at 40 °C. After sputtering with gold, the samples were analyzed by SEM/EDX (JSM-5900LV, Jeol, Akishima, Japan).

2.4. Analytical measurements

2.4.1. ICP-OES

ICP-OES measurements (iCAP 7600 Duo, Thermo Fisher Scientific, Waltham, MA, USA) were performed on the following elements: Li, Na, Mg, Al, Si, K, Ca, Ti, V, Cr, Mn, Fe, Co, Ni, Cu, Zn, As, Sr, Zr, Mo, Ag, Cd, Sn, Sb, Ba, and Pb. A final concentration of 1 mg/l Europium (Eu_2O_3 in 5% nitric acid, Alfa Aesar, Karlsruhe, Germany) was used as the internal standard and analyte signals were corrected by the intensity of the emission line at 381.967 nm (diffraction order 88).

For calibration, ICP multi-element standard solutions IV (23 elements in diluted nitric acid, Merck Millipore, Darmstadt, Germany), XVI (21 elements in diluted nitric acid, Merck Millipore, Darmstadt, Germany), and XII (8 elements in hydrochloric acid/hydrofluoric acid/ammonium hydroxide, Merck Millipore, Darmstadt, Germany) with added Sn single element standard in equal concentration ($SnCl_4$ in 2 mol/l hydrochloric acid, Merck, Darmstadt, Germany) were used.

The digestion solutions were measured at two different dilutions (1:2 in UPW and 1:100 in 3% nitric acid) so that the concentrations of all measured elements would lie within the calibration range. For each of the two digestion dilutions, separate calibration solutions were prepared, which were adjusted to the respective dilution as described in the following.

For the 1:2 in UPW diluted digestion solutions, the calibration solutions were prepared in 6% nitric acid (standard solutions IV and XVI) and 6% hydrochloric acid (standard solution XII + Sn), respectively. Preliminary tests revealed that the internal standard recovery is significantly different in the calibration solutions compared to the 1:2 diluted digestion solutions. Therefore, a final con-

Table 2
Measured concentrations (triplicate average, single measurement in the case of Se), relative standard deviations (RSD) and recoveries for the reference materials BCR 176R and NIST 1633c. For some elements, both the ICP-MS and ICP-OES (for several emission lines if possible) results are given. Concentrations that are below the LOQ are indicated as "<LOQ". The method in bold for each element was ultimately used for real sample measurements.

		Emission line (wavelength in nm and diffraction order) or mass	BCR 176R			NIST 1633c		
			Concentration (mg/kg)	RSD (%)	Recovery (%)	Concentration (mg/kg)	RSD (%)	Recovery (%)
Li	**MS**	**7**	46.1	1.0		209	2.8	
	OES	670.784 (50)	44.7	1.3		196	2.6	
Be	**MS**	**9**	1.36	5.9		17.1	0.6	107
Na	**OES**	**589.592 (57)**	32,457	0.8	93	1584	2.7	93
Mg	OES	279.553 (121)	16,020	0.5		3249	6.9	65
	OES	**280.270 (120)**	18,008	0.5		4218	5.8	85
	OES	285.213 (118)	16,241	0.3		3624	6.1	73
Al	**OES**	**396.152 (85)**	57,364	0.3		102,243	4.8	77
	OES	394.401 (85)	57,458	0.3		101,699	4.7	77
Si	**OES**	**251.611 (134)**	85,670	1.4		169,358	1.8	80
	OES	212.412 (459)	82,796	1.6		165,724	2.7	78
	OES	288.158 (117)	85,212	1.3		169,659	1.9	80
	OES	221.667 (452)	83,276	1.5		166,114	2.5	78
	OES	250.690 (135)	83,425	1.2		165,222	2.0	78
K	**OES**	**766.490 (44)**	34,325	1.6		15,695	2.5	89
	OES	769.896 (44)	32,384	0.5		14,606	2.6	82
Ca	**OES**	**422.673 (80)**	183,230	1.2		11,828	2.6	87
	OES	184.006 (483)	198,112	0.7		15,435	2.2	113
	OES	315.887 (107)	191,153	0.2		14,539	2.5	107
Sc	**MS**	**45**	3.94	3.9	135	33.4	2.6	89
Ti	**OES**	**337.280 (100)**	11,903	0.6		6557	0.5	91
	OES	338.376 (100)	12,110	0.1		6616	0.5	91
	OES	308.802 (109)	11,937	0.5		6539	1.2	90
	OES	323.904 (104)	11,725	0.8		6345	1.0	88
	OES	334.904 (101)	11,979	1.1		6528	1.1	90
V	**MS**	**51**	36.9	1.2	105	293	0.6	102
	OES	292.402 (115)	38.9	1.6	111	265	1.2	93
	OES	292.464 (115)	42.4	2.3	121	273	1.0	95
	OES	290.882 (116)	36.8	1.1	105	282	0.5	99
Cr	**MS**	**52**	785	8.8	97	242	2.3	94
	OES	267.716 (126)	747	6.8	92	229	2.5	89
	OES	284.325 (119)	744	7.1	92	237	1.9	92
	OES	205.560 (464)	750	7.7	93	221	3.1	86
Mn	MS	55	759	0.2	104	241	1.2	101
	OES	257.610 (131)	756	2.3	104	225	1.0	94
	OES	**293.930 (115)**	733	2.2	100	238	0.8	99
	OES	191.510 (476)	727	3.1	100	221	2.1	92
Fe	**OES**	**259.940 (130)**	13,874	0.5	106	107,564	1.1	
	OES	238.204 (142)	14,149	0.7	108	110,517	0.9	
	OES	259.837 (130)	14,710	1.2	112	113,352	1.1	
	OES	261.187 (129)	14,708	1.0	112	113,650	1.1	
Co	**MS**	**59**	28.6	0.6	107	41.7	1.3	97
	OES	230.786 (446)	23.9	2.5	90	35.4	2.4	82
Ni	**MS**	**60**	119	1.9	102	136	0.7	103
	OES	231.604 (446)	112	2.1	96	124	2.1	94
	OES	216.556 (456)	113	2.5	96	139	2.1	105
Cu	**OES**	**324.754 (104)**	1110	1.9	106	176	1.0	101
	OES	327.396 (103)	1094	1.8	104	167	0.6	96
	OES	224.700 (450)	999	1.6	95	156	2.2	90
Rb	**MS**	**85**	105	1.3	103	86.4	11	74
Sr	**MS**	**88**	472	0.4		906	2.9	101
	OES	407.771 (83)	463	1.0		884	2.2	98
	OES	216.596 (456)	451	0.1		848	3.8	94
	OES	215.284 (457)	438	0.1		858	3.6	95
Y	**MS**	**89**	14.5	2.4		81.6	9.2	
Zr	**MS**	**90**	165	0.4		190	0.4	
	OES	339.198 (99)	140	0.9		166	0.7	
	OES	343.823 (98)	143	1.0		167	0.8	
	OES	349.621 (96)	146	0.7		172	1.1	
Nb	**MS**	**93**	14.6	2.0		25.7	0.5	
Mo	**MS**	**95**	38.2	2.4		28.9	1.7	
	OES	202.030 (467)	32.9	0.9		<27.4		
	OES	204.598 (465)	37.1	1.2		<33.1		
	OES	203.844 (465)	33.5	1.4		<23.6		
Ru	**MS**	**101**	<0.18			<0.18		
Rh	**MS**	**103**	0.13	8.1		<0.13		
Pd	**MS**	**105**	<0.38			<0.38		
Ag	MS	107	34.4	0.9	104	<3.29		
	OES	**328.068 (103)**	31.7	1.2	96	<24.8		
Cd	**MS**	**111**	222	0.7	98	<9.24		
	OES	228.802 (447)	231	0.9	102	<23.6		
	OES	226.502 (449)	213	2.6	94	<18.1		
	OES	214.438 (457)	213	3.6	94	<31.3		
In	**MS**	**115**	<0.35			<0.35		
Sn	OES	189.989 (477)	1057	3.0		<58.5		
	OES	**189.989 (478)**	1062	3.0		<52.0		
Sb	OES	206.833 (463)	897	0.8	106	<20.0		
	OES	**217.581 (455)**	877	1.1	103	<14.6		
Ba	**OES**	**455.403 (74)**	5170	0.7	111	1026	1.0	91
	OES	233.527 (445)	5032	0.4	108	993	3.1	88
La	**MS**	**139**	31.8	0.3	105	65.7	9.2	75
Ce	**MS**	**140**	50.7	0.8	106	154	8.6	86
Pr	**MS**	**141**	5.57	2.0		18.9	7.8	
Nd	**MS**	**146**	18.9	1.5		76.5	7.5	88
Sm	**MS**	**147**	3.29	0.5		17.3	6.5	91
Eu	**MS**	**153**	1.11	0.6	128	4.00	7.7	86
Gd	**MS**	**157**	2.99	2.9		18.1	6.7	
Tb	**MS**	**159**	0.56	1.4		2.79	6.6	89
Dy	**MS**	**163**	1.88	2.1		16.7	6.1	89
Ho	**MS**	**165**	0.37	2.4		3.29	6.2	
Er	**MS**	**166**	0.96	2.2		9.07	6.4	
Tm	**MS**	**169**	<0.16			1.26	5.7	
Yb	**MS**	**172**	0.81	1.6		7.97	5.3	103
Lu	**MS**	**175**	<0.22			1.15	5.4	87
Hf	**MS**	**178**	3.89	2.4	80	5.44	2.1	91
Ta	**MS**	**181**	1.99	5.7	99	1.61	0.4	102
W	**MS**	**182**	29.8	1.5	105	7.06	1.2	
Re	**MS**	**185**	<0.10			<0.10		

Zn	**OES**	**213.856 (458)**	17,971	0.7	107	<2616			Ir	**MS**	**193**	<0.15			<0.15		
	OES	202.548 (466)	19,045	1.3	113	<2361			Pt	**MS**	**195**	<0.15			<0.15		
	OES	206.200 (464)	19,957	1.6	119	<1152			Au	**MS**	**197**	0.73	1.8	121	<0.56		
Ga	**MS**	**71**	24.0	1.0		75.7	3.1	138	Tl	**MS**	**205**	1.34	1.1	102	6.13	1.1	
Ge	**MS**	**72**	5.85	4.4		62.3	1.0		Pb	**OES**	**182.205 (485)**	4566	1.5	91	<163		
As	**OES**	**189.042 (478)**	52.4	0.3	97	166	1.3	89		OES	168.215 (501)	4934	3.6	99	<132		
Se	**MS**	**78**	18.3	–	100	16.9	–	122	Bi	**MS**	**209**	69.1	3.6		<5.88		

centration of 1 g/l Ca was added to all calibration solutions, which were prepared for the 1:2 diluted digestion solutions, in order to increase the salt content. For this purpose, a corresponding quantity of $Ca(NO_3)_2$ solution (Ca single element standard in 1 mol/l nitric acid, Bernd Kraft, Duisburg, Germany) was added to all IV and XVI calibration solutions and a solution of $CaCl_2$ (for analysis, Merck, Darmstadt, Germany) in UPW to all XII + Sn calibration solutions. Thus, a plasma loading that is comparable to the 1:2 diluted digestion solutions was obtained, leading to a stable internal standard recovery during the measurement. Ca was chosen for the matrix adaptation because it is the main component in fly ash.

For the 1:100 in 3% nitric acid diluted digestion solutions, the calibration solutions were prepared in 3% nitric acid (standard solution IV) and 3% hydrochloric acid (standard solution XII + Sn), respectively. The internal standard recovery in the calibration solutions was comparable with the 1:100 diluted digestion solutions. Therefore, no matrix adaptation was necessary.

Except alkali and alkaline earth metals, which were measured at a radial plasma observation, all elements were measured at an axial plasma observation.

2.4.2. ICP-MS

ICP-MS measurements (Agilent 7900, Santa Clara, CA, USA) were performed for the following elements: Li, Be, Sc, V, Cr, Mn, Co, Ni, Ga, Ge, Se, Rb, Sr, Y, Zr, Nb, Mo, Ru, Rh, Pd, Ag, Cd, In, La, Ce, Pr, Nd, Sm, Eu, Gd, Tb, Dy, Ho, Er, Tm, Yb, Lu, Hf, Ta, W, Re, Ir, Pt, Au, Tl, and Bi.

For calibration, three multi-element standard solutions obtained from Sigma–Aldrich (St. Louis, MO, USA) were used: Periodic Table Mix 1 for ICP (33 elements in 10% nitric acid), Periodic Table Mix 2 for ICP (17 elements in 5% hydrochloric acid and 1% hydrofluoric acid) and Periodic Table Mix 3 for ICP (16 elements in 5% nitric acid). The digestion solutions were measured at two different dilutions (1:100 in 3% nitric acid and 1:100 in 3% hydrochloric acid).

The nitric acid-diluted digestion solutions were calibrated with Periodic Table Mix 1 and 3. Calibration solutions were prepared in 3% nitric acid. ^{101}Ru (Aldrich Chemical Company, Milwaukee, WIS, USA) and ^{193}Ir (Aldrich Chemical Company, Milwaukee, WIS, USA) were used as internal standards.

The hydrochloric acid-diluted digestion solutions were calibrated with Periodic Table Mix 2. Calibration solutions were prepared in 3% hydrochloric acid. ^{153}Eu (Eu_2O_3 in 5% nitric acid, Alfa Aesar, Karlsruhe, Germany) was used as internal standard.

All elements, except for Li and Be, were measured in helium collision mode to avoid polyatomic interferences. Li and Be were not measured in helium collision mode because these light elements experience higher signal loss through helium than other elements and because no relevant polyatomic interferences exist for Li and Be.

Se was determined by standard addition, because a significant overdetermination due to interferences was observed with external calibration methods (219% recovery for reference material BCR 176R and 312% recovery for reference material NIST 1633c). For standard additions, the ICP multi-element standard solution XVI (21 elements in diluted nitric acid, Merck Millipore, Darmstadt, Germany) was used. Solutions were prepared in 3% HNO_3. ^{101}Ru (Aldrich Chemical Company, Milwaukee, WIS, USA) was used as internal standard. Only one of the three digestion solutions was analyzed by standard addition for each fly ash sample.

Due to isobaric interferences from the ^{115}Sn isotope, ^{115}In was determined by application of a mathematical correction equation. For this purpose, ^{118}Sn was measured in order to indirectly determine the amount of overlapping ^{115}Sn using natural abundance data. The overlapping amount of ^{115}Sn can be subtracted and the equation for In determination is as follows (I = signal intensity):

$$I(^{115}\mathrm{In}) = I(m/z\ 115) - \left[I(^{118}\mathrm{Sn}) \frac{\text{natural abundance of } ^{115}\mathrm{Sn}}{\text{natural abundance of } ^{118}\mathrm{Sn}} \right]$$

2.5. Routine monitoring of Zn, Pb, Cu, Cd, Sb, and Sn at plants A and B

The measurements were conducted by the analytical routine control of plants A and B. The data from Jan. 2015 to Oct. 2017 was kindly provided for this publication. Samples were taken daily and homogenized to weekly composite samples. These composite samples were pressed into pellets and analyzed by ED-XRF (Spectro, Xepos, Kleve, Germany) with matrix adjusted calibration and helium purge.

3. Results and discussion

3.1. Chemical composition of the digestion residues

A small amount of residue remained in the digestion solutions of all samples consisting of colorless crystals and black particles in some cases. SEM/EDX analysis revealed that the residues almost exclusively consisted of F, Ca, Mg, and Al. This indicates that insoluble fluorides were formed. This is frequently described in the literature for these elements if hydrofluoric acid is used for digestion (Croudace, 1981; Karstensen and Lund, 1989). Therefore, the colorless crystals were not an insoluble part of the sample, but a precipitate. Because only elements in comparatively high concentrations were affected, the marginal precipitate was neglected. The black particles were assumed to be soot or graphite.

3.2. Method validation

Table 2 shows the results for the reference materials BCR 176R and NIST 1633c. All listed elements were validated either by reference materials or by analysis with two independent methods, except for the elements: Ge, Y, Nb, Ru, Rh, Pd, In, Sn, Pr, Gd, Ho, Er, Tm, Re, Ir, Pt, and Bi. For these elements either no reference values are available or only one of the applied analytical methods is suitable to analyze these elements e.g. due to too low concentrations. Nevertheless, the concentrations of these elements in the reference materials are listed for completeness.

Due to the presence of a large number of elements at high concentrations, many emission lines in ICP-OES were affected by interference. In Table 2, several suited emission lines are listed as far as possible. The results on different emission lines do not differ much for the respective elements; therefore, significant interference on single lines can be excluded. This list of validated emission lines provides a starting point for future analyses and method developments in other laboratories.

Good recoveries of ±10% were achieved for most elements and the data obtained from ICP-MS and ICP-OES shows a high degree of agreement. It must be considered that the coal fly ash reference material NIST 1633c can only be compared with fly ash from waste combustion to a limited extent. The underestimation of some elements (especially Mg, Al and some rare earth elements) in the digestion solutions of the NIST 1633c reference material is probably due to the formation of insoluble fluorides and coprecipitated elements.

3.3. Concentrations of main and trace elements in fly ash samples from various WTE plants

The measured element concentrations in the fly ash samples are shown in Fig. 2 (main components) and Fig. 3 (trace components) in decreasing concentrations. Rare earth elements are shown in Fig. 4 separately. For elements that were measured with both ICP-OES and ICP-MS, only the results of one method is given (see

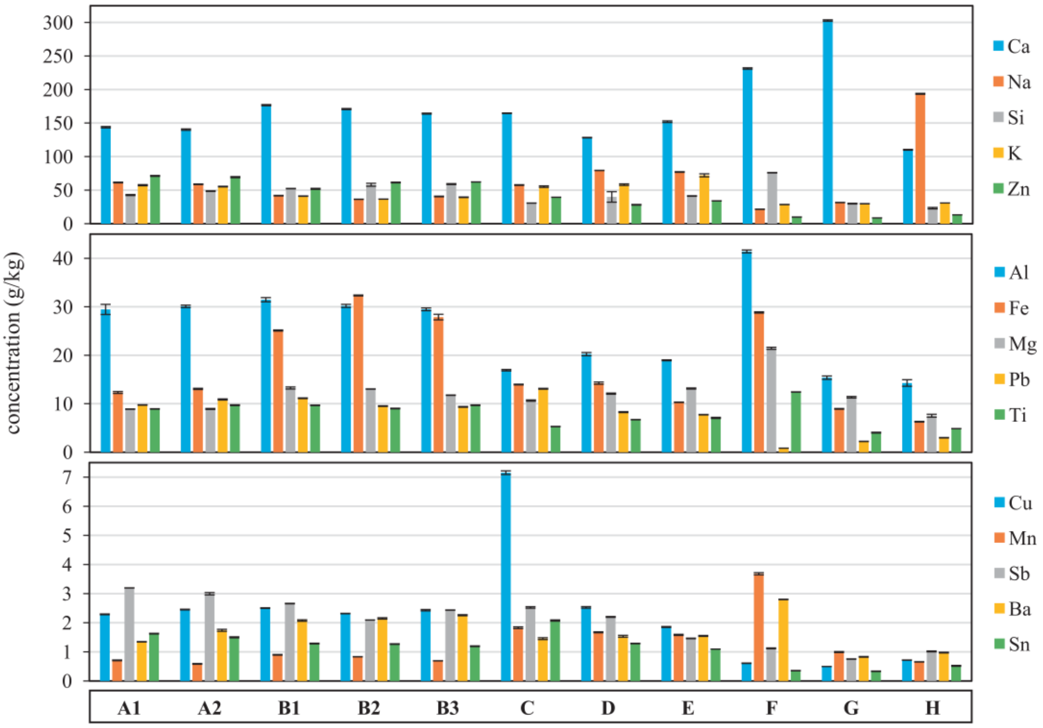

Fig. 2. Concentrations of the main components (triplicate average) in the fly ash samples A–H. The error bars represent the standard deviation of the triplicates.

Fig. 3. Concentrations of trace components (triplicate average, single measurement in the case of Se) except rare earth elements in the fly ash samples A–H. Concentrations that are below the LOQ are not shown in the diagram. The error bars represent the standard deviation of the triplicates.

Table 2) as the differences are below 10% in nearly all cases between both methods. ICP-MS results were preferred for low concentrations.

Ru, Pd, Re, and Ir were always found below the LOQ with the conducted analytical procedure (Ru, Re, and Ir < 0.2 mg/kg, Pd < 0.4 mg/kg). Be, Se, Rh, In, Pt, Au, and the rare earth elements Sm, Eu, Tb, Ho, Tm, and Lu were observed above the LOQ in some of the samples (LOQ values in mg/kg: Be 0.9, Se 9, Rh 0.1, In 1, Pt, Ho, Tm, and Lu 0.2, Au 0.6, Sm 0.7, Eu 0.5, Tb 0.4).

The moisture contents of the fly ash samples were relatively low at 0.4–1.3%. Due to the high aluminum content in all fly ash samples, contaminations with aluminum through abrasion from the grinding tools were negligible. Fly ash is a fine-grained and homogenous material. A short milling process was sufficient to ensure a representative measurement and most elements could be determined with high accuracy. Apart from a few exceptions, the RSD values were below 5%. Higher deviations of mostly 10–20% were observed in all samples only for Ta. Due to sufficient high signal intensities during the measurements, these consistently high RSD values are not related to low concentrations. The same applies for Cr, which shows higher RSD values compared to other high concentrated elements. Probably elements with higher RSD values are present as unevenly distributed particles in the fly ash and show therefore different concentrations in the three milled replicates. It might also be possible that the particles cannot be crushed by the applied milling process, so they remain inhomogeneous distributed within the milled replicates.

Despite the high accuracy of the measurements, it must be considered that only a small portion of the entire amount of fly ash arising from a WTE plant, which amounts to several thousand tons

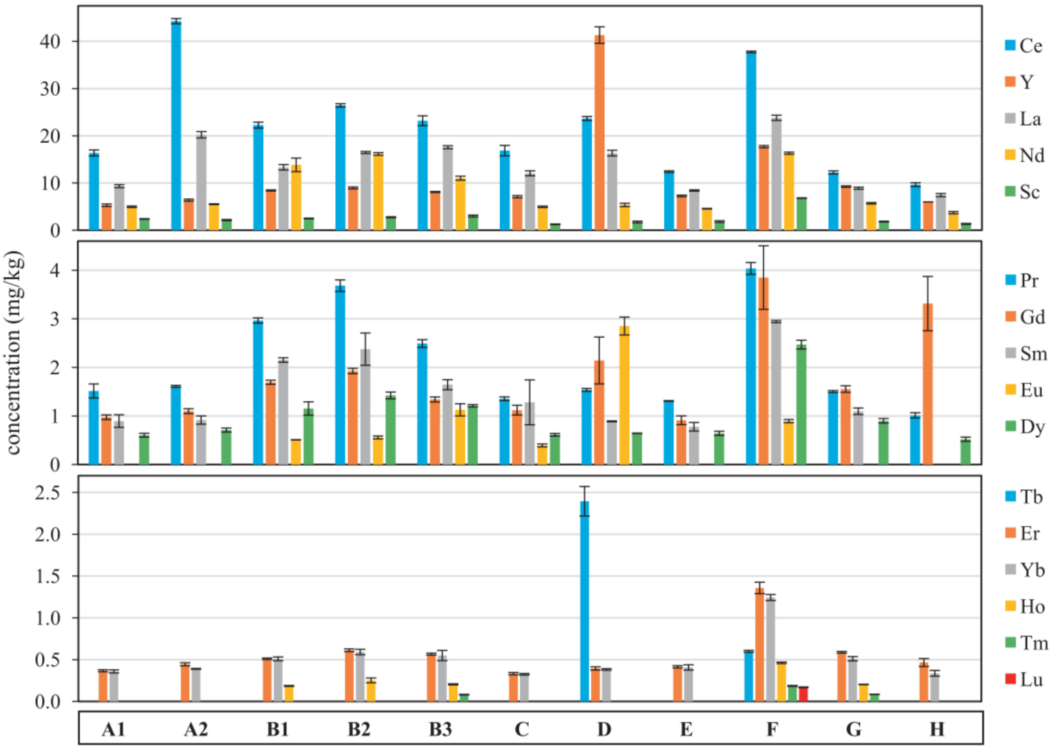

Fig. 4. Concentrations of rare earth elements (triplicate average) in the fly ash samples A–H. Concentrations that are below the LOQ are not shown in the diagram. The error bars represent the standard deviation of the triplicates.

per year, can be taken for analysis. This complicates extrapolation of element concentrations for an entire WTE plant. Nevertheless, by taking composite samples over one month, we attempted to diminish this issue.

Fly ash G and H contained additives from the flue gas cleaning system (G: lime milk, H: $NaHCO_3$ and activated carbon). Therefore, the calcium content in G and the sodium content in H were significantly higher compared to the other ashes. The content of other elements was lower due to dilution caused by the additives. Therefore, these two ashes were only comparable with the other ashes to a limited extent. From the point of view of precious metal recovery, mixing with additives should be avoided to maintain the potential accumulation of these metals.

In general, the elemental composition of fly ash is influenced by many parameters, such as waste composition, combustion temperature and time, redox conditions, and the content of chlorine and reaction partners during combustion (Belevi and Moench, 2000). However, as the data shows, there were no large differences between the WTE plants for most elements disregarding the ashes containing additives. At 13–23%, Ca was the main component of fly ash, followed by the elements Na, Si, K, Zn, Al, and Fe, which all show concentrations between 1% and 8%. All other investigated elements were found at approximately 1% and lower. Nearly all of the elements were in the same order of magnitude in various samples. Only fly ash F showed larger differences in elemental composition compared to the ashes A–E. This is probably because the waste input almost exclusively consisted of municipal solid waste (99%) and only a negligible percentage of commercial waste (1%). The amount of commercial waste is significantly higher in the other WTE plants. Due to the request of the plant operators to keep the plants anonymous, the results are not correlated to operational set-up details to prevent that conclusions about the plants can be drawn.

The Swiss fly ash data (plants A and B) allows a comparison of temporal variations between different months in one WTE plant along with variations between different WTE plants. Most of the elements in higher concentrations show low temporal differences of <10%. Fluctuations in concentration between different months are only caused by changes in waste composition if no changes in WTE plant operations are done. This was the case at all plants during the considered sampling periods. On the whole, temporal fluctuations tend to be lower than spatial differences.

3.4. Temporal fluctuations of Zn, Pb, Cu, Cd, Sb, and Sn within plants A and B

The comparison of two and three months, respectively, in Section 3.3 gives only a rough overview of the temporal concentration fluctuations in fly ash. Therefore, variations in concentrations over time are examined in more detail for Zn, Pb, Cu, Cd, Sb, and Sn as these are some of the most promising valuable metals in fly ash. In Fig. 5, the concentration profiles of these elements are shown from Jan. 2015 to Oct. 2017 for plants A and B, which routinely monitor these elements among others.

The average concentrations and the corresponding standard deviations over the considered time period are listed in Table 3. Standard deviations around 20% are observed for all regarded elements. The fluctuations of the individual elements are very similar at both plants. At some time points, a correlation between both plants is visible. During 2016 for example, an increase of Zn can be observed at both plants. In spring 2015, the Cu content increased temporary for a few weeks. The fluctuations are primarily caused by changes in waste composition, which is similar at both plants. The concentrations of all regarded elements remain at a very constant level over time. No significant increase or

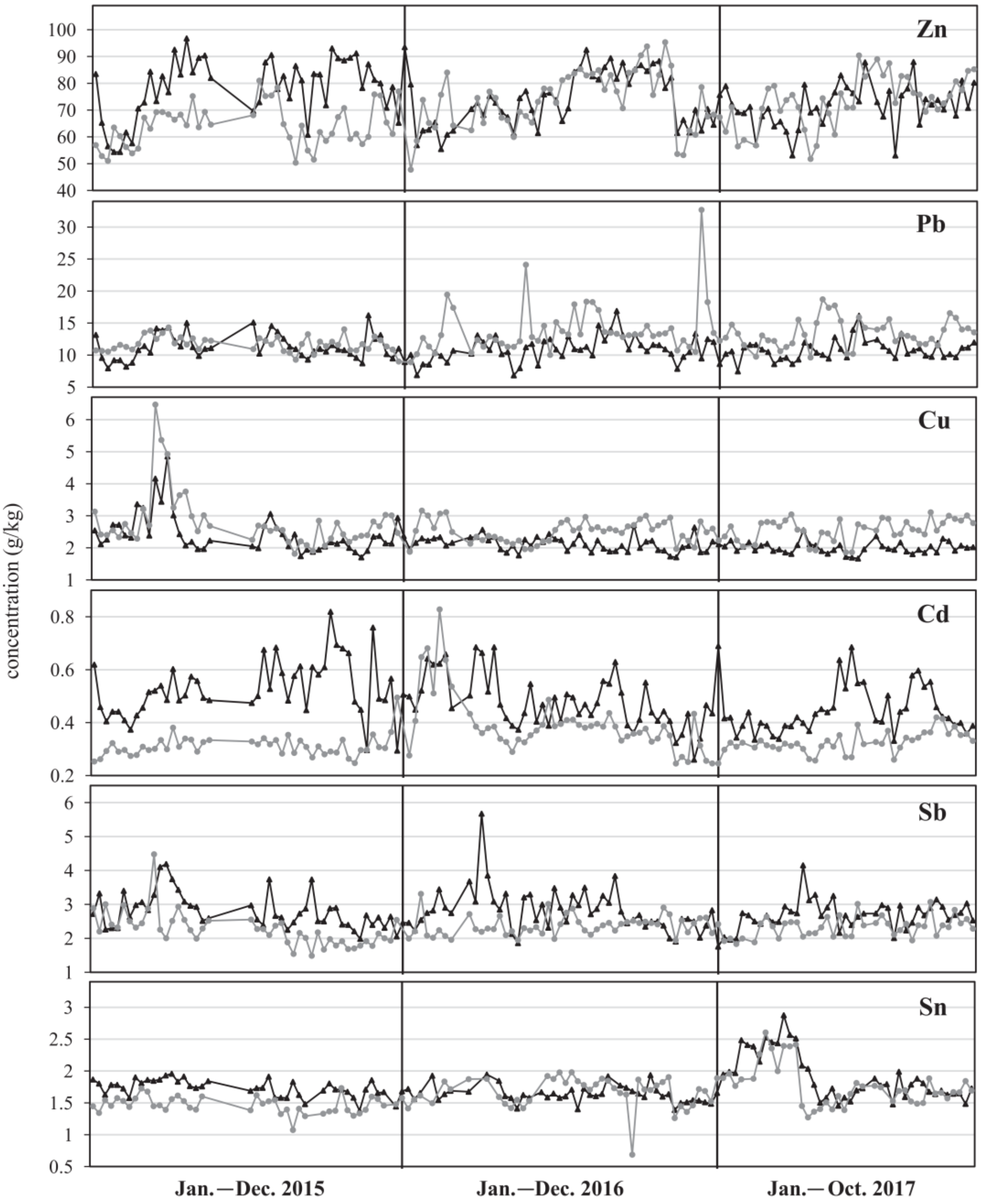

Fig. 5. Concentrations of Zn, Pb, Cu, Cd, Sb, and Sn in fly ash from plants A (black graph) and B (grey graph) from Jan. 2015 to Oct. 2017 based on weekly composite samples.

Table 3
Average concentrations and corresponding standard deviations in g/kg for Zn, Pb, Cu, Cd, Sb, and Sn in fly ash from plants A and B from Jan. 2015 to Oct. 2017.

	Plant A	Plan B
Zn	75 ± 10	70 ± 10
Pb	11 ± 2	13 ± 3
Cu	2.2 ± 0.4	2.6 ± 0.6
Cd	0.5 ± 0.1	0.3 ± 0.1
Sb	2.8 ± 0.5	2.3 ± 0.4
Sn	1.8 ± 0.3	1.6 ± 0.3

decrease in concentration over the years is observed. Consequently, these valuable metals arise in constant quantities which is advantageous with regard to the use of fly ash as secondary raw material. The average concentrations in Table 3 match very well with the results obtained for the few monthly composite samples described in Section 3.3.

3.5. Evaluation of the resource potentials of Sb, Sn, and Bi in Germany

In 2013, 68 waste incineration plants were in operation in Germany with an overall throughput of about 19 million t/a

(Löschau, 2014). The amount of the remaining fly ash is usually stated with 2–4% of the waste input (Bavarian State Ministry of the Environment and Consumer Protection, 2002; Jung et al., 2004). Morf et al. (2013) report a generation rate of 2.2% for a Swiss WTE plant. As no detailed information is available on the total amount of fly ash arising in Germany every year, this amount can be calculated at approximately 380,000–760,000 t/a (assuming a generation rate of 2–4%). In the following, we want to take a closer look at the resource potentials of Sb, Sn, and Bi by comparing the annual consumption with the estimated annual material flow of these elements.

The European Commission classified Sb, which shows high concentrations up to 3 g/kg in the fly ash samples, as one of the most critical raw materials in the EU regarding supply risk and economic importance (European Commission, 2017). The relatively high amount of Sb in fly ash probably originates from combusted polymers containing Sb_2O_3 as a flame retardant synergist, which is one of the main applications of Sb (German Mineral Resources Agency, 2013; Nakamura et al., 1996; Wiel and Levchik, 2016). Sb in Germany is completely imported (German Mineral Resources Agency, 2013). According to the German Mineral Resources Agency (2013), Sb was imported in following quantities and commodities in 2011: 8 t ore, 447 t raw metal, 6954 t trioxide, and 28,835 t antimony-containing lead, containing 1–5% Sb. Taking the different Sb content into account, this corresponds to a consumption of about 7000 t Sb in 2011 neglecting Sb from recycling. Assuming a concentration of about 2 g/kg Sb in the fly ash of all 68 German WTE plants, this sums up to 760–1520 to/a Sb, which is about 11–22% of the annual consumption of Sb in Germany.

Sn is not jet classified as critical, but due to the economic importance and relatively high concentration up to 2 g/kg in the fly ash samples nevertheless interesting. According to the German Mineral Resources Agency (2014), Germany is completely dependent on import and recycling of Sn and the consumption was 21,100 t in 2012. Analogous to Sb, the Sn content in German fly ash can be estimated to 380–760 t/a assuming a concentration of about 1 g/kg. This corresponds to 2–4% of the annual consumption of Sn in Germany.

Bi, which was found in this study up to 0.5 g/kg, was newly added to the list of critical raw materials in the EU in 2017 (European Commission, 2017). Morf et al. (2013) report a significant accumulation of Bi in fly ash compared to the bottom ash and propose fly ash as an interesting source to recover this metal. According to the German Mineral Resources Agency (2015), the consumption of Bi in recent years was about 1000 t/a in Germany. The Bi content in German fly ash can be estimated to 38–76 t/a assuming a concentration of about 0.1 g/kg. This corresponds to 4–8% of the annual consumption of Bi in Germany.

Although the numbers are only roughly estimated, they indicate that the quantities are not negligible, especially the high amount of Sb. Jung et al. (2004) also report high amounts of Sb, Sn, and Bi getting lost in incineration residues (including bottom ashes) in Japan compared to the annual consumption of these metals. They found 132% Sb, 1% Sn and 31% Bi of the annual consumption of these metals in incineration residues. Fly ash can therefore be considered as a possible secondary raw material source for these elements, in particular for Sb.

4. Conclusions and outlook

The element concentrations vary only slightly between various plants when the flue gas cleaning system is similar. Additives during flue gas cleaning lead to a significant reduction of the precious metal enrichment in the originally pure fly ash, which should therefore be collected separately. As concentration fluctuations within single plants are relatively low even over long periods, fly ash would be a continuous and constant source of valuable metals. The contained valuable metals sum up to significant amounts considering the high quantity of fly ash arising from all plants every year. Fly ash could be a promising source of secondary raw material especially for Sb, Sn, and Bi beside of Zn, Pb, Cu, and Cd.

Currently, 27 raw materials are classified as critical by the European Commission (2017). Apart from Sb and Bi, further metals like for example Co, Ga, Ge, In, Mg, Nb, W, and rare earth elements are classified as critical. These elements are also contained in fly ash in notable concentrations. When concentrations in primary deposits reach low levels, or when these are depleted, fly ash could become a worthwhile and important raw material source.

The next step would be the development of selective recovery processes. Fly ash samples from this work will be used to study the solubility behavior for a large number of elements by applying a sequential extraction procedure that will help to develop an efficient separation technology.

Acknowledgement

This work was funded in part by the German Federal Ministry of Education and Research (BMBF) [grant number 033R140]. The authors thank the plant operators for preparation and providing the fly ash composite samples and the ED-XRF data.

References

Bavarian State Ministry of the Environment and Consumer Protection, 2002. Müllverbrennung: Die thermische Behandlung von Abfällen, München.

Belevi, H., Moench, H., 2000. Factors determining the element behavior in municipal solid waste incinerators. 1 Field studies. Environ. Sci. Technol. 34, 2501–2506.

Bogush, A., Stegemann, J.A., Wood, I., Roy, A., 2015. Element composition and mineralogical characterisation of air pollution control residue from UK energy-from-waste facilities. Waste Manage. 36, 119–129.

Chang, C.-Y., Wang, C.-F., Mui, D., Cheng, M.-T., Chiang, H.-L., 2009. Characteristics of elements in waste ashes from a solid waste incinerator in Taiwan. J. Hazard. Mater. 165, 766–773.

Croudace, I.W., 1981. A possible error source in silicate wet-chemistry caused by insoluble fluorides. Chem. Geol. 31, 153–155.

Derie, R., 1996. A new way to stabilize fly ash from municipal incinerators. Waste Manage. 16, 711–716.

DIN 32645:2008-11, Chemical analysis - Decision limit, detection limit and determination limit under repeatability conditions - Terms, methods, evaluation.

European Commission, 2017. On the 2017 list of Critical Raw Materials for the EU.

Fellner, J., Lederer, J., Purgar, A., Winterstetter, A., Rechberger, H., Winter, F., Laner, D., 2015. Evaluation of resource recovery from waste incineration residues–The case of zinc. Waste Manage. 37, 95–103.

Fermo, P., Cariati, F., Pozzi, A., Demartin, F., Tettamanti, M., Collina, E., Lasagni, M., Pitea, D., Puglisi, O., Russo, U., 1999. The analytical characterization of municipal solid waste incinerator fly ash: methods and preliminary results. Fresenius J. Anal. Chem. 365, 666–673.

Ferreira, C., Ribeiro, A., Ottosen, L., 2003. Possible applications for municipal solid waste fly ash. J. Hazard. Mater. 96, 201–216.

German Mineral Resources Agency, Federal Institute for Geosciences and Natural Resources, 2013. DERA Rohstoffinformationen 18 – Antimon.

German Mineral Resources Agency, Federal Institute for Geosciences and Natural Resources, 2014. Rohstoffwirtschaftliche Steckbriefe – Zinn.

German Mineral Resources Agency, Federal Institute for Geosciences and Natural Resources, 2015. DERA Rohstoffinformationen 27 – Bismut.

Hong, K.-J., Tokunaga, S., Kajiuchi, T., 2000a. Extraction of heavy metals from MSW incinerator fly ashes by chelating agents. J. Hazard. Mater. 75, 57–73.

Hong, K.J., Tokunaga, S., Ishigami, Y., Kajiuchi, T., 2000b. Extraction of heavy metals from MSW incinerator fly ash using saponins. Chemosphere 41, 345–352.

Huang, S.-J., Chang, C.-Y., Chang, F.-C., Lee, M.-Y., Wang, C.-F., 2007. Sequential extraction for evaluating the leaching behavior of selected elements in municipal solid waste incineration fly ash. J. Hazard. Mater. 149, 180–188.

Jung, C., Matsuto, T., Tanaka, N., Okada, T., 2004. Metal distribution in incineration residues of municipal solid waste (MSW) in Japan. Waste Manage. 24, 381–391.

Karlfeldt Fedje, K., Ekberg, C., Skarnemark, G., Steenari, B.-M., 2010. Removal of hazardous metals from MSW fly ash—An evaluation of ash leaching methods. J. Hazard. Mater. 173, 310–317.

Karstensen, K.H., Lund, W., 1989. Multi-element analysis of a city waste incineration ash reference sample by inductively coupled plasma atomic emission spectrometry. J. Anal. At. Spectrom. 4, 357–359.

Lam, C.H., Ip, A.W., Barford, J.P., McKay, G., 2010. Use of incineration MSW ash: a review. Sustainability 2, 1943–1968.

Li, M., Xiang, J., Hu, S., Sun, L.-S., Su, S., Li, P.-S., Sun, X.-X., 2004. Characterization of solid residues from municipal solid waste incinerator. Fuel 83, 1397–1405.

Löschau, M., 2014. Reinigung von Abgasen: unter besonderer Berücksichtigung der thermischen Abfallbehandlung. TK-Verlag, Neuruppin.

Mangialardi, T., Paolini, A., Polettini, A., Sirini, P., 1999. Optimization of the solidification/stabilization process of MSW fly ash in cementitious matrices. J. Hazard. Mater. 70, 53–70.

Morf, L.S., Gloor, R., Haag, O., Haupt, M., Skutan, S., Di Lorenzo, F., Böni, D., 2013. Precious metals and rare earth elements in municipal solid waste–sources and fate in a Swiss incineration plant. Waste Manage. 33, 634–644.

Nakamura, K., Kinoshita, S., Takatsuki, H., 1996. The origin and behavior of lead, cadmium and antimony in MSW incinerator. Waste Manage. 16, 509–517.

Pan, Y., Wu, Z., Zhou, J., Zhao, J., Ruan, X., Liu, J., Qian, G., 2013. Chemical characteristics and risk assessment of typical municipal solid waste incineration (MSWI) fly ash in China. J. Hazard. Mater. 261, 269–276.

Purgar, A., Winter, F., Blasenbauer, D., Hartmann, S., Fellner, J., Lederer, J., Rechberger, H., 2016. Main drivers for integrating zinc recovery from fly ashes into the Viennese waste incineration cluster. Fuel Process. Technol. 141, 243–248.

Schlumberger, S., Schuster, M., Ringmann, S., Koralewska, R., 2007. Recovery of high purity zinc from filter ash produced during the thermal treatment of waste and inerting of residual materials. Waste Manage. Res. 25, 547–555.

Weibel, G., Eggenberger, U., Schlumberger, S., Mäder, U.K., 2017. Chemical associations and mobilization of heavy metals in fly ash from municipal solid waste incineration. Waste Manage. 62, 147–159.

Wiel, E.D., Levchik, S.V., 2016. Flame Retardants for Plastics and Textiles. Practical Applications, Hanser, Munich.

Wu, H.-Y., Ting, Y.-P., 2006. Metal extraction from municipal solid waste (MSW) incinerator fly ash—Chemical leaching and fungal bioleaching. Enzyme Microb. Technol. 38, 839–847.

8.2. Publikation 2

Solubility of elements in waste incineration fly ash and bottom ash under various leaching conditions studied by a sequential extraction procedure

Jasmin Haberl *, Michael Schuster

Division of Analytical Chemistry, Department of Chemistry, Technical University of Munich, 85748 Garching, Lichtenbergstrasse 4, Germany

* Corresponding author.
E-Mail: jasmin.haberl@tum.de

Abdruck des Artikels mit allgemeiner Genehmigung von Elsevier (siehe Kapitel 7.2) aus

Waste Management, 2019, 87, 268–278

DOI: 10.1016/j.wasman.2019.02.001

Waste Management 87 (2019) 268–278

Contents lists available at ScienceDirect

Waste Management

journal homepage: www.elsevier.com/locate/wasman

Solubility of elements in waste incineration fly ash and bottom ash under various leaching conditions studied by a sequential extraction procedure

Jasmin Haberl [*], Michael Schuster

Division of Analytical Chemistry, Department of Chemistry, Technical University of Munich, 85748 Garching, Lichtenbergstrasse 4, Germany

ARTICLE INFO

Article history:
Received 17 September 2018
Revised 4 January 2019
Accepted 1 February 2019

Keywords:
Waste incineration residues
Fly ash
Bottom ash
Sequential extraction
pH-dependent solubility
Metal leaching

ABSTRACT

An optimized 7-step sequential extraction was applied to fly ash samples from two waste incineration plants and a bottom ash sample. The solubility of 37 elements in water under alkaline and neutral conditions, ion exchange, acid solubility as well as the influence of reducing and oxidizing agents, were investigated using reagents which are typically applied in sequential extractions. Potential error sources and the suitability and selectivity of individual steps and extracting agents were also evaluated. Additionally, the amounts of total dissolved solids were determined for each extraction step, and the results were validated by comparison with the analysis data of the elemental composition.

All the investigated incineration residues exhibited a very similar solubility behavior. Only the alkali metals in the bottom ash were considerably less water-soluble than those in the fly ash. The solubility behavior among the rare earth elements was alike. The pH of the fly ash suspensions in water increased over several hours from neutral to alkaline. Concentration changes of water-soluble elements were investigated during the pH increase and to what extent precipitated elements can be re-dissolved by a subsequent neutralization.

Meanwhile, it was shown that chloride ions in commonly used sequential extraction agents (e.g., $MgCl_2$ and $NH_2OH{\cdot}HCl$) can influence the extractability of individual elements, which can lead to misinterpretations of the results. Using $MgCl_2$ to study Mg^{2+} ion exchange led to the dissolution of Ag and Cd only caused by the chloride ions. Furthermore, the order of the reducing and oxidizing step was found to be interchangeable.

1. Introduction

Sequential extractions are a common tool to divide elements into different fractions depending on their leachability from a sample. The leachability is determined by the mineralogical form of the element in the sample. Sequential extractions are conducted in several steps using progressively stronger leaching solutions. They were originally developed for element speciation in sediments and soils. The Tessier procedure (Tessier et al., 1979) and the BCR procedure (Rauret et al., 1999) are most widely used.

Sequential extractions have also been applied to waste incineration residues like fly ash (Huang et al., 2007; Jiao et al., 2016; Van Herck and Vandecasteele, 2001) and bottom ash (Bruder-Hubscher et al., 2002).

One general problem of sequential extractions is the limited comparability of different studies because they mostly used different procedures. There are only few studies which applied the same sequential extraction procedure to different waste incineration residues. Buchholz and Landsberger (1995) investigated fly ash and bottom ash and also size-fractioned fly ash, while Pan et al. (2013) and Xiong et al. (2014) compared several different fly ash samples. However, most studies covered only a few elements. Therefore, we considered it necessary to conduct a more comprehensive study with 37 elements comparing different incineration residues. Furthermore, a large number of steps were conducted to obtain a detailed fractionation. The fly ash samples used in this work were described and analyzed in detail in our previous publication (Haberl et al., 2018).

The concept of sequential extractions is often criticized (Bacon and Davidson, 2008; Martin et al., 1987; Nirel and Morel, 1990). The main criticisms are the lack of selectivity and specificity, and only little valuable information about the element species and binding forms. Waste incineration residues have a very different composition and mineralogy compared to sediments and soils for which sequential extraction was originally developed. Therefore,

---

[*] Corresponding author.
E-mail address: jasmin.haberl@tum.de (J. Haberl).

https://doi.org/10.1016/j.wasman.2019.02.001
0956-053X/© 2019 Elsevier Ltd. All rights reserved.

the common sequential extraction procedures are not directly transferable to waste incineration residues. For this reason, we developed a modified concept of the sequential extraction in this work. Sequential extraction was used as a method of identifying the minimum necessary conditions to bring an element into solution. It is not our objective to precisely determine the binding forms. Rather, an insight into the necessary leaching conditions shall be provided. The leaching solutions in the extraction steps were not chosen in a way that certain element species are selectively dissolved, like for example in the Tessier procedure. Tessier defined some of the fractions as *bound to carbonates* (using acid), *bound to Fe-Mn oxides* (using a reducing agent), and *bound to organic matter* (using an oxidizing agent). In contrast, our approach defined them in more general terms, such as an *acid soluble fraction*, a *reducible fraction*, and an *oxidizable fraction*. This approach can already be found in several publications, but the applied procedures were usually still mixed with the original approach to obtain fractions of certain element species. For example, when defining an acid soluble fraction, a reducible fraction, or an oxidizable fraction, other possible influences on the solubility beside the investigated parameters must be excluded. This includes a constant pH in consecutive steps when the aim is to investigate another parameter than the pH. This was already suggested by Van Herck and Vandecasteele (2001). Another example is the influence of anions in salts, which are used to investigate cation-exchange reactions. These aspects were all considered and studied in this work aiming to obtain clear information about which parameters influence the dissolution of an element.

Knowing the solubility behavior of incineration residues is for example essential for recovery approaches comprising a leaching procedure and a subsequent separation of individual metals out of the leaching solution. It is useful to know whether ashes from different plants have a similar solubility behavior because then it is unnecessary to adjust the leaching procedure for each ash from different plants. Fly ash leaching is already conducted at several waste incineration plants with the commercially available FLUWA (abbreviation for the German word *Flugaschen-Wäsche*, engl.: *fly ash washing*) process, which is a fly ash washing process using acidic scrubbing water. More details on the FLUWA process can be found in Quina et al. (2018).

2. Materials and methods

For all experiments ultrapure water (UPW), obtained from a water purification system Direct-Q® 5 UV (Merck Millipore), was used. The following acids were used: nitric acid (65% for analysis, Merck, purified by sub-boiling distillation), hydrochloric acid (30% Suprapur®, Merck), hydrofluoric acid (47% ultrapure Normatom®, VWR), acetic acid (100% for analysis, Merck) and boric acid (Suprapur®, Merck).

2.1. Description of the samples and analysis of the elemental composition

The fly ash (FA) samples originated from three different waste incineration plants (A, B, and C) and have already been the subject of our previous study, where detailed descriptions and comprehensive analysis data of the samples can be found (Haberl et al., 2018). The fly ash sample from the plant C was created as a project internal reference material by the German Federal Institute of Hydrology (SESAM project BMBF, cf. Acknowledgment, Fabricius et al., in preparation). Each sample was a composite sample consisting of daily samples collected over a month. The focus in this work was on the fly ash samples from plants A (FA-A, sample A2) and C (FA-C). The sample from plant B (FA-B) was only used for an additional experiment. The abbreviations refer to the abbreviations used in the publication by Haberl et al. (2018). All ashes were electrostatic filter ashes, partially mixed with boiler ash and fabric filter ash.

The bottom ash originated from a waste incineration plant with dry discharge (plant B). For the experiments, the fine fraction of the bottom ash (BA) with a particle size of <0.3 mm was used (12% of the entire bottom ash at the incineration plant). This fraction was separated from the bottom ash by sieving, which is one bottom ash processing step at the incineration plant. Sample preparation and analysis of the bottom ash were done similarly to the fly ash samples (Haberl et al., 2018), only the homogenization was intensified (30 min dry ball milling at 450 rpm). Triplicates were digested and analyzed by ICP-OES (iCAP 7600 Duo, Thermo Fisher Scientific) and ICP-MS (Agilent 7900).

2.2. Performance of the sequential extraction procedure

The extractions were done with sample quantities of 500 mg in centrifuge tubes. The fly ash samples were used without homogenization, whereas the bottom ash was used after homogenization (see Section 2.1). The extraction procedure comprised seven extraction steps (Table 1). The general experimental procedure was as follows. The leaching solution of the respective step was added to the sample or residue of the previous step. 15 min before the end of a defined leaching time, the suspension was centrifuged for 10 min at 5000 rpm (Z 206A, Hermle) to separate the extraction solution from the solid residue. The supernatant was separated with a pipette at the end of the leaching time, and the residue was washed with 5–10 mL of UPW after each step. After several seconds of manual shaking, the solid residue was separated again by centrifugation. The washing water was separated with a pipette and combined with the extraction solution. In steps 1–3, the extraction solutions were acidified with 0.5 mL of 65% nitric acid in order to stabilize the solutions until measurement.

The leaching time, the volume of leaching solution, and the detailed experimental conditions in the extraction steps were as follows.

Step 1: 40 mL of UPW was added to the sample. The suspension was continuously agitated on a horizontal shaker for 47 h (FA-A) or 24 h (FA-C and BA).

Step 2: 30 mL of UPW (FA-A and FA-C) or 20 mL of UPW (BA) were added to the residue of step 1. The suspension was neutralized with 0.5% acetic acid to pH = 7 under gentle stirring with the pH electrode at the suspension surface so that the solid particles were whirled up with taking care not to scratch the pH electrode's glass membrane. The neutralization required continuous pH readjustments since the pH immediately rose when the addition of acid was interrupted. It took 1–2 h until the pH stabilized at 7. As the amount of the consumed acid

Table 1
Overview of the sequential extraction procedure.

Extraction step	Dissolved fraction	Leaching solution
1	Water-soluble (alkaline pH)	UPW
2	Water-soluble (neutral pH)	UPW, neutralized to pH = 7 with acetic acid
3	Ion-exchangeable	1 M $MgCl_2$
4	Acid-soluble	Acetic acid, pH = 3
5	Reducible	0.3 M $NH_2OH{\cdot}HCl$, pH = 3 with acetic acid
6	Oxidizable	H_2O_2, pH = 3 with HNO_3
7	Residue	Digestion with HNO_3, HCl, and HF

for the neutralization was higher for the bottom ash, only 20 mL of UPW was used to obtain a comparable final volume of the extraction solution after neutralization. The total leaching time was 3 h.

Step 3: 20 mL of 1 M $MgCl_2$ (for analysis, Merck) was added to the residue of step 2. The suspension was continuously agitated on a horizontal shaker for 6 h.

Step 4: 30 mL of diluted acetic acid (pH = 3) was added to the residue of step 3. The pH of the suspension was adjusted to 3 with 100% acetic acid. The suspension was continuously agitated on a horizontal shaker for 24 h. The pH was regularly checked and adjusted, if necessary.

Step 5: 20 mL of 0.3 M $NH_2OH{\cdot}HCl$ (for analysis, Merck) was added to the residue of step 4. The pH was adjusted to 3 with 25% acetic acid. The suspension was heated to 50 °C in a water bath and shaken occasionally by hand. The pH was regularly checked and adjusted, if necessary. After 22 h, the suspension was continuously agitated on a horizontal shaker for another 2 h at room temperature before the extraction solution was separated.

Step 6: 16 mL of 30% H_2O_2 (Suprapur®, Merck) and 4 mL of UPW were added to the residue of step 5. The pH was adjusted to 3 with 0.05 M nitric acid. The suspension was heated to 50 °C in a water bath and shaken occasionally by hand. The pH was regularly checked and adjusted, if necessary. After 22 h, the suspension was continuously agitated on a horizontal shaker for another 2 h at room temperature before the extraction solution was separated.

Step 7: The residue was dried at 60 °C and digested with nitric acid, hydrochloric acid, and hydrofluoric acid by microwave-assisted pressure digestion as described by Haberl et al. (2018).

For the horizontal shaking, an HS 501 Digital Shaker (IKA) was used at 300 rpm. A blank solution was prepared for each step. The acid concentrations used for the pH adjustments were chosen so that only micro- or a few milliliters had to be added to the suspensions. A high liquid-to-solid ratio was used in order to prevent saturation effects. The volumes of the leaching solutions were roughly adjusted to the extracted amounts in the individual steps. All the extraction solutions were filled up with UPW to a final volume of 50 mL. The extraction solutions were allowed to stand for several hours or centrifuged for a few minutes before an aliquot for ICP analysis was withdrawn. By this, it was ensured that no residual particles in the extraction solutions got into the ICP analysis. An aliquot of each extraction solution was diluted with a ratio of 1:100 in 3% nitric acid and analyzed using both ICP-OES and ICP-MS.

The sequence of the extraction steps and the used reagents $MgCl_2$, acetic acid, $NH_2OH{\cdot}HCl$ and H_2O_2 were adopted from Tessier et al. (1979) with modified concentrations in some cases. The additional step 1, the sample quantity of 500 mg, the concentration of 0.3 M $NH_2OH{\cdot}HCl$ and the idea of a constant pH during the steps 4–6 were adopted from Van Herck and Vandecasteele (2001). Step 2 is not a common step in sequential extractions in literature and was newly introduced.

2.3. Determination of the necessary leaching times

The change in concentration of several elements was monitored during the extraction steps 1, 3, 4, and 5 to determine the necessary contact time between the sample/residue and the leaching solution. Fly ash FA-A was used in all the experiments. Fly ash FA-B was additionally used as a comparison in step 1. The sequential extraction was conducted as described in Section 2.2. Aliquots of 1 mL were taken from the extraction solution every few hours over a specified period. The suspensions were centrifuged (10 min, 5000 rpm) before each sampling. The aliquots were then stabilized with 100 µL of 65% nitric acid in steps 1 and 3.

2.4. Modifications of the sequential extraction procedure

The influence of the following modifications on the sequential extraction procedure described in Section 2.2 was evaluated.

- Replacement of $MgCl_2$ by $Mg(NO_3)_2$ in the ion exchange step: 1 M $Mg(NO_3)_2$ (for analysis, Merck) was used instead of 1 M $MgCl_2$ (using FA-C as an example).
- Interchange of the reducing and the oxidizing step: these steps were carried out in reverse order (using FA-A as an example).
- Replacement of $NH_2OH{\cdot}HCl$ by NaCl in the reducing step: 0.3 M NaCl (Normapur®, VWR) was used instead of 0.3 M $NH_2OH{\cdot}HCl$ (using FA-C as an example).

2.5. Determination of the total dissolved solids in each extraction step

The residues were washed twice after each extraction step, dried at 60 °C, and weighed afterward. These experiments were conducted separately from the experiments in which the extraction solutions were analyzed in order to exclude the potential influences of the drying process on the element binding forms.

3. Results and discussion

3.1. Elemental composition of the fly ashes and the bottom ash

Table 2 shows the elemental composition of the investigated incineration residues. The concentrations of Rb, Zn, Cd, Sb, Tl, Pb, and Bi were significantly lower in the bottom ash compared to those in the fly ashes. Mainly volatile elements were accumulated in the fly ash, and more rare earth elements were found in the bottom ash. The concentrations of other elements were similar in both fly ashes and bottom ash.

3.2. Solubility of elements in the different extraction steps

The sequential extraction was conducted with the fly ashes (FA-A and FA-C) and the bottom ash, to investigate the elements listed in Table 2. The concentrations of all the extraction steps were added up and normalized to 100% for each element. The element distributions between the fractions are shown in Figs. 1–3. The error bars represent the standard deviation of three replicates. The procedure showed a high reproducibility as the error bars were very small. In this section, an overview of all extraction steps is given. The individual steps are discussed and investigated in more detail in Section 3.3.

The solubility behavior of the two fly ash samples was very similar as seen from the high agreement of their distribution patterns. Thus, it is safe to say that the binding forms, which determine the solubility, must be quite similar for both fly ash samples, despite the different elemental concentrations. Moreover, the solubility behavior of the bottom ash was similar to that of the fly ashes. This was even the case for elements with a significantly different concentration. However, there was one significant difference. The alkali metals in the fly ashes had a high solubility of about 60–80% for Li and 90% for Na, K, and Rb in water (step 1). In contrast, only 10–25% of the alkali metals in the bottom ash were soluble in water. A significant amount of the alkali metals was not even soluble in acid (step 4) and thus remained in the residue. Hence, the binding forms of the alkali metals were significantly different between the fly ash and the bottom ash. The lower water solubility of bottom ash was

Table 2
Elemental composition of the fly ashes FA-A and FA-C and the bottom ash sample. Average and standard deviation of the analyzed triplicates are given below. The analysis data of the fly ashes was previously published (Haberl et al., 2018). The concentration of Tl in the bottom ash was below the limit of quantification.

Alkali and alkaline earth metals											
	Li (mg/kg)	Na (g/kg)	K (g/kg)	Rb (mg/kg)	Ca (g/kg)	Sr (mg/kg)	Ba (g/kg)				
FA-A	61 ± 2	59 ± 0.5	55 ± 0.5	183 ± 1	140 ± 1	359 ± 7	1.7 ± 0.03				
FA-C	135 ± 12	58 ± 0.5	55 ± 1	205 ± 2	165 ± 0.4	285 ± 2	1.5 ± 0.03				
BA	45 ± 0.3	17 ± 0.2	10 ± 0.2	27 ± 1	208 ± 2	626 ± 9	3.1 ± 0.02				
Other elements											
	Al (g/kg)	Si (g/kg)	Ti (g/kg)	V (mg/kg)	Cr (mg/kg)	Mn (g/kg)	Fe (g/kg)	Co (mg/kg)	Ni (mg/kg)	Cu (g/kg)	Zn (g/kg)
FA-A	30 ± 0.2	49 ± 0.4	10 ± 0.08	28 ± 0.3	350 ± 17	0.6 ± 0.01	13 ± 0.1	26 ± 1	103 ± 7	2.5 ± 0.01	69 ± 0.8
FA-C	17 ± 0.1	31 ± 0.1	5.3 ± 0.04	23 ± 0.6	463 ± 12	1.8 ± 0.03	14 ± 0.07	46 ± 4	122 ± 6	7.2 ± 0.06	39 ± 0.1
BA	45 ± 0.4	120 ± 2	11 ± 0.07	57 ± 2	661 ± 50	1.1 ± 0.01	51 ± 0.02	72 ± 5	319 ± 8	3.5 ± 0.09	6.6 ± 0.05
	Ga (mg/kg)	Mo (mg/kg)	Ag (mg/kg)	Cd (mg/kg)	Sb (g/kg)	Tl (mg/kg)	Pb (g/kg)	Bi (mg/kg)			
FA-A	24 ± 0.7	30 ± 1	63 ± 1	540 ± 6	3.0 ± 0.04	3.3 ± 0.01	11 ± 0.1	269 ± 8			
FA-C	12 ± 0.5	61 ± 1	59 ± 2	373 ± 2	2.5 ± 0.03	5.2 ± 0.06	13 ± 0.1	474 ± 12			
BA	11 ± 0.4	27 ± 1	23 ± 5	14 ± 2	0.2 ± 0.002	<0.24	1.2 ± 0.05	38 ± 13			
Rare earth elements											
	Sc (mg/kg)	Y (mg/kg)	La (mg/kg)	Ce (mg/kg)	Pr (mg/kg)	Nd (mg/kg)	Sm (mg/kg)	Gd (mg/kg)	Dy (mg/kg)	Er (mg/kg)	Yb (mg/kg)
FA-A	2.2 ± 0.1	6.4 ± 0.2	20 ± 0.7	44 ± 0.6	1.6 ± 0.02	5.5 ± 0.1	0.9 ± 0.1	1.1 ± 0.05	0.7 ± 0.04	0.4 ± 0.02	0.3 ± 0.005
FA-C	1.3 ± 0.1	7.1 ± 0.2	12 ± 0.5	17 ± 1	1.4 ± 0.04	5.0 ± 0.2	1.3 ± 0.5	1.1 ± 0.1	0.6 ± 0.03	0.3 ± 0.01	0.3 ± 0.009
BA	4.7 ± 0.1	12 ± 0.3	26 ± 0.8	42 ± 2	6.3 ± 0.1	23 ± 0.7	2.9 ± 0.4	2.8 ± 0.08	2.1 ± 0.05	1.1 ± 0.04	3.4 ± 0.3

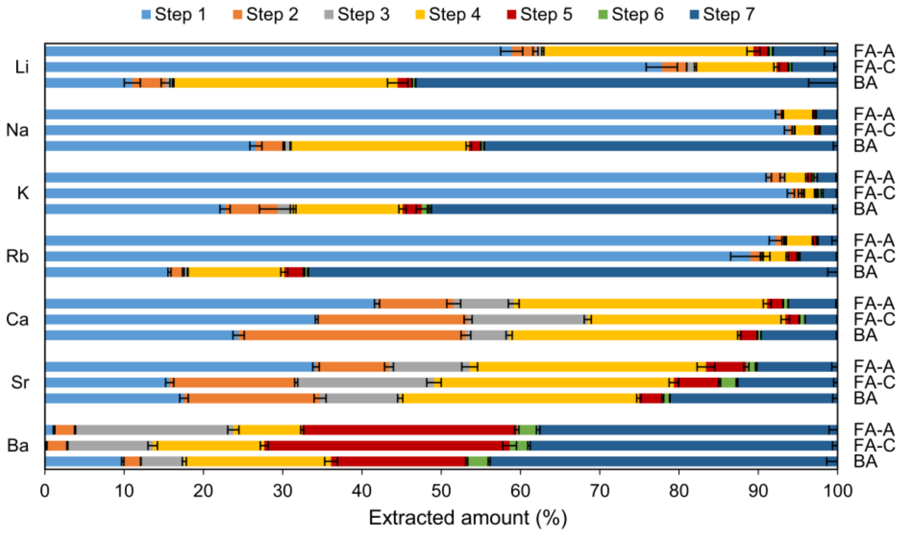

Fig. 1. Solubility of the alkali and alkaline earth metals in the extraction steps 1–7 for the fly ash samples (FA-A and FA-C) and the bottom ash sample.

reported in the literature (Abbas et al., 2003), and based on our study, the difference was only caused by a lower solubility of the alkali metals in the bottom ash.

Additionally, X-ray diffraction (XRD) analysis was performed on the two fly ash samples and on the bottom ash sample. Details on the XRD analysis and the results can be found in the Supplementary data in Appendix A. Only the main minerals could be detected with XRD due to the low sensitivity. The main mineralogy of the two fly ash samples was very similar. The XRD analysis confirmed that the alkali metals Na and K were present as easily soluble salts (mainly chlorides and sulfates, e.g. NaCl, KCl, $K_3Na[SO_4]_2$, K_2ZnCl_4). This agrees with other studies about the mineralogy of fly ash (Weibel et al., 2017; Zhao et al., 2017). No water-soluble Na- or K-minerals could be detected in the bottom ash. The main mineralogy of the bottom ash was quite different to the fly ashes although the solubility behavior was similar apart from the alkali metals.

All rare earth elements exhibited a striking similar solubility pattern among each other. This observation matches with the generally known fact that the rare earth elements have similar chemical properties. This indicates that the rare earth elements were present as similar minerals in the incineration residues. Most rare earth elements were about 50% dissolved at pH = 3 (step 4) in all the investigated incineration residues, but only Sc had a lower acid solubility of about 15% compared to the other rare earth elements.

A sufficient leaching time must be chosen in each leaching step to achieve complete dissolution of all the soluble compounds. This is important to avoid carryover into the next leaching step. For several steps, the necessary contact time between the sample/residue and the leaching solution was determined by monitoring the change in the concentration of several elements over time. It turned out that longer leaching times than for example in the procedures of Tessier et al. (1979) and Van Herck and Vandecasteele

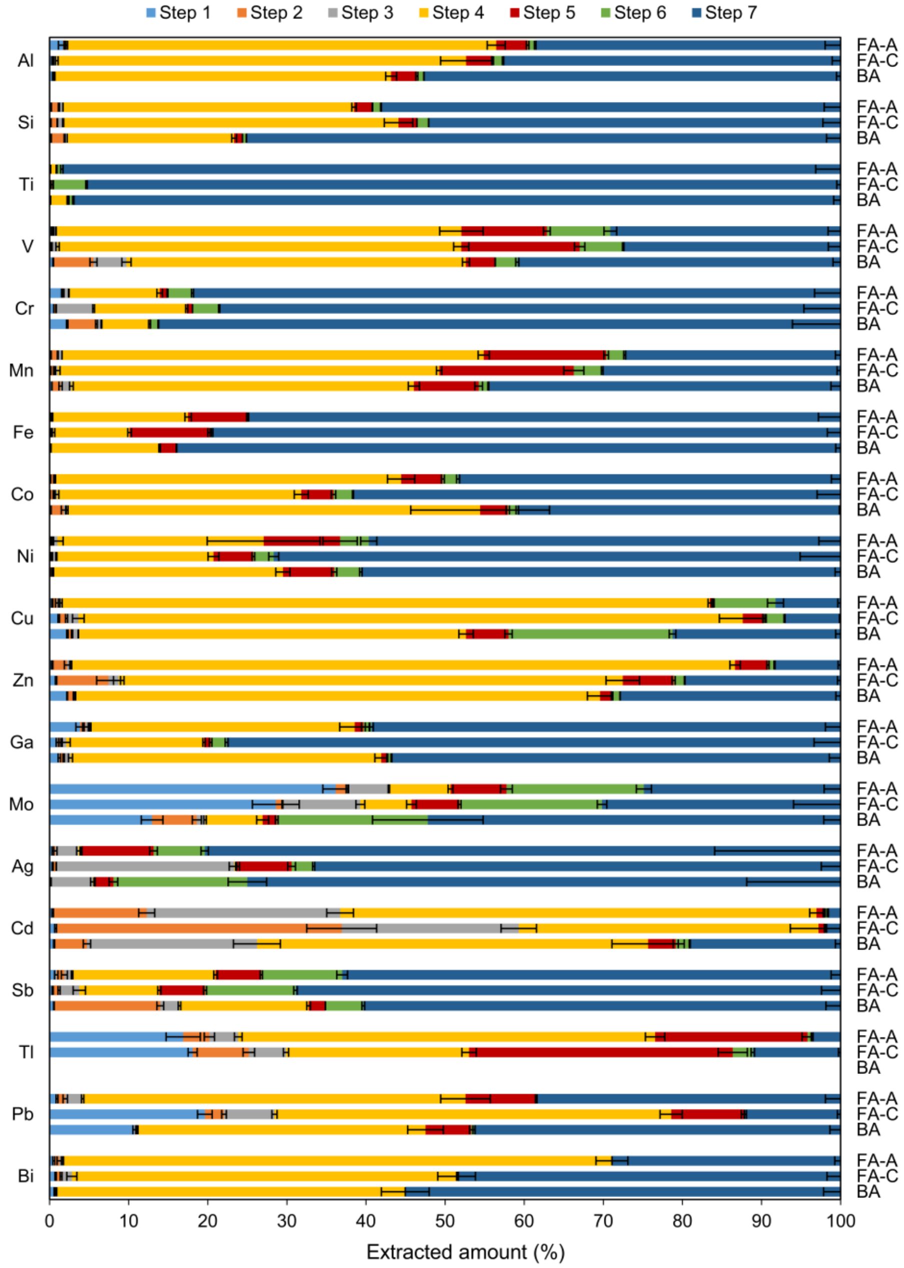

Fig. 2. Solubility of other elements in the extraction steps 1–7 for the fly ash samples (FA-A and FA–C) and the bottom ash sample. The alkali and alkaline earth metals, as well as the rare earth elements, are shown separately in Figs. 1 and 3, respectively. Tl was not quantified in the bottom ash extraction solutions because its concentration in the bottom ash was below the limit of quantification.

(2001) were necessary. For details, please refer to the Supplementary data in Appendix A. The concentration change during step 1 is discussed in more detail in Section 3.3.1.

3.3. Detailed investigation and discussion of each extraction step

3.3.1. Step 1 – Water-soluble fraction (alkaline conditions)

Fly ashes and bottom ashes are known to be highly reactive in water to form alkaline solutions, mainly due to the contained $CaCO_3$ and CaO (Johnson et al., 1995; Weibel et al., 2017). The pH of the bottom ash suspension in water immediately reached 12 and remained constant over time. The same was observed for the fly ash FA-C. Due to some technical reasons at the incineration plant C, some amount of $Ca(OH)_2$ was mixed with the pure fly ash during the separation of the ash from the flue gas. Therefore, FA-C was considered as a special case. The fly ash samples FA-A and FA-B, which contained no additives from the flue gas cleaning, could not reach the final alkaline pH immediately despite vigorous stirring with a magnetic stir bar (Fig. 4). This might be due to the buffer capacity of the fly ashes. The pH curves show two buffer areas probably belonging to the carbonate buffer system (Karlfeldt Fedje et al., 2010). The pH increased by slowly dissolving

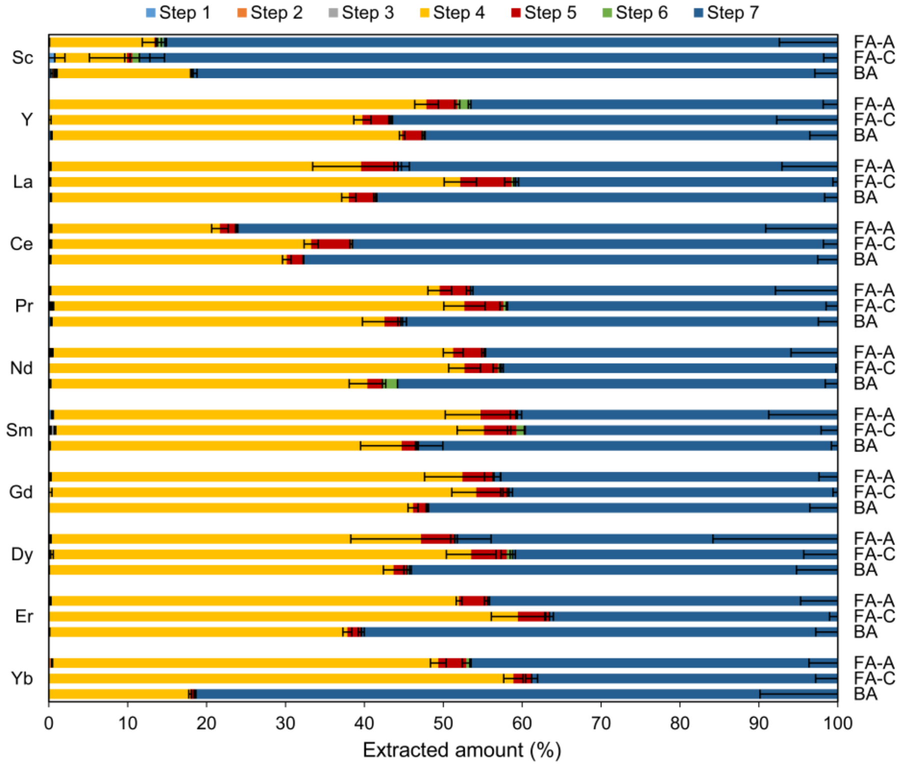

Fig. 3. Solubility of the rare earth elements in the extraction steps 1–7 for the fly ash samples (FA-A and FA-C) and the bottom ash sample.

alkaline compounds. When the buffer capacity was exceeded the pH reached the final value between 10 and 11. Both fly ashes had the same pH curves but differed only in the time to reach the final pH.

The time difference must generally be considered in fly ash leaching experiments. A longer leaching time was chosen for FA-A in step 1 in order to ensure the complete dissolution of all soluble components and a comparable pH with FA-C at the end of this step. As a result, the alkali metals were mostly dissolved, as previously discussed in Section 3.2. Additionally, we measured significant amounts of Ca, Sr, Mo, and Tl, and for some samples also Ba and Pb in the alkaline extraction solutions.

The slow pH increases during the water extraction of FA-A and FA-B enabled an investigation of the pH-dependent solubility of elements in the alkaline range. The elements dissolved in significant amounts in water were investigated. The concentration curves over time and the pH at each sampling point are shown in Fig. 5. The pH changed slower than in Fig. 4 probably because the suspensions were agitated by horizontal shaking instead of stirring with a magnetic stir bar in this experiment.

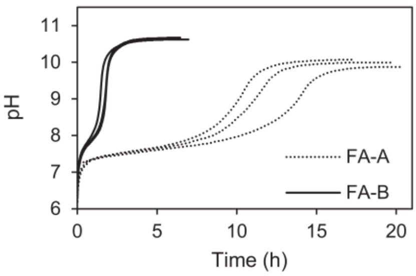

Fig. 4. pH curves of the fly ash suspensions in water. Each pH curve was recorded three times. The suspensions were stirred with a magnetic stir bar in this experiment, because horizontal shaking like in step 1 prevented a continuous pH measurement.

The concentrations of Na, K, and Rb no longer changed significantly after 1 h of leaching time. The solubility of these metals was hence not influenced by the pH. The concentrations of Li, Ca, and Sr increased slightly with time. This was caused by slow dissolution of these elements, and no pH correlation was observed. Meanwhile, the concentrations of Cd, Tl, Zn, Ba, and Pb decreased with the increasing pH because they precipitated as hydroxides and carbonates (Karlfeldt and Steenari, 2007; Mizutani et al., 1996; Van Herck et al., 2000). The concentrations of these elements correlated clearly with the pH for both fly ash samples. Therefore it could be concluded that these elements were not precipitated by anions as soon as they enter the solution (e.g., precipitation of Ba^{2+} by SO$_4^{2-}$). Also, the solubility of Mo was strongly pH dependent. There was hardly any Mo dissolved under neutral conditions, but as soon as the pH increased, the concentration of Mo rose rapidly. Mo is present as MoO$_4^{2-}$ under alkaline conditions (Cornelis et al., 2008).

The final concentrations in this experiment agreed well with the concentrations of the first step in the sequential extraction (Figs. 1 and 2).

3.3.2. Step 2 – Water-soluble fraction (neutral conditions)

In the second extraction step, the residues of step 1 were leached once again with water and the suspensions were still strongly alkaline (pH > 10 for all samples). The mixtures were then neutralized to pH 7. In this extraction step mainly those elements were dissolved which precipitated during step 1. All other water-soluble

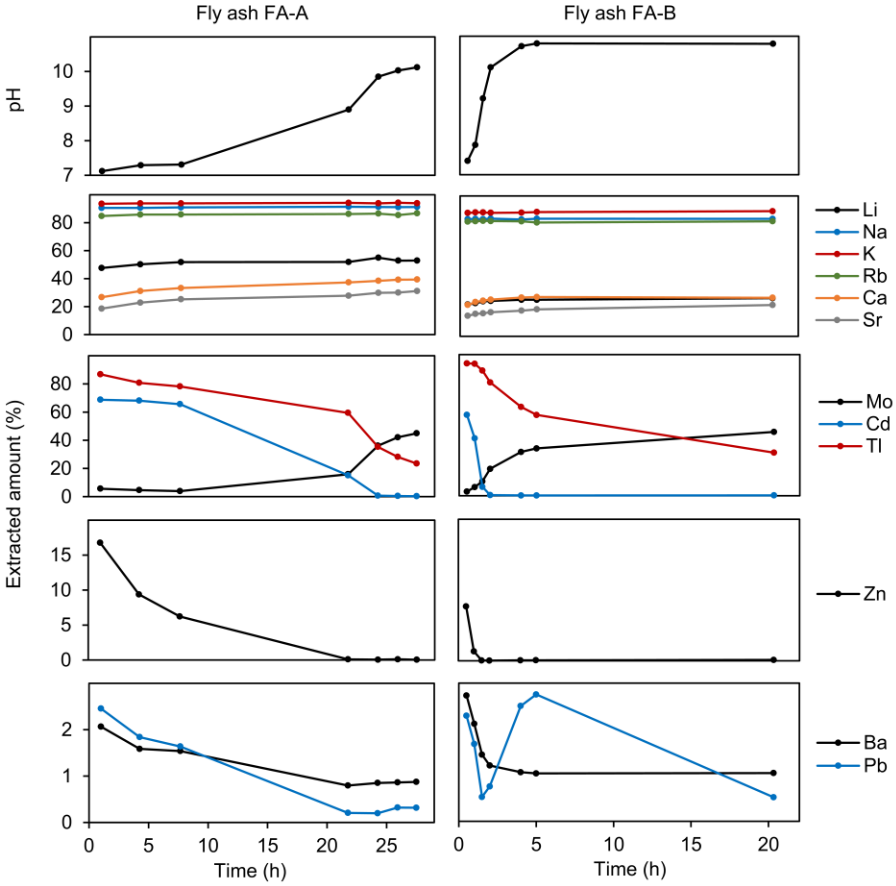

Fig. 5. pH curves and corresponding concentration curves of water-soluble elements during step 1 for fly ashes FA-A and FA-B. The extracted amounts at different time points are relative to the total content of the respective element given in Table 2.

elements were removed in step 1. This extraction step provided the extent of the precipitated elements to be re-dissolved at neutral pH. When comparing the precipitated amounts in the fly ash FA-A during step 1 (Fig. 5) with the amounts that re-entered the solution after the neutralization in step 2 (Figs. 1 and 2), most precipitated elements could not be completely re-dissolved. This applied particularly to Tl and Cd, whereby 87% of Tl and 69% of Cd were dissolved from the fly ash FA-A after 1 h at a pH of 7.1. When the suspension reached an alkaline pH, the dissolved amounts dropped to 23% for Tl and 0% for Cd. After re-neutralization in step 2, only 3% Tl and 12% Cd were dissolved; these amounts were much less than the precipitated amounts. This means that these elements were transformed from water-soluble compounds, which were dissolved at the beginning of step 1, to largely water-insoluble compounds at the end of step 1. Apart from Tl and Cd, significant amounts of Ca and Sr were also found in step 2. Although the concentrations of Ca and Sr increased during step 1, parts of them must have nevertheless precipitated simultaneously.

Consequently, for some elements, there is a significant difference on how long the fly ash is in contact with water. Separating the extraction solution from the residual fly ash before the buffer capacity is exceeded can prevent precipitation.

3.3.3. Step 3 – Ion exchange fraction

The extraction with 1 M $MgCl_2$ provided information about which elements could be exchanged by Mg^{2+} ions. Most sequential extraction procedures in the literature contained an ion exchange step, often after leaching with water (Huang et al., 2007; Jiao et al., 2016; Van Herck and Vandecasteele, 2001), but the pH differences between the water-soluble and the ion-exchange fractions were often not considered. In our study, the pH during the ion exchange was around 8 for all samples. By performing step 2 under neutral conditions before, it could be ruled out that the elements were dissolved because of a lower pH than that in the step 1. This increases the informative value of the ion exchange step significantly. The suspensions have been neutralized to pH 7 in step 2. The slightly higher pH of 8 in the subsequent ion exchange was probably caused by small amounts of residual alkaline compounds which dissolved only during the ion exchange step. As mentioned in Section 3.3.2, the pH was still >10 when water was added to the washed residues of step 1. It is interesting to note that significant lower pH values (also around 8) were observed in preliminary experiments when 1 M $MgCl_2$ was added instead (i.e. skipping step 2). The reason for the lower pH is probably the precipitation of hydroxide ions in form of sparingly soluble $Mg(OH)_2$.

With $MgCl_2$ ion exchange, most of the Ca, Sr, Ba, Ag, Cd and small amounts of the Mo, Tl, and Pb went into solution. In order to check if the chloride ions influenced the extractability, sequential extraction was repeated with 1 M $Mg(NO_3)_2$ (Fig. 6). As a result, Ag and Cd were not extracted. Their dissolution was hence triggered only by the chloride ions from $MgCl_2$ probably by forming chloro-complexes and not by the ion exchange with Mg^{2+}. Therefore, the influence of anions must be considered when studying metal ion exchanges to avoid misinterpretations. However, the chloride ions did not influence the extractability of other elements, as there was no significant difference between using $MgCl_2$ and $Mg(NO_3)_2$ except for Ba, which was extracted in higher quantities with $Mg(NO_3)_2$.

In conclusion, mainly the alkaline earth metals were exchanged by Mg^{2+} probably because Mg is itself an alkaline earth metal and thus has similar properties. Also, it is a small alkaline earth metal and thus could easily replace the larger alkaline earth metals.

Fly ashes usually contain high amounts of chloride. Therefore, varying chloride concentrations in fly ash can influence the extractability of certain elements. Additionally, chloride ions are of particular relevance in the FLUWA process, which is mentioned in the introduction. In this process, fly ash is washed with the wastewater from the flue gas scrubbers, which contains hydrochloric acid.

3.3.4. Step 4 – Acid-soluble fraction

Acid is needed to dissolve significant quantities of most elements. Acetic acid was chosen because acetate does not form sparingly soluble salts and has no oxidizing effect, unlike for example nitric acid, which was used in step 6 (oxidizable fraction) for this reason. Furthermore, with acetic acid, a constant pH could be achieved due to its buffer effect. In contrast, with strong acids, the pH always changed after each pH adjustment, and thus a pH-stat system would be necessary.

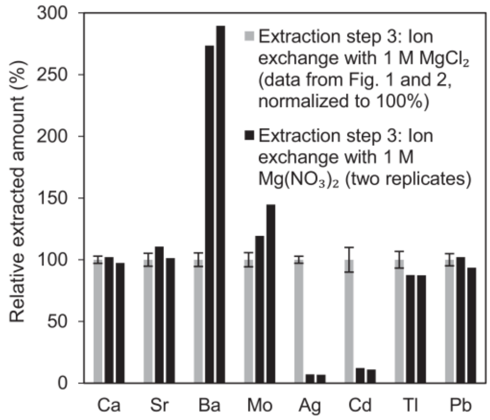

Fig. 6. Comparison of the extractability of several elements using $MgCl_2$ and $Mg(NO_3)_2$ in the extraction step 3 (ion exchange) using the fly ash FA-C as an example.

3.3.5. Steps 5 and 6 – Reducible and oxidizable fraction

The effect of changing the redox conditions was investigated in the extraction steps 5 and 6. In both steps, only relatively small quantities of most elements were dissolved. The pH was kept constant at 3 during steps 4–6 in order to eliminate the influences of pH variations as suggested by Van Herck and Vandecasteele (2001).

One characteristic feature of sequential extractions is the increasing strength and aggressiveness of the leaching solution with every step. Only the order of the reducing and the oxidizing step should be exchangeable, as they have an equivalent strength and only affect the redox conditions. By changing the order, the validity of these two steps can be checked because the interchange should not affect the extracted quantities in both steps. In Fig. 7, the extracted quantities when the reducing step was conducted before the oxidizing step are compared with the extracted quantities when the order was reversed. Only the elements dissolved significantly in the steps 5 and/or 6 were considered. The results show that the interchange had no significant influence on the extracted amounts in both steps for the majority of the elements. The reason there was a slight difference might be the fact that the residues were different at the beginning of steps 5 and 6 when the sequence was changed.

As both steps were interchangeable, a carryover from step 4 due to an insufficient washing of the residue or an inadequate leaching time could be excluded. The results prove that there was no significant extraction caused only by the increase in temperature after step 4. The temperature was increased in steps 5 and 6 to increase the reaction speed. In conclusion, by interchanging the reducing and the oxidizing step, influencing factors other than the reducing or oxidizing effect can be inspected.

The following discussion will investigate the reducing step in more detail. $NH_2OH{\cdot}HCl$ is commonly used in sequential extractions in the literature to determine the reducible fraction (Huang et al., 2007; Van Herck and Vandecasteele, 2001). NH_2OH is usually used in the form of its hydrochloride acid salt. As already shown in the ion exchange step, the chloride ions had a significant influence on

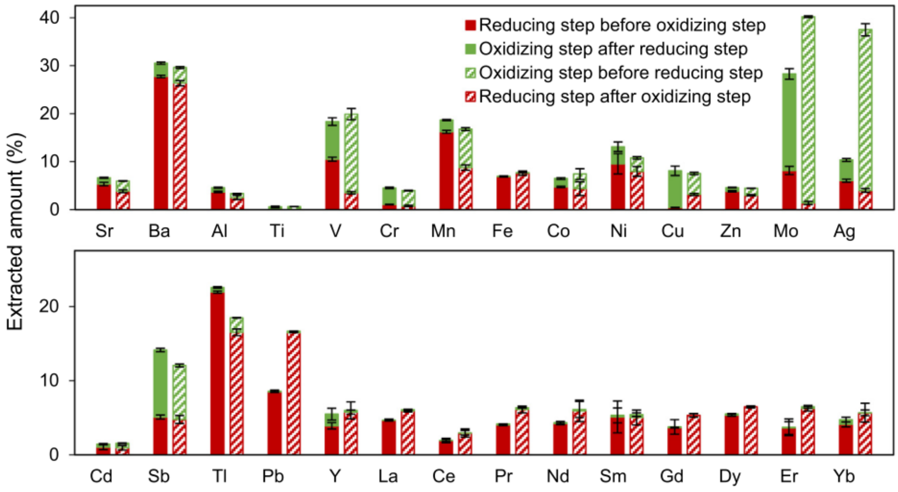

Fig. 7. Comparison of the extracted element quantities when the order of the reducing ($NH_2OH{\cdot}HCl$) and oxidizing step (H_2O_2) were reversed using the fly ash FA-A as an example. The extracted amounts are relative to the total content of the respective element given in Table 2. The error bars represent the standard deviation of three replicates.

the extractability of some elements. Therefore, we investigated the reducing extent of the $NH_2OH{\cdot}HCl$ responsible for the dissolution of the elements and which type of influence the chloride ions have.

For this purpose, the sequential extraction was repeated using 0.3 M NaCl (to obtain an equal chloride concentration as in 0.3 M $NH_2OH{\cdot}HCl$) in the reducing step. The influence of pH was eliminated by adjusting the pH to 3 with acetic acid in both experiments. Using 0.3 M HCl instead of NaCl was proven unsuitable because the pH of 0.3 M HCl was lower than 3.

In Fig. 8, the extracted quantities using $NH_2OH{\cdot}HCl$ and NaCl are compared for several elements using the fly ash FA-C as an example. Two replicates were extracted again with $NH_2OH{\cdot}HCl$ in parallel to the experiments with NaCl in order to verify the reproducibility of the data presented in Figs. 1–3. The concentrations of the verification experiment and with NaCl are relative to the extracted concentrations in the reducing step presented in Figs. 1–3, which are normalized to 100%. Although the extracted amounts with $NH_2OH{\cdot}HCl$ were rather small, the results still show a high reproducibility.

It can be seen clearly that significant amounts of those elements, which were dissolved with $NH_2OH{\cdot}HCl$, were also readily dissolved with NaCl. This means that the reducing effect of $NH_2OH{\cdot}HCl$ was only partly responsible for the dissolution. Only the dissolution of V, Fe, Mo, and partly Mn were explained by the reducing effect since these elements were not or only slightly dissolved with NaCl. This behavior was in accordance with the literature for Fe and Mn. Tessier et al. (1979) used $NH_2OH{\cdot}HCl$ to identify the elements bound to Fe-Mn oxides. In fly ashes, $NH_2OH{\cdot}HCl$ also dissolved V and Mo beside Fe and Mn. All other elements were already dissolved at around 50% or more with NaCl, compared to the extracted amount with $NH_2OH{\cdot}HCl$. Therefore, their extraction was not mainly driven by reduction.

The extraction of Ag appeared to be inhibited during the reducing condition because it was dissolved more significantly with NaCl than with $NH_2OH{\cdot}HCl$. As already shown with $MgCl_2$, the chlorides significantly influenced the solubility of Ag.

In conclusion, the effect of the chloride ions should also be considered, especially when $NH_2OH{\cdot}HCl$ is used to investigate which elements can be dissolved under a reducing condition.

3.3.6. Step 7 – Residue

The residue after the step 6 formed one of the most substantial fractions for most elements. With around 80% and more, the largest residues were observed for Ti, Cr, Fe, and Sc.

3.4. Total dissolved solids in each extraction step

The determination of total dissolved solids considers both the different amounts of metals in the ashes and the dissolved anions. Fig. 9 shows the total dissolved solids in each extraction

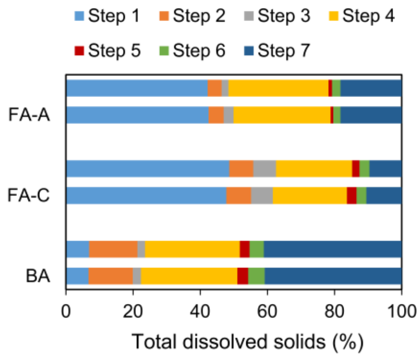

Fig. 9. Total dissolved solids in each extraction step for the fly ashes FA-A and FA-C, as well as for the bottom ash (two replicates each).

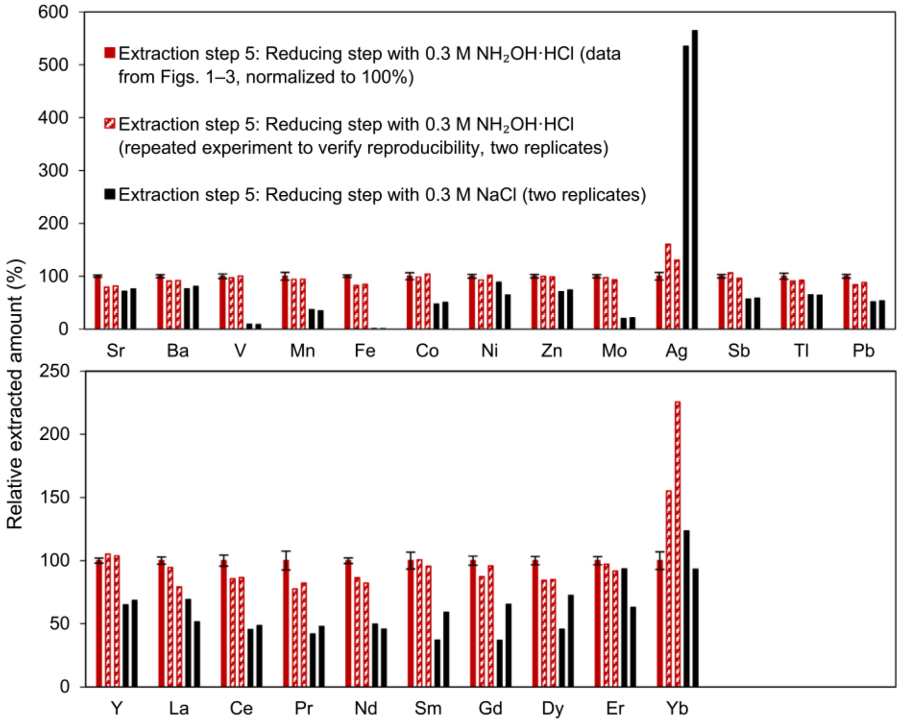

Fig. 8. Quantity comparison of the extracted elements in the reducing step with 0.3 M $NH_2OH{\cdot}HCl$ and 0.3 M NaCl using the fly ash FA-C as an example.

Table 3
Comparison of the total element contents in all the extraction steps with the analysis results of elemental composition. The sum of the extraction steps is given in percent relative to the analysis results (≙100%).

Alkali and alkaline earth metals

	Li	Na	K	Rb	Ca	Sr	Ba
FA-A	125	99	101	104	97	105	103
FA-C	157	100	124	85	98	95	93
BA	101	103	103	95	103	102	91

Other elements

	Al	Si	Ti	V	Cr	Mn	Fe	Co	Ni	Cu	Zn	Ga	Mo	Ag	Cd	Sb	Tl	Pb	Bi
FA-A	93	108	91	98	110	105	92	91	99	98	92	87	116	67	101	88	114	95	101
FA-C	99	116	87	91	101	95	90	85	96	96	94	79	110	111	91	93	107	68	105
BA	102	105	91	98	101	103	94	91	95	91	100	92	144	72	92	102	-*	107	93

Rare earth elements

	Sc	Y	La	Ce	Pr	Nd	Sm	Gd	Dy	Er	Yb
FA-A	116	97	100	91	107	108	114	95	128	102	116
FA-C	76	113	95	91	97	104	66	89	108	98	93
BA	93	96	94	93	92	97	86	97	102	101	86

[*] No data available, because Tl was below the limit of quantification.

step, for the fly ashes FA-A and FA-C, as well as for the bottom ash sample. The amount of total dissolved solids was very similar for both fly ashes in each extraction step. The water-soluble fraction (step 1) in the fly ashes was significantly higher than that in the bottom ash. As shown in Section 3.2, this was due to the higher water solubility of the alkali metals in the fly ash. Especially large quantities of Na and K were found in the fly ash, leading to a high proportion of dissolved solids. The water-soluble fraction after neutralization (step 2) was higher for the bottom ash, mainly due to the large quantities of dissolved Ca in this step. The amounts of dissolved solids in the extraction steps 3–6 were similar for all ashes. The mass loss due to the ion exchange (step 3) could be explained by the exchange of heavier ions by Mg^{2+}. The residual fraction of the bottom ash was higher than that of the fly ashes.

3.5. Validation of the results

In order to validate the measured concentrations in the extraction solutions, the element contents of all extraction steps were added up and then compared to the analysis results of the elemental composition given in Table 2. A high agreement of mostly ±10% was observed (Table 3). This verifies the results of the sequential extraction. It must be considered that all the extraction steps were afflicted with a certain error, which accumulated over all the extraction steps. Despite this fact, the results agreed very well.

4. Conclusion

Fly ashes from different incineration plants with similar flue gas cleaning had similar solubility behavior. Due to the observed similar extractability of individual elements from the two investigated fly ash samples, the binding forms must be similar too. Even though the bottom ash consisted of several elements at significantly different concentrations compared to the fly ashes, their solubility behavior was also similar. The main difference between fly ash and bottom ash was the solubility of the alkali metals, whereby those in the bottom ash were less soluble than in the fly ash. This information can for example be useful to assess whether the bottom ash fine fraction could be extracted together with the fly ash for example to obtain extracts for a subsequent metal recovery.

The fact that it can take several hours for a fly ash suspended in water to reach a strong alkaline pH is a substantial detail to note. Therefore, it can be necessary to check whether a fly ash sample either does not or only slightly react alkaline so that the buffering effect maintains a roughly neutral pH or whether it simply takes some time until the suspension becomes significantly alkaline. This has to be considered for example in applications where fly ashes are pre-washed with water, because the dissolved amounts of particularly Cd, Tl, and Mo depend mainly on the pH at the end of the washing process with the pH being strongly time-dependent. Therefore, it can be necessary to adjust the washing time for each fly ash sample, because the speed of the pH increase can differ widely between different samples.

The proposed sequential extraction procedure in this work should not be interpreted as an improvement of the Tessier procedure because this procedure was developed for a different purpose. In contrast to classical sequential extraction procedures, the presented modified procedure is better suited to obtain clear information about the factors determining the solubility of individual elements. For this, we recommend to change only one parameter compared to the previous step, and to exclude interfering parameters, such as pH differences. When cation ion exchange is investigated, the effect of the anions must also be considered.

The comprehensive leaching data in this work is useful in all processes where leaching of waste incineration residues is involved. The data can for example help to find optimal leaching conditions or to estimate the co-extraction of trace elements, which might be undesired or interfere, beside the target elements in a leaching process. The stepwise dissolution shows which conditions are necessary for each element to be dissolved and to what extent elements can be separated from each other by using different leaching solutions.

The presented sequential extraction procedure could be modified; for example, investigating ion exchange via other ions than Mg^{2+}, using a different acid or pH to obtain the acid-soluble fraction, or testing different reducing or oxidizing agents. Since only small amounts were dissolved using the reducing agent $NH_2OH{\cdot}HCl$ and oxidizing agent H_2O_2, other reducing/oxidizing agents might have a greater impact on the solubility. Moreover, the procedure could also be utilized for other samples beside waste incineration residues.

Acknowledgment

This work was funded in part by the German Federal Ministry of Education and Research (BMBF) [grant number 033R140]. We thank Wolfgang Zucha and Dr. Urs Eggenberger (University of Bern, Institute of Geological Sciences) for the XRD measurements.

Appendix A. Supplementary material

Supplementary data to this article can be found online at https://doi.org/10.1016/j.wasman.2019.02.001.

References

Abbas, Z., Moghaddam, A.P., Steenari, B.-M., 2003. Release of salts from municipal solid waste combustion residues. Waste Manage. 23, 291–305.

Bacon, J.R., Davidson, C.M., 2008. Is there a future for sequential chemical extraction? Analyst 133, 25–46.

Bruder-Hubscher, V., Lagarde, F., Leroy, M., Coughanowr, C., Enguehard, F., 2002. Application of a sequential extraction procedure to study the release of elements from municipal solid waste incineration bottom ash. Anal. Chim. Acta 451, 285–295.

Buchholz, B., Landsberger, S., 1995. Leaching dynamics studies of municipal solid waste incinerator ash. J. Air Waste Manage. Assoc. 45, 579–590.

Cornelis, G., Johnson, C.A., Van Gerven, T., Vandecasteele, C., 2008. Leaching mechanisms of oxyanionic metalloid and metal species in alkaline solid wastes: a review. Appl. Geochem. 23, 955–976.

A.-L. Fabricius, M. Renner, S. Fromm, A. Perfoll, M. Funk, L. Duester. Method Validation and Characterization of time-dependent Element Distributions in Waste Incineration Fly Ashes, in preparation.

Haberl, J., Koralewska, R., Schlumberger, S., Schuster, M., 2018. Quantification of main and trace metal components in the fly ash of waste-to-energy plants located in Germany and Switzerland: an overview and comparison of concentration fluctuations within and between several plants with particular focus on valuable metals. Waste Manage. 75, 361–371.

Huang, S.-J., Chang, C.-Y., Chang, F.-C., Lee, M.-Y., Wang, C.-F., 2007. Sequential extraction for evaluating the leaching behavior of selected elements in municipal solid waste incineration fly ash. J. Hazard. Mater. 149, 180–188.

Jiao, F., Zhang, L., Dong, Z., Namioka, T., Yamada, N., Ninomiya, Y., 2016. Study on the species of heavy metals in MSW incineration fly ash and their leaching behavior. Fuel Process. Technol. 152, 108–115.

Johnson, C.A., Brandenberger, S., Baccini, P., 1995. Acid neutralizing capacity of municipal waste incinerator bottom ash. Environ. Sci. Technol. 29, 142–147.

Karlfeldt Fedje, K., Ekberg, C., Skarnemark, G., Steenari, B.-M., 2010. Removal of hazardous metals from MSW fly ash—an evaluation of ash leaching methods. J. Hazard. Mater. 173, 310–317.

Karlfeldt, K., Steenari, B.-M., 2007. Assessment of metal mobility in MSW incineration ashes using water as the reagent. Fuel 86, 1983–1993.

Martin, J., Nirel, P., Thomas, A., 1987. Sequential extraction techniques: promises and problems. Mar. Chem. 22, 313–341.

Mizutani, S., Yoshida, T., Sakai, S.-I., Takatsuki, H., 1996. Release of metals from MSW I fly ash and availability in alkali condition. Waste Manage. 16, 537–544.

Nirel, P.M.V., Morel, F.M.M., 1990. Pitfalls of sequential extractions. Water Res. 24, 1055–1056.

Pan, Y., Wu, Z., Zhou, J., Zhao, J., Ruan, X., Liu, J., Qian, G., 2013. Chemical characteristics and risk assessment of typical municipal solid waste incineration (MSWI) fly ash in China. J. Hazard. Mater. 261, 269–276.

Quina, M.J., Bontempi, E., Bogush, A., Schlumberger, S., Weibel, G., Braga, R., Funari, V., Hyks, J., Rasmussen, E., Lederer, J., 2018. Technologies for the management of MSW incineration ashes from gas cleaning: new perspectives on recovery of secondary raw materials and circular economy. Sci. Total Environ. 635, 526–542.

Rauret, G., Lopez-Sanchez, J., Sahuquillo, A., Rubio, R., Davidson, C., Ure, A., Quevauviller, P., 1999. Improvement of the BCR three step sequential extraction procedure prior to the certification of new sediment and soil reference materials. J. Environ. Monit. 1, 57–61.

Tessier, A., Campbell, P.G., Bisson, M., 1979. Sequential extraction procedure for the speciation of particulate trace metals. Anal. Chem. 51, 844–851.

Van Herck, P., Van der Bruggen, B., Vogels, G., Vandecasteele, C., 2000. Application of computer modelling to predict the leaching behaviour of heavy metals from MSWI fly ash and comparison with a sequential extraction method. Waste Manage. 20, 203–210.

Van Herck, P., Vandecasteele, C., 2001. Evaluation of the use of a sequential extraction procedure for the characterization and treatment of metal containing solid waste. Waste Manage. 21, 685–694.

Weibel, G., Eggenberger, U., Schlumberger, S., Mäder, U.K., 2017. Chemical associations and mobilization of heavy metals in fly ash from municipal solid waste incineration. Waste Manage. 62, 147–159.

Xiong, Y., Zhu, F., Zhao, L., Jiang, H., Zhang, Z., 2014. Heavy metal speciation in various types of fly ash from municipal solid waste incinerator. J. Mater. Cycles Waste Manage. 16, 608–615.

Zhao, J., Wei, X., Li, T., Li, H., Bin, F., 2017. Behavior of alkali metals in fly ash during waste heat recovery for municipal solid waste incineration. Energy Fuels 32, 4417–4423.

Solubility of elements in waste incineration fly ash and bottom ash under various leaching conditions studied by a sequential extraction procedure

Jasmin Haberl*, Michael Schuster

Division of Analytical Chemistry, Department of Chemistry, Technical University of Munich,
85748 Garching, Lichtenbergstrasse 4, Germany

* Corresponding author.
E-mail address: jasmin.haberl@tum.de (J. Haberl).

Appendix A. Supplementary data

A.1. X-ray diffraction (XRD) analysis

Method

A mixture of 4 g ash and 1 g corundum (internal standard) was grinded for 6 min at 55 Hz in an XRD-Mill McCrone (Retsch) without the addition of any liquid. The powder mix (grain size 1–10 µm) was then mounted on a sample holder, disorientated and measured on an X'Pert^3 PRO Powder XRD (Malvern Panalytical) with the settings stated below. The data was evaluated using the software TOPAS-Academic-64 V6 and Rietveld refinement.

Start Position:	5.0044°2θ	Divergence Slit Type:	Fixed
End Position:	74.9764°2θ	Divergence Slit Size:	0.25°
Step Size:	0.017°2θ	Anode Material:	Cu
Scan Step Time:	200.025 s	Generator Settings:	40 mA, 40 kV

Results

Table A.1. Mineralogical composition of the fly ash samples FA-A and FA-C as well as of the bottom ash (BA) sample determined by XRD.

Mineral phase	Abbreviation	Chemical formula		wt.%	
			FA-A	FA-C	BA
Halite	Ha	$NaCl$	12.4	12.8	n.d.
Sylvite	Sy	KCl	2.4	3.2	n.d.
Anhydrite	An	$CaSO_4$	8.5	8.8	2.9
Quartz	Qtz	SiO_2	3.4	1.2	13.6
Calcite	Cc	$CaCO_3$	3.7	3.7	4.8
Portlandite	Por	$Ca(OH)_2$	0.8	2.8	4.3
Aphthitalite	Aph	$K_3Na(SO_4)_2$	2.6	6.8	n.d.
Bassanite	Bas	$CaSO_4 \cdot 0.5\ H_2O$	4.8	6.2	n.d.
Yavapaiite	Y	$KFe(SO_4)_2$	4.5	2.1	n.d.
Larnite	Lar	Ca_2SiO_4	10.4	7.4	10.3
K-Zn-Chloride		K_2ZnCl_4	9.4	n.d.	n.d.
Rutile	Rt	TiO_2	0.9	n.d.	0.2
Ankerite		$CaFe(CO_3)_2$	2.2	n.d.	n.d.
Periclase		MgO	0.4	n.d.	1.2
Albite	Ab	$Na(AlSi_3O_8)$	n.d.	n.d.	1.9
Gehlenite	Ge	$Ca_2Al(AlSiO_7)$	n.d.	n.d.	7.1
Hematite	He	Fe_2O_3	n.d.	n.d.	3.5
Wollastonite		$CaSiO_3$	n.d.	n.d.	4.9
Amorph + unidentified			33.7	45.0	45.3

n.d. = not detectable

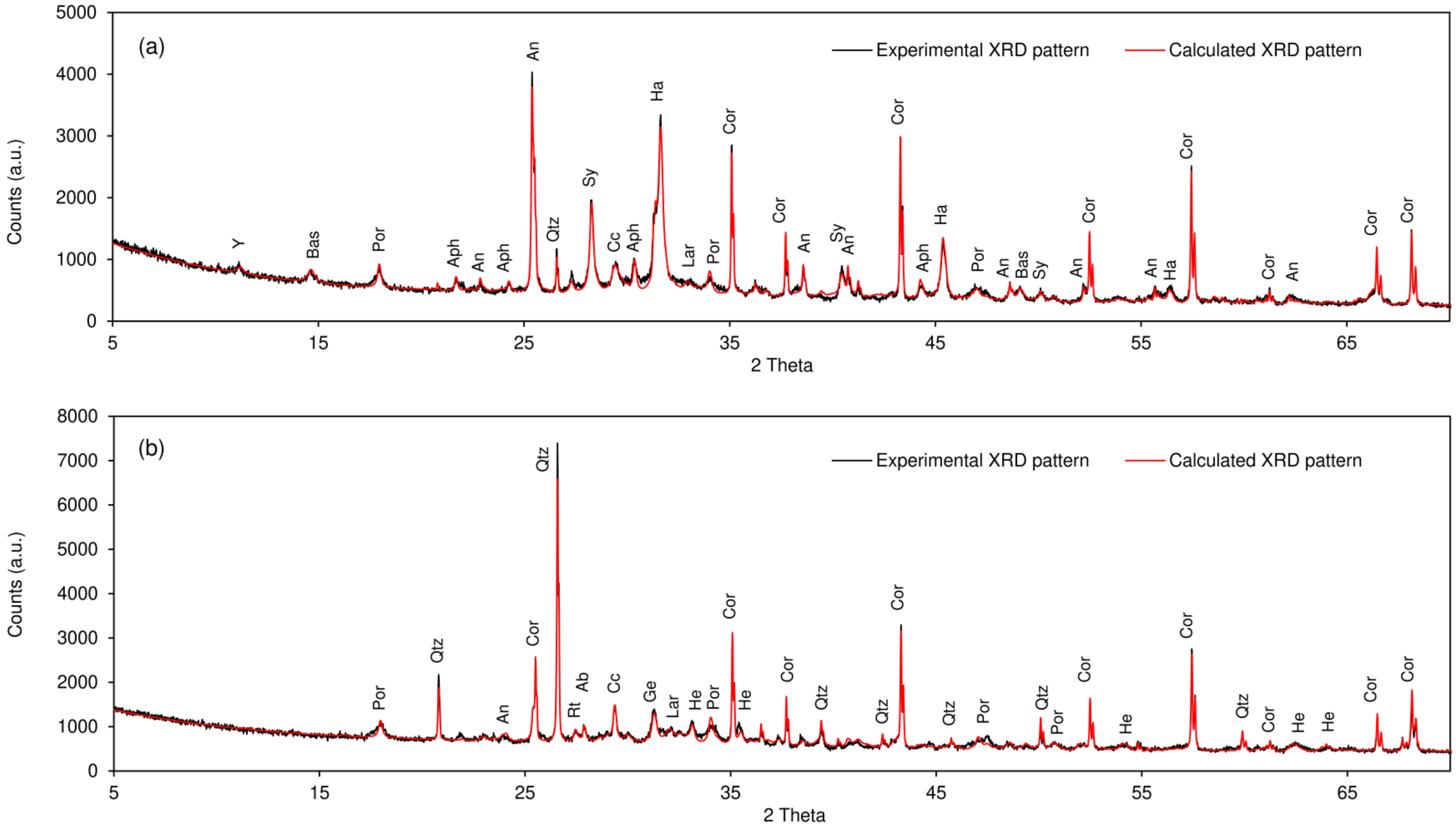

Fig. A.1. Experimental and calculated XRD patterns of the fly ash FA-C (a) and of the bottom ash (b). For the meaning of the abbreviations, please refer to Table A.1. Cor = Corundum.

A.2. Determination of the necessary leaching times

This section gives information about the chosen leaching times and the change in the concentration of several elements during the extraction steps. These concentration curves were the basis of decision-making for the required leaching time. The temporal leaching behavior varied for different elements. Thus, compromises were made between a complete dissolution and a reasonable experiment duration. The pH values were equal at each sampling.

Step 2 – Water-soluble fraction (neutral conditions)

It was assumed that compounds precipitated during step 1 re-dissolved fairly quickly because they were not enclosed by the fly ash matrix anymore. Therefore, a leaching time of 3 h was considered to be sufficient.

Step 3 – Ion-exchange fraction

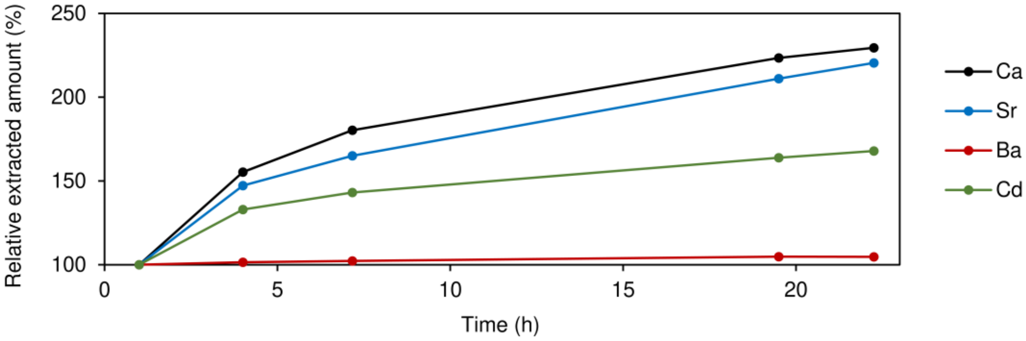

Fig. A.2. Concentration curves for several elements during the step 3 using the fly ash FA-A as an example. The extracted amounts at different time points are relative to the first sampling after 1 h. A leaching time of only 6 h was chosen in the final sequential extraction experiments because this step aimed to get qualitative rather than quantitative information about the exchangeable elements.

Step 4 – Acid-soluble fraction

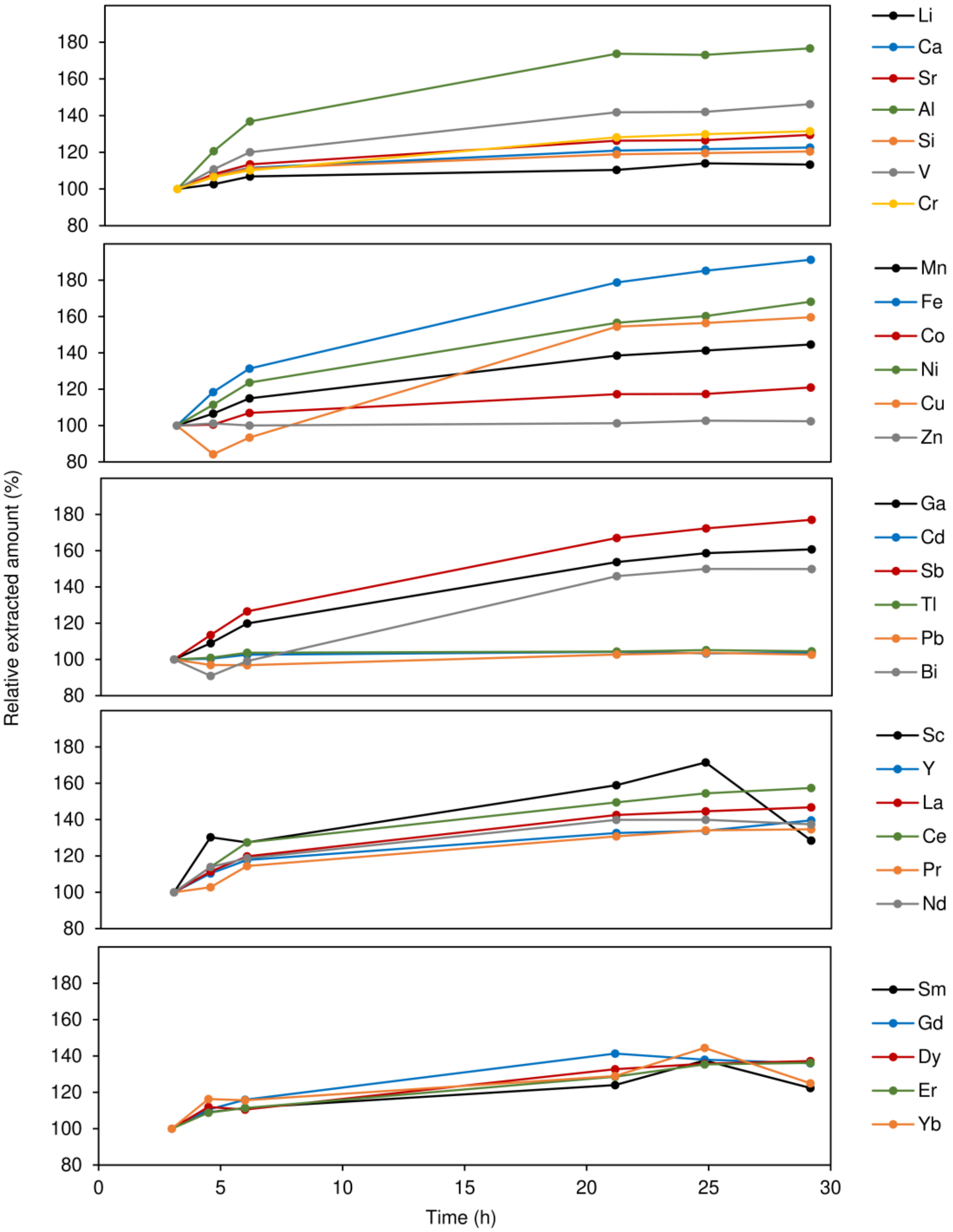

Fig. A.3. Concentration curves for several elements during the step 4 using the fly ash FA-A as an example. The extracted amounts at different time points are relative to the first sampling after 3 h. A leaching time of 24 h was chosen in the final sequential extraction experiments.

Step 5 – Reducible fraction

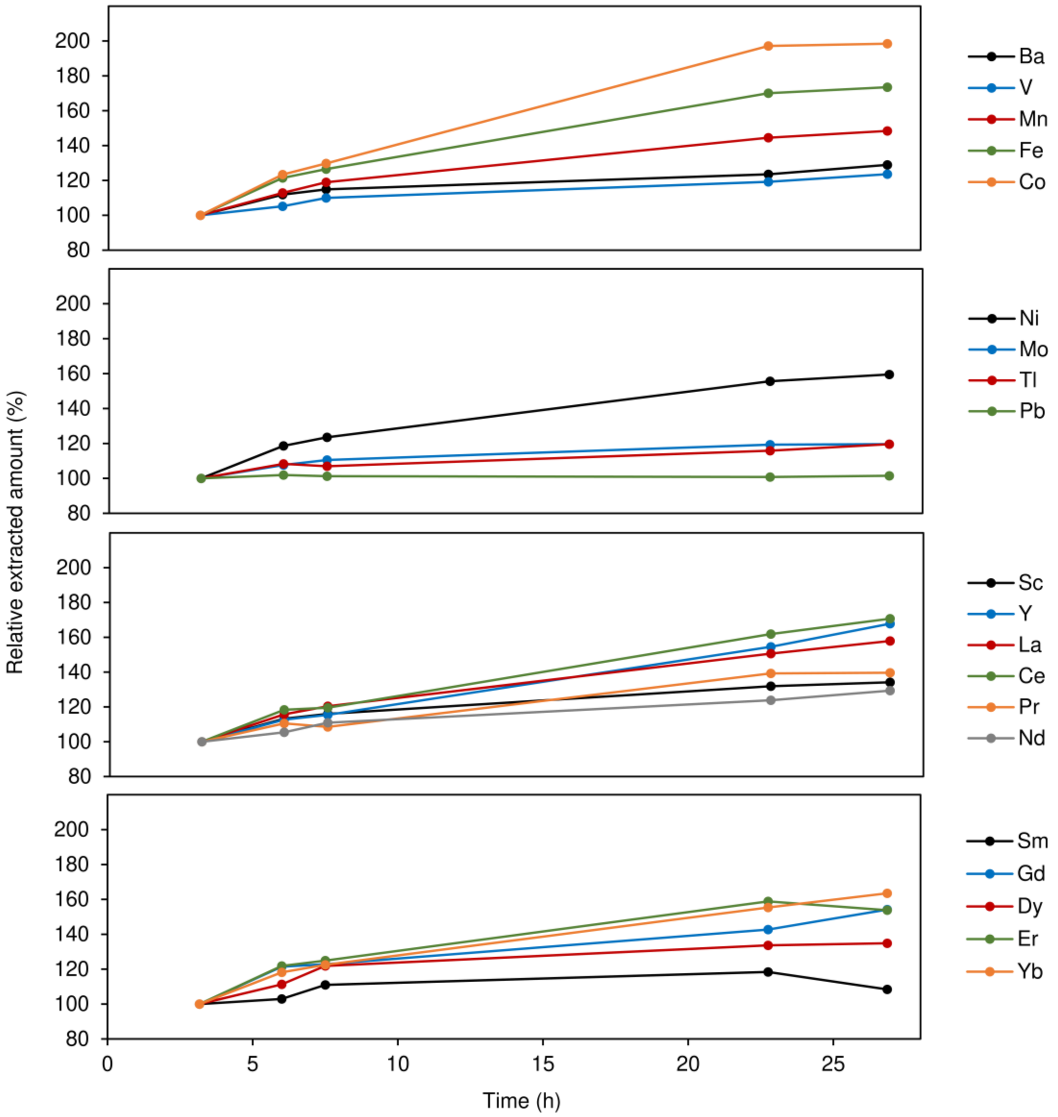

Fig. A.4. Concentration curves for several elements during the step 5 using the fly ash FA-A as an example. The extracted amounts at different time points are relative to the first sampling after 3 h. A leaching time of 24 h was chosen in the final sequential extraction experiments.

Step 6 – Oxidizable fraction

The leaching time in the step 6 was set to 24 h when the gas evolution by decomposing H_2O_2 had largely finished.

8.3. Publikation 3

Digestions vs. suspensions: The influence of sample preparation on precision and accuracy in total-reflection X-ray fluorescence analysis by the example of waste incineration fly ash

Jasmin Haberl *, Stephan Fromm, Michael Schuster

Division of Analytical Chemistry, Department of Chemistry, Technical University of Munich, 85748 Garching, Lichtenbergstrasse 4, Germany

* Corresponding author.
E-Mail: jasmin.haberl@tum.de

Abdruck des Artikels mit allgemeiner Genehmigung von Elsevier (siehe Kapitel 7.3) aus

Spectrochimica Acta Part B, 2019, 154, 82–90

DOI: 10.1016/j.sab.2019.02.004

Spectrochimica Acta Part B 154 (2019) 82–90

Contents lists available at ScienceDirect

Spectrochimica Acta Part B

journal homepage: www.elsevier.com/locate/sab

Digestions vs. suspensions: The influence of sample preparation on precision and accuracy in total-reflection X-ray fluorescence analysis by the example of waste incineration fly ash

Jasmin Haberl*, Stephan Fromm, Michael Schuster

Division of Analytical Chemistry, Department of Chemistry, Technical University of Munich, 85748 Garching, Lichtenbergstrasse 4, Germany

ARTICLE INFO

Keywords:
Total-reflection X-ray fluorescence spectrometry
Waste incineration fly ash
Sample preparation
Slurry sampling
Angle scan

ABSTRACT

The elements K, Ca, Ti, Mn, Fe, Cu, Zn, Rb, Sr, Pb, and Br in a fly ash sample from municipal waste incineration were determined by total-reflection X-ray fluorescence (TXRF) spectrometry. The fly ash was analyzed after microwave-assisted digestion and in the form of suspensions, each with several modifications. The results of the different sample preparation methods were compared with regard to precision and accuracy. Multiple sample spots were prepared for each sample preparation method, and the spread of the results was used as a measure of the precision. Accuracy was evaluated by comparing the median of the results with ICP–OES/ICP–MS analysis results. Additionally, the results were validated using a waste incineration fly ash reference material.

Different internal standards and the influence of adding a surfactant were tested for the digestion solution. For the suspensions, the fly ash sample was subjected to different grinding levels and suspended both in water and in 1% w/w nitric acid. Light microscope images were taken of the dried sample spots on the sample carrier, and their size and shape were visually compared.

Some sample preparation methods led to an inhomogeneous depth distribution of the analytes and/or the internal standard within the sample spots. This inhomogeneity was detected by angle scans and was found to be a main reason for systematic errors and/or a low precision. With optimized preparation of the suspension and of the digestion solution, comparable precision could be achieved, even in the range of the instrument precision. A suited sample preparation method that requires the least effort and least use of chemicals is presented for each element.

1. Introduction

Fly ashes are fine-grained particles produced during the incineration of waste. They are carried in the flue gas and usually separated by filters or cyclones. They are classified as a hazardous material because of their high concentrations of heavy metals. They are usually stored in landfills, where they can pose a risk to the environment. However, in the past few years, they have been increasingly regarded as a source for secondary raw materials [1–3]. In Switzerland, an industrial process was established for recovering, inter alia, Zn, Pb, and Cu from fly ash (FLUREC process) [4]. The recovery of metals is even prescribed by law from 2021 onwards (VVEA, art. 54, 1/1/2016). These examples demonstrate why a fast and simple analytical method to monitor the elemental composition of fly ashes is needed. Because of the various compositions of fly ashes from different incineration plants, matrix-dependent X-ray fluorescence (XRF) spectrometry is only suitable to a limited extent. Total-reflection X-ray fluorescence (TXRF) spectrometry is a less matrix-independent and more sensitive alternative which additionally enables simple measurements of suspensions. TXRF was already successfully applied for monitoring the metal concentrations in metallurgical slag before and after a recycling process [5].

Many different sample preparation techniques have been developed for solid samples for TXRF analysis. Mineralization, usually achieved by digestion, is the most common technique, being applied in 31% of the publications related to TXRF analysis from 2008 to 2012. Suspended samples were used in only 12% of cases even though this method is less elaborate than mineralization [6]. The literature includes only a few studies in which TXRF was used to analyze waste incineration fly ash [7–11]. In many cases, only a reference material was analyzed and the ash was usually digested prior to measurement. The ability to directly measure solids, thus enabling rapid sample preparation, is one of the greatest strengths of TXRF, and this advantage should be exploited.

---

* Corresponding author.
E-mail address: jasmin.haberl@tum.de (J. Haberl).

https://doi.org/10.1016/j.sab.2019.02.004
Received 6 November 2018; Received in revised form 8 February 2019; Accepted 11 February 2019

In this study, the analytical results of digestions and suspensions were compared with regard to precision and accuracy and the reasons for differences were identified. Because the preparation of suspensions is less elaborate, we evaluated whether the same precision could be achieved as with homogenous digestion solutions. We aimed to identify the sample preparation method for each element that requires the least effort and least use of chemicals.

Emphasis was placed on angle scans. We recorded the fluorescence intensity as a function of the incidence angle in the range below the critical angle of total reflection. This approach enables investigation of the depth distribution of the analytes and the internal standard within a sample spot. According to Mori and Uemura [12], the depth distribution is often overlooked and difficult to control and is therefore the most important error factor in TXRF analysis. In the literature, angle scans have been used only in a few studies to verify a homogenous depth distribution and, thus, the reliability of the measured values [13,14]. However, the course of the angle-dependent intensity profiles has been well investigated for different types of residues on the sample carrier like different particle sizes and shapes or layer structures [15,16].

2. Material and methods

In all experiments, ultrapure water (UPW) obtained from a Direct-Q® 5 UV water purification system (Merck Millipore) was used.

2.1. Description of the fly ash samples

The experiments were conducted with a fly ash sample originating from a municipal waste incineration plant in Germany. This sample has already been the subject of previous studies. A detailed description as well as validated analysis data for K, Ca, Ti, Mn, Fe, Cu, Zn, Rb, Sr, and Pb determined by inductively coupled plasma optical emission spectroscopy (ICP–OES) or inductively coupled plasma mass spectrometry (ICP–MS) can be found in previous work [17]. The experiments were conducted with fly ash sample C (this sample labeling refers to that used in Ref. [17]). In the present study, we used the analysis data given in Ref. [17] to validate the TXRF measurements. Fly ash C was used in two additional studies [18,19]. The reference material BCR 176R (fly ash collected in the electrostatic filters of a waste incineration plant) was used for additional validation.

2.2. Preparation of the fly ash digestion solutions

A sample quantity of 300 mg was digested with microwave assistance using 8 mL of nitric acid (65% w/w for analysis, Merck, purified by subboiling distillation), 1 mL of hydrochloric acid (30% w/w suprapur, Merck), and 1.5 mL of hydrofluoric acid (47% w/w ultrapur, VWR). Excess hydrofluoric acid was neutralized with 9 mL of saturated boric acid (suprapur, Merck) solution. A detailed description of the applied digestion procedure can be found in our previous work [17]. An aliquot of the digestion solution was diluted with UPW in a centrifuge tube so that 50 mg of digested fly ash were finally dissolved in a volume of approximately 40 mL.

When Se was used as an internal standard, 0.25 mL of a 1000 mg/L Se standard solution (in 0.5 mol/L nitric acid, Bernd Kraft) was added. When Ni was used as internal standard, 0.5 mL of a 1000 mg/L Ni standard solution (in 2% w/w nitric acid, Sigma-Aldrich) was added (a higher amount than Se due to the lower fluorescence yield). When a surfactant was used, 400 µL of Triton X-100 (Alfa Aesar) was added, corresponding to a surfactant concentration of approximately 1% v/v.

2.3. Preparation of the fly ash suspensions

Fly ash was ground by wet ball milling using zirconium oxide grinding tools (PM 100, Retsch). 10 g of ash was ground with 10 mL of ethanol (absolute for analysis, Merck Millipore) at 650 rpm for different grinding times (5 min, 20 min, and 60 min). Wet milling prevented the fly ash from caking on the grinding bowl. The ethanol was allowed to evaporate at room temperature before the samples were dried at 105 °C to constant weight (HE53, Mettler-Toledo).

Sample quantities of 100 mg fly ash were suspended in centrifuge tubes in 40 mL of water or 40 mL of 1% w/w nitric acid (prepared from a 65% w/w nitric acid solution for analysis, Merck, purified by subboiling distillation). 0.5 mL of a 1000 mg/L Se standard solution (in 0.5 mol/L nitric acid, Bernd Kraft) were added as an internal standard. Unless otherwise stated, the suspensions were treated ultrasonically for 30 min in a water bath (37 kHz, 160 W, Proclean 3.0DSP, Ulsonix).

2.4. Sample spot preparation on the sample carrier and TXRF measurements

TXRF measurements were performed with an Atomika 8010 TXRF spectrometer operated at 50 kV and 40 mA. The instrument was equipped with a Mo-target X-ray tube and a 80 mm^2 Si(Li) detector (due to an 8 mm diameter aperture, the detector can view an area with a diameter of up to 8 mm). During the measurements, the measuring chamber was flushed with nitrogen from a connected gas bottle. In a laminar flow cabinet, 1 µL of a prepared solution/suspension was pipetted on a Si wafer (sample carrier), which provides space for several spots. With 1 µL, the deadtime was in an ideal range. A stencil was used to ensure an exact positioning of the spots on defined positions (see graphical abstract). Suspensions were either shaken directly before each pipetting or continuously stirred with a stir bar during pipetting. Samples were pipetted from the upper layer of the suspension. The solvent was either gently evaporated on a heating plate or allowed to evaporate at room temperature. The incidence angle of the excitation radiation was set to 0.6 mrad and the lifetime (effective measurement time) was 120 s. For studies of the angular dependence of the signal intensity, angle scans were performed. The incidence angle was increased in 0.1 mrad increments from 0.1 to 1.7 mrad (1.8 mrad is the critical angle of total-reflection for Mo–Kα radiation on Si) by tilting the sample stage relative to the incidence beam as shown in Fig. 1. A spectrum of the same sample spot was acquired at each angle.

The Atomika 8010 TXRF spectrometer was introduced in the 1980s with software running under the operating system MS-DOS. Consequently, the evaluation software is quite user-unfriendly and cumbersome compared with modern software. Additionally, spectra processing is severely restricted due to low computing power. The Atomika software was therefore just used for spectra acquisition. For spectra evaluation, the software Spectra 5.3® was used. This software was developed by Bruker AXS Microanalysis GmbH for acquisition and evaluation of XRF spectra and is integrated into modern Bruker TXRF spectrometers. The raw spectra recorded with the Atomika software were converted into the Spectra 5.3®-compatible file format in an automated process.

2.5. Particle size measurements

Particle size distributions were determined by laser diffraction using a SALD-2201 particle size analyzer (Shimadzu). Samples were dispersed

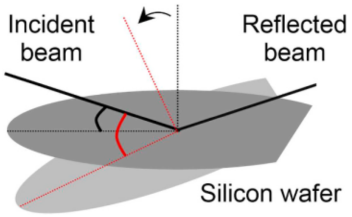

Fig. 1. Schematic illustration of the angle scans.

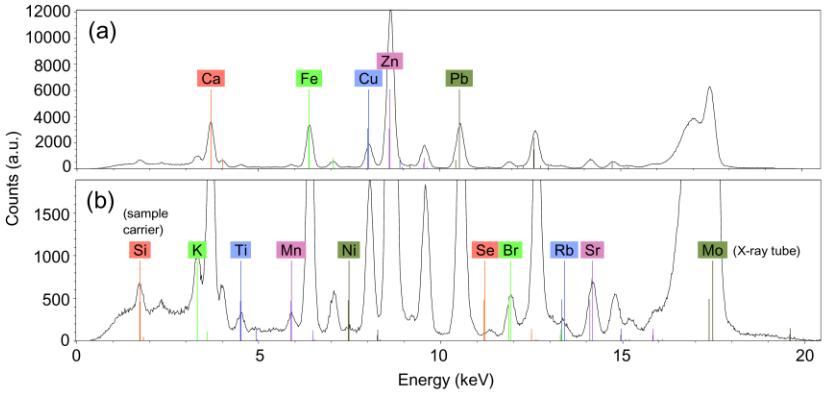

Fig. 2. TXRF spectrum of fly ash C (a: entire spectrum, b: magnification). The emission lines of the analytes K, Ca, Ti, Mn, Fe, Cu, Zn, Br, Rb, and Sr (K-series) and of Pb (L-series) are labeled. Additionally, the K-series emission lines of possible internal standards (Ni and Se) are labeled.

in isopropyl alcohol and treated with ultrasound for 1 min before measurement.

2.6. XRF measurements

For XRF measurements pressed pellets were prepared from 100 mg of sample and 20 mg of wax (Cereox, BM-0002-1, Fluxana) as a binding agent. The sample and wax were gently mixed to maintain the particle size of the sample and then pressed into pellets. Measurements were performed with an EDX-800HS spectrometer (Shimadzu) equipped with a Rh-target X-ray tube (voltage 50 kV, current 23–25 μA, excitation time 100 s, collimator diameter 5 mm, vacuum).

2.7. Microscope images of sample spots

To compare the size and shape of different sample spots on the Si wafer, light microscope images were taken (MZ8, Leica Microsystems).

3. Results and discussion

3.1. General applicability of TXRF spectrometry on waste incineration fly ash

Waste incineration fly ash contains a broad range of elements over a wide concentration range. Fig. 2 shows a TXRF spectrum of the fly ash used in this study. TXRF analysis of the detected elements K, Ca, Ti, Mn, Fe, Cu, Zn, Pb, Br, Rb, and Sr was the focus in this work. As fluorescence signals were present over the whole energy range, the choice of possible internal standards was limited. The main requirements for a suitable internal standard are a negligible concentration in the sample and no substantial overlap with other fluorescence signals. This applied, for example, to Ni and Se, which were both tested in this study. At 38 mg/kg, Se was present in a lower concentration than Ni (122 mg/kg) in the fly ash sample and was therefore preferred.

3.2. Overview of the various sample preparation methods

An overview of all investigated sample preparation methods M1–M15 is given in Table 1. The influence of the different sample preparation methods on the precision and accuracy of the results was determined. For this, 10 sample spots of each solution/suspension were prepared on the sample carrier. The spread of the results is a measure of the precision. Accuracy is defined as the closeness of the measured value to the true value, which is, by nature, indeterminable. Therefore, the agreement of the median of the 10 sample spots with the validated ICP–OES/ICP–MS analysis results was used to evaluate the accuracy.

The precision and accuracy of the different sample preparation methods of the fly ash are shown in Figs. 3 and 4. Additionally, the

Table 1
Overview of the various sample preparation methods M1–M15.

	Sample	Internal standard and additives	Ultrasonic treatment	Suspension homogenization	Sample spot drying
Digestion solutions					
M1	–	Se	–	–	Heating
M2	–	Se	–	–	Room temperature
M3	–	Se + 1% v/v Triton X-100	–	–	Heating
M4	–	Ni	–	–	Heating
Suspensions in water					
M5	Original ash	Se	30 min	Shaking	Heating
M6	Original ash	Se	30 min	Stirring	Heating
M7	Ground ash (5 min)	Se	30 min	Shaking	Heating
M8	Ground ash (20 min)	Se	30 min	Shaking	Heating
M9	Ground ash (60 min)	Se	30 min	Shaking	Heating
Suspensions in 1% v/v nitric acid					
M10	Original ash	Se	30 min	Shaking	Heating
M11	Ground ash (5 min)	Se	30 min	Shaking	Heating
M12	Ground ash (20 min)	Se	30 min	Shaking	Heating
M13	Ground ash (60 min)	Se	30 min	Shaking	Heating
M14	Original ash	Se	3 min	Shaking	Heating
M15[a]	Ground ash (60 min)	Se	30 min	Shaking	Room temperature

[a] Only for microscopic investigation in Section 3.5.

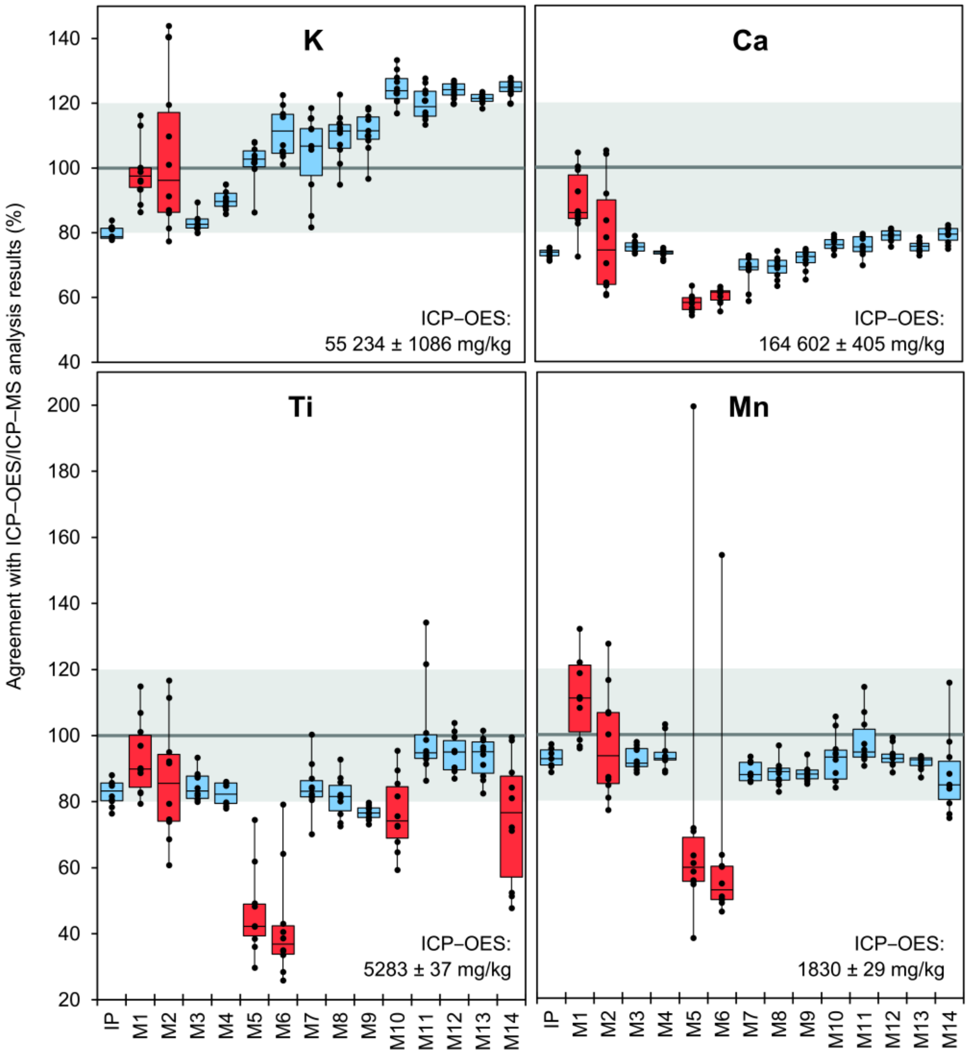

Fig. 3. Instrument precision (IP) and TXRF results for K, Ca, Ti, and Mn with sample preparation methods M1–M14. The data of the 10 sample spots prepared with each method are shown separately and as box plots with whiskers from the minimum to the maximum value. Measurements associated with problems discussed in the text are marked in red color. The validated ICP–OES/ICP–MS analysis data [17] are given in the bottom right corners. (For interpretation of the references to color in this figure legend, the reader is referred to the web version of this article.)

instrument precision (IP) was determined by measuring one sample spot (M3) 10 times to determine the maximally possible precision that can be achieved with the instrument used in this work. The results are discussed in Sections 3.3 and 3.4.

3.3. Measurement of fly ash digestion solutions

In the following section, the measurement of fly ash digestion solutions with TXRF is discussed. Specifically, the results of digestion preparation methods M1–M4 shown in Figs. 3 and 4 are discussed.

In method M1, the internal standard Se was added to the diluted digestion solution of the fly ash and 10 sample spots were gently dried on a heating plate. Because the solutions were fully homogenous, a high precision was expected. However, high scattering of the results was observed. Allowing the sample spots to dry at room temperature (M2) did not improve the precision. With both methods, only Cu showed a slightly better precision compared with the other elements.

To explain these phenomena, an angle scan of some spots was conducted. The angular dependences of the signal intensities of one spot are shown in Fig. 5 (M1). Se and Cu exhibited a substantially different angular behavior than the other elements. This observation can be explained as follows [14]. For an accurate quantification, all analytes as well as the internal standard must be evenly distributed within the sample spot to achieve an even excitation by the field of standing waves. In this case, the fluorescence intensity ratios of all elements are independent of the incidence angle. If the analytes or the internal standard exhibit an inhomogeneous depth distribution within the sample spot, different amounts of these elements are excited at various angles, which leads to different intensity ratios between the analytes and the internal standard at different angles, in turn leading to inaccurate results. The Se/Cu intensity ratio varied less with the incidence angle, whereas the intensity ratio between Se and the other elements varied more. This indicates that Se and Cu had a similar depth distribution within the sample spot. The other elements had the same depth distribution among each other, as evident from their constant intensity ratios at each angle, but their depth distribution differed from

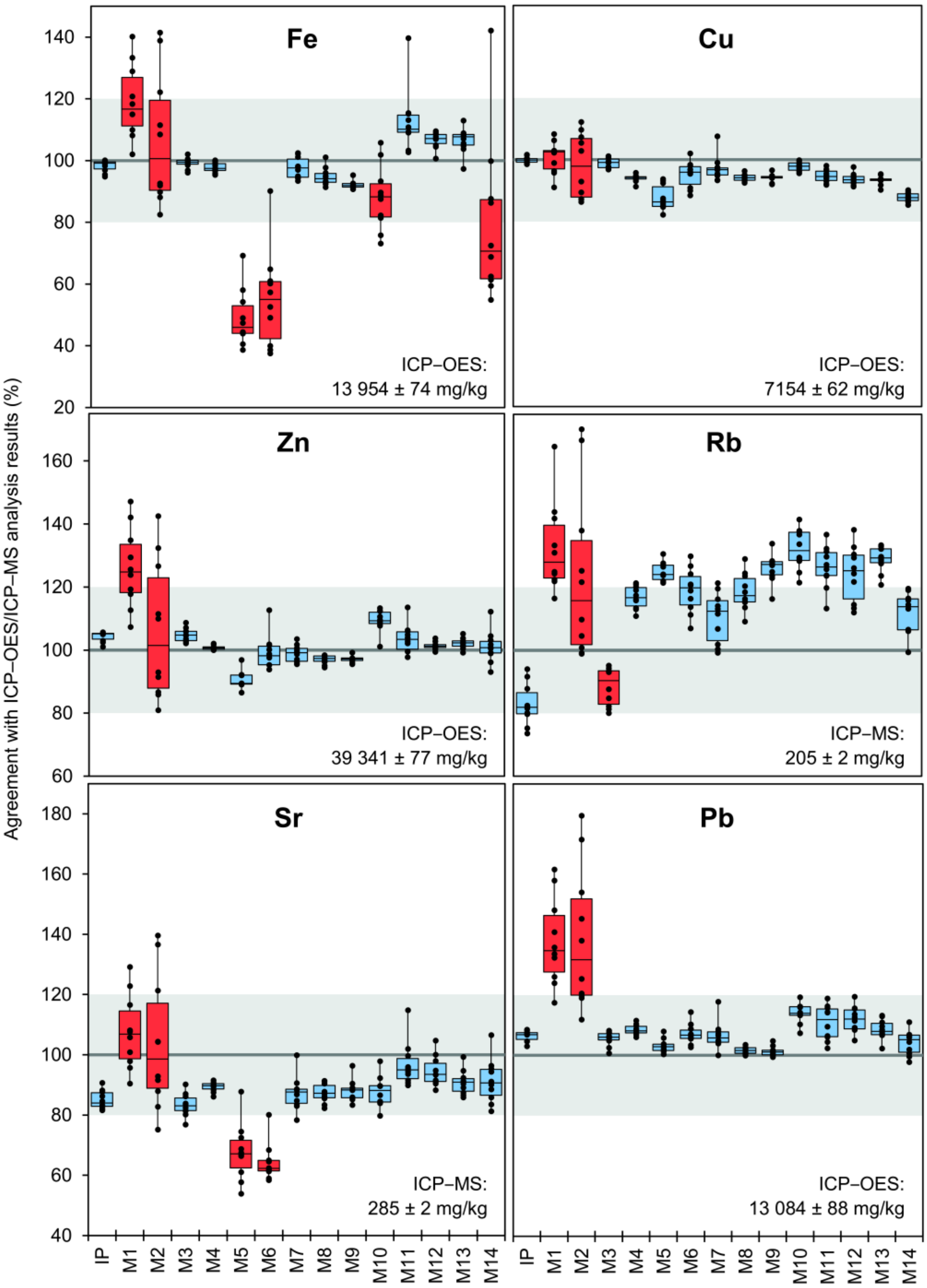

Fig. 4. Continuation of Fig. 3 for the elements Fe, Cu, Zn, Rb, Sr, and Pb.

those of Se and Cu. The weak angle dependency of the Se/Cu intensity ratio was likely caused by the proportion of Se and Cu distributed differently. Because of the varying intensity ratio with the internal standard, different concentrations were obtained at different angles. Considering all these issues, the high scattering between several spots may be explained. The depth distribution of Se is probably not the same in each spot. The measurement of several spots at the same incidence angle thus led to different results i.e. a high scattering.

The formation of an inhomogeneous depth distribution was prevented by adding a surfactant. In sample preparation method M3, Se was added again as an internal standard to the diluted digestion solution, along with the surfactant Triton X-100 with a final concentration of 1% v/v. Surfactants lead to the formation of a thinner sample layer on the sample carrier during the drying process (see Section 3.5). Triton X-100 is commonly used in the sample preparation of suspensions but is not usually used for digested samples [6]. Very precise results and good accuracy were achieved with the surfactant, confirming that the high scattering of the results without surfactant (M1 and M2) was caused by the inner structure of the sample spots. Triton X-100 is therefore also useful in the sample preparation of solutions.

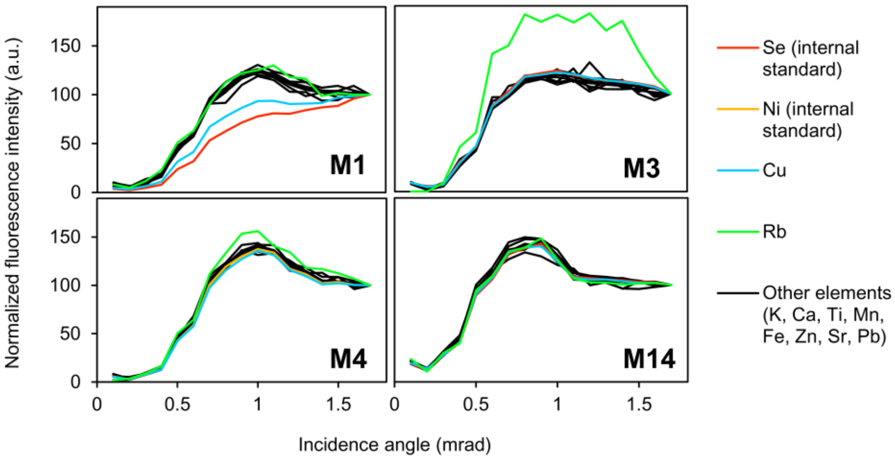

Fig. 5. Angle scan of one sample spot prepared with methods M1, M3, M4, and M14, respectively. The signal intensities at 1.7 mrad are normalized to 100%.

An angle scan was performed again to investigate the depth distribution (Fig. 5, M3). Se and the analytes showed the same angular behavior, except for Rb. Although the measured values for Rb exhibited low scattering and the median agreed to 90% with the ICP–MS analysis result, the angle scan revealed that potential error remained.

For this reason, a further modification in sample preparation was tested (M4). Ni was added as internal standard instead of Se, without a surfactant. The obtained precision and accuracy was comparable with those achieved with Se and surfactant (M3); however, the concentration of Rb was higher (117% agreement with the ICP–MS result). An angle scan revealed that all elements showed the same angular behavior (Fig. 5, M4). Therefore, we concluded that method M4 (Ni), not method M3 (Se and surfactant), gives the correct results for Rb and that a surfactant is not necessary when Ni is used as the internal standard. This is advantageous because the use of a surfactant has some drawbacks, such as foaming, and the use of Triton X-100 led to a substantially higher scattering of the Mo excitation radiation, causing a significant increase of the Mo signal. This increase in Mo signal intensity in turn increased the deadtime of the Si(Li) detector. The instrument precision and the precision achieved with the digestion solution using Ni as internal standard (M4) were comparable; therefore, no further optimization of the precision was possible with the used instrument.

The presented results show the importance of angle scans in the TXRF method development and validation. A clear statement of which method provides the correct result for Rb would not have been possible based solely on the degree of agreement with the ICP–MS analysis result. Some other studies have reported similar observations regarding angle scans. Fernández-Ruiz and Garcia-Heras [13] analyzed suspensions of archaeological ceramics with TXRF. They also found an anomalous angular behavior for the elements that had a poor recovery. Prange et al. [14] analyzed both a suspended and a digested coal fly ash reference material with Se as the internal standard. They found an anomalous angular behavior for Se only for the suspended sample. In the present study, we found that anomalous angular behaviors can also occur when solutions are measured and that such effects cannot be predicted with certainty.

For an additional validation, a digestion solution of the BCR 176R reference material was analyzed applying both methods M3 (Se and surfactant) and M4 (Ni) (Table 2). Again, the recovery of Rb with method M4 was approximately 20% higher than that with method M3 and the recovery was better with method M4 (81% vs. 102%). The recovery differences for Cu can be explained by an insufficient deconvolution of the signal overlapped with that of the internal standard Ni in method M4. As the Cu content was lower in the reference material compared to that in fly ash C (1050 mg/kg vs. 7154 mg/kg, respectively), this had a greater influence on the result for the reference material than for fly ash C.

Table 2
Concentrations of several elements in the BCR 176R reference material and in the measurement solutions (50 mg of the reference material dissolved in 40 mL). The recoveries with sample preparation methods M3 and M4 are given (median and relative standard deviation of 10 sample spots).

	Concentration in		Recovery (%)	
	Solid (mg/kg)	Measurement solution (mg/L)	M3	M4
Mn	730[b]	0.9	99 ± 8	99 ± 5
Fe	13,100[a]	16.4	96 ± 4	95 ± 2
Cu	1050[a]	1.3	103 ± 4	89 ± 6
Zn	16,800[a]	21.0	105 ± 1	97 ± 1
Rb	102[c]	0.1	81 ± 10	102 ± 3
Pb	5000[a]	6.3	100 ± 2	93 ± 2

[a] Certified values.
[b] Indicative values.
[c] Additional material information.

The results presented in this section were also observed for a fly ash sample from another waste incineration plant. The differences and characteristics of the investigated sample preparation methods were therefore not only valid for fly ash C.

3.4. Measurement of fly ash suspensions

In contrast to homogenous digestion solutions, fly ash suspensions are inhomogeneous through the contained particles. The particle size distribution of the original fly ash C and of different grinding levels are shown in Fig. 6. The particle size distribution of fly ash C was in a similar range like fly ash samples from other incineration plants. A comparison with fly ash samples originating from five other plants can be found in Fig. S1 in the Supplementary data in Appendix A. Suspensions were prepared both in water (M5–M9) and in 1% w/w nitric acid (M10–M14) using the original fly ash C as well as fly ash C samples subjected to the different grinding levels. Again, the precision and accuracy of different sample preparation methods was compared. The precision and accuracy of the TXRF measurements shown in Figs. 3 and 4 are discussed in this section.

Se proved to be suitable as an internal standard for the suspension measurements and was used for this reason. Fly ashes are alkaline in water [19,20]. Because the added Se standard solution contained nitric acid, the pH of the suspensions in water was in the approximate range

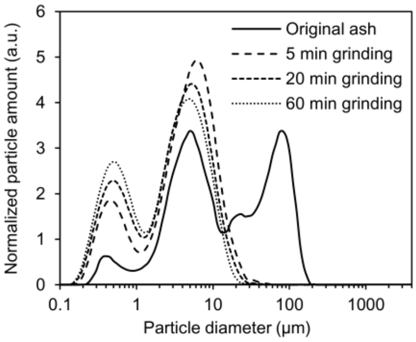

Fig. 6. Particle size distribution of fly ash C and of different grinding levels.

5–7. An ultrasonic treatment was necessary for all of the suspensions to break agglomerates, which were already visible to the naked eye. Ultrasound also accelerates the dissolution of solids [21–23].

Suspending the original fly ash in water (M5) led to an underestimation of several elements, especially Ca, Ti, Mn, Fe, and Sr. Grinding was necessary to achieve accurate values and also to achieve better precision for these elements. In contrast to the digestion measurements, a significantly lower scattering was observed with suspensions when Se was used as internal standard. Maybe the particles in the suspensions inhibit the inhomogeneous crystallization of Se within the sample spot. The acid mixture in the digestion solution could also influence the processes occurring within the sample spot during drying. No significant difference was observed between the different grinding times (M7–M9). The underestimations indicate that Ca, Ti, Mn, Fe, and Sr were mainly present as large and insoluble particles that quickly settled, resulting in an unrepresentative aliquot withdrawn from the upper layer of the suspension. After particle size reduction, the particles settled slower and were therefore more evenly distributed in the suspension. To avoid particle settling in the suspensions prepared from original fly ash, sample spots were prepared with 1-µL aliquots withdrawn while the solution was continuously stirred with a stir bar (M6) instead of being withdrawn after the solution was shaken (M5). This approach did not affect the underestimation of Ca, Ti, Mn, Fe, and Sr. Therefore, particle settling was not the main reason for the underestimation.

XRF measurements were performed with pressed pellets prepared from the original fly ash and from the ground fly ash (60 min). The fluorescence intensities were compared for each element (Fig. 7). Again, a substantially lower signal intensity was observed for Ca, Ti, Mn, and Fe with the original fly ash even though the particles were fixed in the pellets in contrast to the suspensions where particle settling occurs. Because the precision was high, the possibility that the differences were caused by inhomogeneities within the pellets was excluded. The reason for the differences is losses through X-ray absorption within the particles. The intensity of the emitted X-ray fluorescence is lower for large particles than for the same mass of small particles [24], indicating that Ca, Ti, Mn, Fe, and likely also Sr are present as large and insoluble particles in the fly ash. It must be noted, that the XRF and TXRF measurements are not directly comparable because the excitation conditions were different and because, unlike the fly ash in the pellets, the fly ash in the suspensions was partly dissolved. XRF could nevertheless be useful in distinguishing between particle settling effects and X-ray absorption effects caused by too large particles.

The TXRF results of the other elements (K, Cu, Zn, Rb, and Pb) showed no or only a small difference between the original and the ground fly ash. Grinding was therefore not necessary for analysis of these elements. However, accurate determination of Ca, Ti, Mn, Fe, and Sr requires reduction of the particle size.

Because grinding is quite elaborate, diluted acid was tested as a suspension liquid instead of water to achieve a particle size reduction through stronger dissolution of the ash. The original fly ash and the fly ash samples subjected to three different grinding levels were suspended in 1% w/w nitric acid (M10–M13). The recoveries were similar or slightly higher than those for the ground ashes in water; only the results for Ti and Fe were still underestimated and imprecise with the original ash. For all of the other elements, no substantial difference in accuracy and precision was observed between the original and the ground fly ash in 1% w/w nitric acid. Grinding was therefore not necessary if 1% w/w nitric acid was used as a suspension liquid. Grinding or digestion of the fly ash was necessary only for the determination of Ti and Fe.

To further shorten the sample preparation time, the ultrasonic treatment was reduced to 3 min (M14). This modification only marginally affected the results. Additionally, the element distribution between the solid and the liquid phase was determined in a suspension prepared via method M14. After centrifugation, the elements K, Ca, Cu, Zn, Rb, Sr, and Rb were found almost completely in the liquid phase (92–106% relative to the median values obtaines with method M13), although substantial amounts of solids remained in the suspension. Ti, Mn, and Fe were only partly in the liquid phase (23%, 75%, and 41%, respectively, relative to the median values obtaines with method M13). Details can be found in Fig. S2 in the Supplementary data in Appendix A.

Additionally, an angle scan was performed on a spot prepared via method M14 (Fig. 5, M14). The angular behavior of all elements was found to be equal. Suspensions of the BCR 176R reference material were not examined because the reference material is only available in

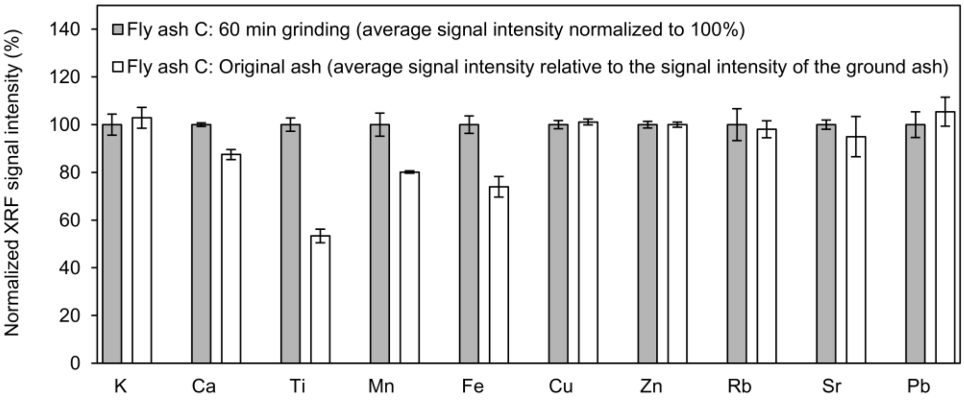

Fig. 7. XRF measurements of the original and the 60-min-ground fly ash C. The signal intensities of the original ash were relative to the signal intensities of the ground ash. Two pellets were prepared for each sample and were measured on both sides, resulting in four replicate measurements.

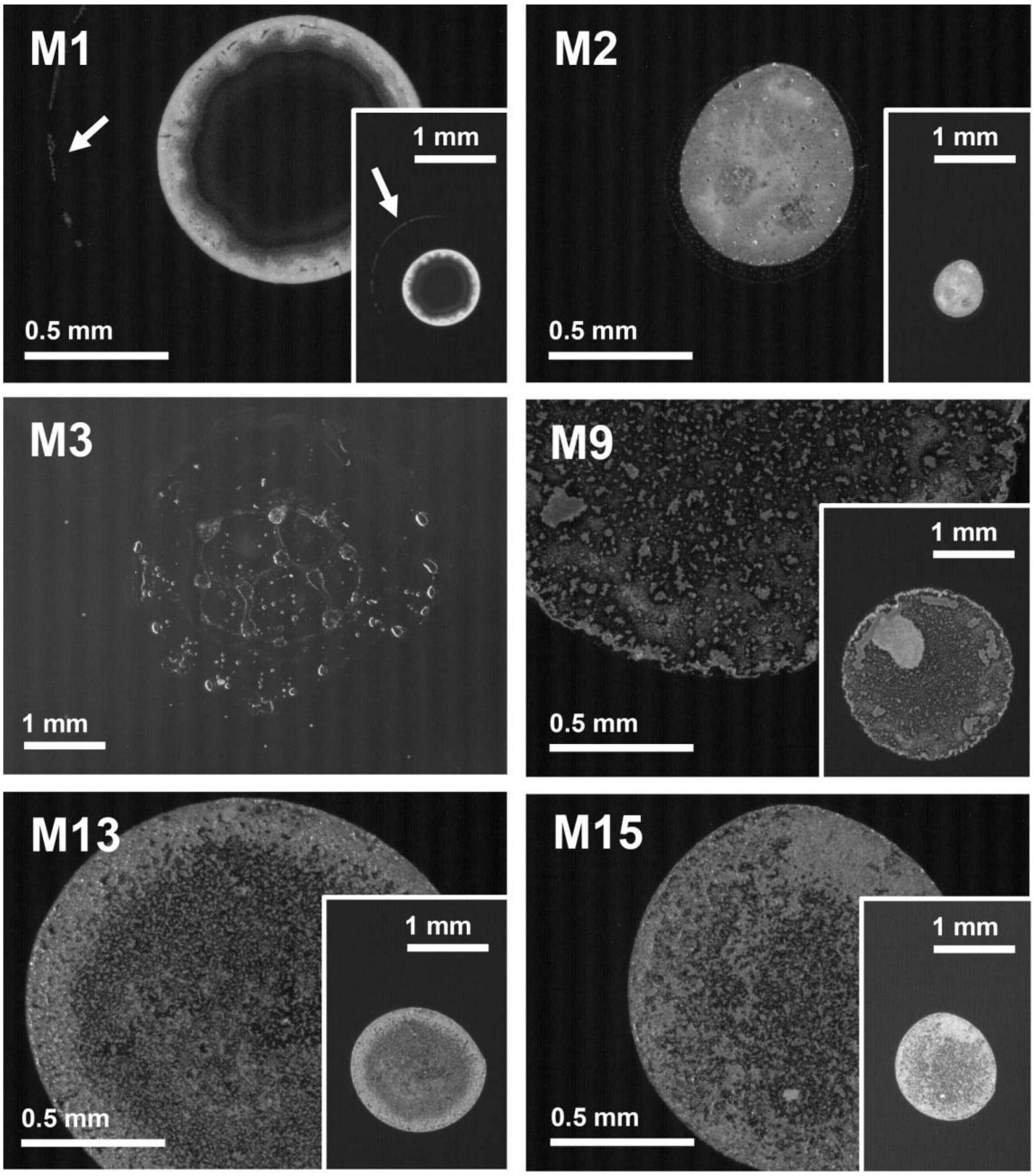

Fig. 8. Light microscope images of representative sample spots prepared with methods M1, M2, M3, M9, M13, and M15, respectively.

ground form. Analogous to the digestion solution measurements, the presented results in this section were also observed for a fly ash sample from another waste incineration plant. The differences and characteristics of the investigated sample preparation methods were therefore not only valid for fly ash C.

3.5. Influence of the sample preparation method on the shape of the sample spots

The different sample preparation methods also led to visual differences in the shape and size of the sample spots. Light microscope images of some representative sample spots are shown in Fig. 8.

Spots prepared from digestion solutions with Triton X-100 (M3) were considerably larger than those prepared without surfactant (M1). On the one hand, the use of surfactant leads to a thinner sample layer; on the other hand, the spreading of the sample on the carrier can lead to an exceedance of the detectable area. Spots without surfactant formed a ring due to the coffee-ring effect when they were dried on a heating plate (M1). Spots dried at room temperature (M2) did not exhibit this effect and had a dot-like shape instead. However, as shown previously, the shape did not influence the measurement results.

Sample spots of suspensions (M9, M13, and M15) were larger than the digestion solution spots (without surfactant). The digestion droplets likely first shrank without deposition of solids until solids began to crystallize. This effect is evident from a thin outer ring, which was likely the initial border of the droplet (see arrows in Fig. 8). The suspension spots were larger because particles immediately deposited as soon as the droplet started drying, leading to a larger spot area. The ring formation was less significant than in the digestion spots (M1) and even less significant when the suspension spots were dried at room temperature (M15).

3.6. Special case: analysis of Br

The determination of Br is complicated by the fact that bromide volatilizes as HBr from acid solutions [25]. The majority of Br volatilized from sample spots prepared from digestion solutions and suspensions in 1% w/w nitric acid. Because of the volatility, we assume that Br is predominantly present in the form of bromides. Br must therefore be determined in aqueous suspensions.

The Br concentration in the BCR 176R reference material is stated as 836 mg/kg as additional material information. With sample preparation method M5 (Se as internal standard, 30 min ultrasonic treatment, sample spot drying on a heating plate), a recovery of 88 ± 3% was achieved using the as-received reference material. The pH of the suspension was 7. Comparable recoveries were obtained with a reduced ultrasonic treatment time of 3 min (89 ± 1%) and when the spots were dried at room temperature (85 ± 2%). Because the reference material is only available in ground form, the necessity of grinding was determined for fly ash C. No influence of the grinding process on the obtained concentration or on the precision was observed, likely because the water solubility of bromides is usually high.

4. Conclusion

TXRF proved to be a suitable technique for the fast and simple determination of a broad range of elements in waste incineration fly ash. The same accuracy and precision can be achieved with suspensions as with digestion solutions. The precision was even in the range of the instrument precision in this study. An elaborate digestion is therefore not necessary. For an accurate and precise determination of Cu, Zn, Rb, and Pb, preparing a suspension of the fly ash in water without grinding is sufficient. As mentioned in the introduction, the elements Cu, Zn, and Pb are of main interest in the recovery of valuable metals from fly ash. It is advantageous, that these elements can be determined with this simple sample preparation method. When K, Ca, Mn, and Sr are also to be determined, 1% w/w nitric acid is recommended instead of water to obtain accurate and precise results. Grinding of the ash is necessary only for the determination of Ti and Fe. Because of the volatilization of Br as HBr, this element must be determined in a neutral aqueous suspension. Depending on the desired accuracy and precision of the results, the sample preparation can be selected accordingly. Measuring several replicates is highly recommended for the suspensions because inhomogeneity of the suspensions can cause outliers.

Angle scans of sample spots are an important tool for method development and validation to identify inhomogeneous depth distributions within a sample spot. These inhomogeneous depth distributions are hardly predictable and are dependent on the sample. Such inhomogeneities can lead to both low precision and systematic deviation.

As the results in this study could be reproduced with a further fly ash sample from a different waste incineration plant, the presented results are not only valid for the sample investigated in this study but are transferable to similar fly ash samples.

Acknowledgement

This work was funded by the German Federal Ministry of Education and Research (BMBF) [grant number 033R140]. The authors would like to thank the Bruker AXS Microanalysis GmbH for providing the Spectra software.

Appendix A. Supplementary data

Supplementary data to this article can be found online at https://doi.org/10.1016/j.sab.2019.02.004.

References

[1] J. Fellner, J. Lederer, A. Purgar, A. Winterstetter, H. Rechberger, F. Winter, D. Laner, Evaluation of resource recovery from waste incineration residues–The case of zinc, Waste Manag. 37 (2015) 95–103.

[2] V. Funari, R. Braga, S.N.H. Bokhari, E. Dinelli, T. Meisel, Solid residues from Italian municipal solid waste incinerators: a source for “critical” raw materials, Waste Manag. 45 (2015) 206–216.

[3] M.J. Quina, E. Bontempi, A. Bogush, S. Schlumberger, G. Weibel, R. Braga, V. Funari, J. Hyks, E. Rasmussen, J. Lederer, Technologies for the management of MSW incineration ashes from gas cleaning: New perspectives on recovery of secondary raw materials and circular economy, Sci. Total Environ. 635 (2018) 526–542.

[4] S. Schlumberger, M. Schuster, S. Ringmann, R. Koralewska, Recovery of high purity zinc from filter ash produced during the thermal treatment of waste and inerting of residual materials, Waste Manage. Res. 25 (2007) 547–555.

[5] I. De La Calle, M. Quade, T. Krugmann, U. Fittschen, Determination of residual metal concentration in metallurgical slag after acid extraction using total reflection X-ray fluorescence spectrometry, X-Ray Spectrom. 43 (2014) 345–352.

[6] I. De La Calle, N. Cabaleiro, V. Romero, I. Lavilla, C. Bendicho, Sample pretreatment strategies for total reflection X-ray fluorescence analysis: A tutorial review, Spectrochim. Acta B 90 (2013) 23–54.

[7] P. Fermo, F. Cariati, A. Pozzi, F. Demartin, M. Tettamanti, E. Collina, M. Lasagni, D. Pitea, O. Puglisi, U. Russo, The analytical characterization of municipal solid waste incinerator fly ash: methods and preliminary results, Fresenius J. Anal. Chem. 365 (1999) 666–673.

[8] N. Rodella, A. Bosio, R. Dalipi, A. Zacco, L. Borgese, L. Depero, E. Bontempi, Waste silica sources as heavy metal stabilizers for municipal solid waste incineration fly ash, Arab. J. Chem. 10 (2017) S3676–S3681.

[9] A.K. Detcheva, S.E. Mitsiev, P.S. Vassileva, J.H. Jordanov, M.G. Karadjov, E. Ivanova, Total reflection X-ray fluorescence analysis of fly ash from Bulgarian coal-fired power plants, Chem. Pap. 69 (2015) 650–654.

[10] W. Gerwinski, D. Goetz, Multielement analysis of standard reference materials with total reflection X-ray fluorescence (TXRF), Fresenius Z. Anal. Chem. 327 (1987) 690–693.

[11] M. Guarienti, A. Gianoncelli, E. Bontempi, S.M. Cardozo, L. Borgese, D. Zizioli, S. Mitola, L.E. Depero, M. Presta, Biosafe inertization of municipal solid waste incinerator residues by COSMOS technology, J. Hazard. Mater. 279 (2014) 311–321.

[12] Y. Mori, K. Uemura, Error Factors in Quantitative Total Reflection X-Ray Fluorescence Analysis, X-Ray Spectrom. 28 (1999) 421–426.

[13] R. Fernández-Ruiz, M. Garcia-Heras, Study of archaeological ceramics by total-reflection X-ray fluorescence spectrometry: Semi-quantitative approach, Spectrochim. Acta B 62 (2007) 1123–1129.

[14] A. Prange, U. Reus, H. Schwenke, J. Knoth, Optimization of TXRF measurements by variable incident angles, Spectrochim. Acta B 54 (1999) 1505–1511.

[15] R. Klockenkamper, J. Knoth, A. Prange, H. Schwenke, Total-reflection X-ray fluorescence, Anal. Chem. 64 (1992) 1115A–1123A.

[16] A. von Bohlen, M. Krämer, C. Sternemann, M. Paulus, The influence of X-ray coherence length on TXRF and XSW and the characterization of nanoparticles observed under grazing incidence of X-rays, J. Anal. At. Spectrom. 24 (2009) 792–800.

[17] J. Haberl, R. Koralewska, S. Schlumberger, M. Schuster, Quantification of main and trace metal components in the fly ash of waste-to-energy plants located in Germany and Switzerland: An overview and comparison of concentration fluctuations within and between several plants with particular focus on valuable metals, Waste Manag. 75 (2018) 361–371.

[18] A.-L. Fabricius, M. Renner, S. Fromm, A. Perfoll, M. Funk, L. Duester, Method validation and characterization of time-dependent element distributions in waste incineration fly ashes, (in preparation).

[19] J. Haberl, M. Schuster, Solubility of elements in waste incineration fly ash and bottom ash under various leaching conditions studied by a sequential extraction procedure, Waste Manag. 87 (2019) 268–278.

[20] G. Weibel, U. Eggenberger, S. Schlumberger, U.K. Mäder, Chemical associations and mobilization of heavy metals in fly ash from municipal solid waste incineration, Waste Manag. 62 (2017) 147–159.

[21] I. De La Calle, N. Cabaleiro, I. Lavilla, C. Bendicho, Ultrasound-assisted single extraction tests for rapid assessment of metal extractability from soils by total reflection X-ray fluorescence, J. Hazard. Mater. 260 (2013) 202–209.

[22] I. De La Calle, N. Cabaleiro, I. Lavilla, C. Bendicho, Analytical evaluation of a cup-horn sonoreactor used for ultrasound-assisted extraction of trace metals from troublesome matrices, Spectrochim. Acta B 64 (2009) 874–883.

[23] I. De La Calle, N. Cabaleiro, I. Lavilla, C. Bendicho, Ultrasound-assisted extraction of antimony and cobalt from inorganic environmental samples using a cup-horn sonoreactor prior to their determination by electrothermal-atomic absorption spectrometry, Int. J. Environ. Anal. Chem. 91 (2011) 1401–1411.

[24] J.W. Criss, Particle size and composition effects in X-ray fluorescence analysis of pollution samples, Anal. Chem. 48 (1976) 179–186.

[25] P.A. Fecher, A. Nagengast, Trace analysis in high matrix aqueous solutions using helium microwave induced plasma mass spectrometry, J. Anal. At. Spectrom. 9 (1994) 1021–1027.

Digestions vs. suspensions: The influence of sample preparation on precision and accuracy in total-reflection X-ray fluorescence analysis by the example of waste incineration fly ash

Jasmin Haberl*, Stephan Fromm, Michael Schuster

Division of Analytical Chemistry, Department of Chemistry, Technical University of Munich, 85748 Garching, Lichtenbergstrasse 4, Germany

* Corresponding author.

E-mail address: jasmin.haberl@tum.de (J. Haberl).

Appendix A. Supplementary data

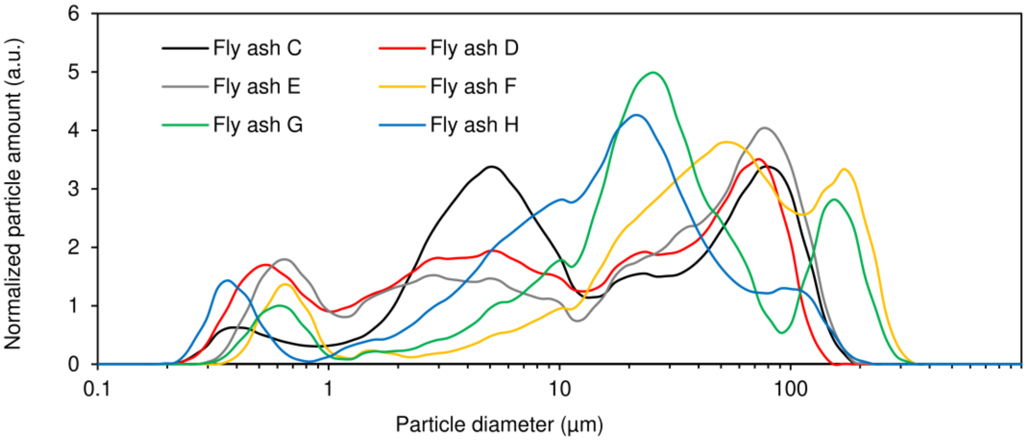

Fig. S1: Particle size distribution of fly ash samples from various waste incineration plants C–H. These samples are described in more detail in previous work [1]. The sample labeling refers to that used in Ref. [1].

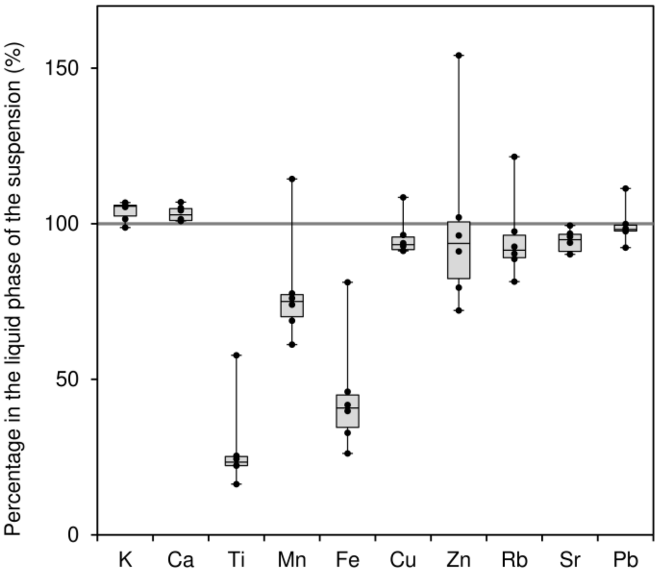

Fig. S2: Percentage of the elements in the supernatant of a suspension prepared with method M14 after centrifugation (20 min at 5000 rpm). Six aliquots from the supernatant were analyzed. The results of the six sample spots are shown separately and as box plots with whiskers from the minimum to the maximum value. The results are relative to the median values obtained with method M13 (cf. Figs. 3 and 4).

References

[1] J. Haberl, R. Koralewska, S. Schlumberger, M. Schuster, Quantification of main and trace metal components in the fly ash of waste-to-energy plants located in Germany and Switzerland: An overview and comparison of concentration fluctuations within and between several plants with particular focus on valuable metals, Waste Manage., 75 (2018) 361–371.

9. Vollständige Publikationsliste

Publikationen

1. Jasmin Haberl, Ralf Koralewska, Stefan Schlumberger, Michael Schuster, Quantification of main and trace metal components in the fly ash of waste-to-energy plants located in Germany and Switzerland: An overview and comparison of concentration fluctuations within and between several plants with particular focus on valuable metals, Waste Management, 2018, 75, 361–371.

2. Jasmin Haberl, Michael Schuster, Solubility of elements in waste incineration fly ash and bottom ash under various leaching conditions studied by a sequential extraction procedure, Waste Management, 2019, 87, 268–278.

3. Jasmin Haberl, Stephan Fromm, Michael Schuster, Digestions vs. suspensions: The influence of sample preparation on precision and accuracy in total-reflection X-ray fluorescence analysis by the example of waste incineration fly ash, Spectrochimica Acta Part B, 2019, 154, 82–90.

Poster

1. Jasmin Haberl, Michael Schuster, Vergleich des Rohstoffpotentials in Flugaschen aus verschiedenen Müllverbrennungsanlagen: Quantifizierung von Haupt- und Spurenelementen mittels ICP-OES, ICP-MS und TXRF. ANAKON 2017, Tübingen, Deutschland.

2. Jasmin Haberl, Michael Schuster, Determination of Metal Contents in Fly Ash from Waste Incineration Plants in Germany and Switzerland with Focus on Total Reflection X-Ray Fluorescence (TXRF) Spectroscopy. 101st Canadian Chemistry Conference 2018, Edmonton, Kanada.

Vortrag

1. Jasmin Haberl, Michael Schuster, Optimierung der Probenvorbereitung zur Analyse von Flugaschen aus Müllverbrennungsanlagen mittels Totalreflexions-Röntgenfluoreszenzanalyse. 8. XRF- und µXRF Workshop 2016, Münster, Deutschland.

10. Literatur

[1] A. Tisserant, S. Pauliuk, S. Merciai, J. Schmidt, J. Fry, R. Wood, A. Tukker, Solid waste and the circular economy: a global analysis of waste treatment and waste footprints, Journal of Industrial Ecology, 2017, 21, 628–640.

[2] Dritte allgemeine Verwaltungsvorschrift zum Abfallgesetz (TA Siedlungsabfall), Technische Anleitung zur Verwertung, Behandlung und sonstigen Entsorgung von Siedlungsabfällen vom 14. Mai 1993 (Bundesanzeiger Nr. 99a vom 29. Mai 1993), online abrufbar unter https://www.rh-entsorgung.de/de/Unternehmen/Rechtliche-Grundlagen/Rechtliche-Grundlagen/tasi-ges.pdf (aufgerufen am 08.10.2018).

[3] Verordnung über die umweltverträgliche Ablagerung von Siedlungsabfällen und über biologische Abfallbehandlungsanlagen vom 20. Februar 2001 (Bundesanzeiger Nr. 10 vom 27. Februar 2001). Online verfügbar unter: http://www.bgbl.de/xaver/bgbl/start.xav?startbk=Bundesanzeiger_BGBl&jumpTo=bgbl101s0305b.pdf (aufgerufen am 10.11.2018).

[4] Bayerisches Staatsministerium für Landesentwicklung und Umweltfragen (Hrsg.), Müllverbrennung: Die thermische Behandlung von Abfällen, München, 2002.

[5] H.-P. Fahrni, Schweizerische Technische Verordnung über Abfälle (TVA) – Verwertungsbedingungen für Rückstände aus Metallindustrie, Abfallverwertungsanlagen und Kraftwerken –, in: K.J. Thomé-Kozmiensky (Hrsg.), Aschen Schlacken Stäube – aus Abfallverbrennung und Metallurgie – , TK Verlag Karl Thomé-Kozmiensky, Neuruppin, 2013.

[6] Bundesamt für Umwelt BAFU, Abfallstatistik 2000: Fast die Hälfte der Siedlungsabfälle wird wiederverwertet, Medienmitteilung, Bern, 2002. Online verfügbar unter: https://www.admin.ch/gov/de/start/dokumentation/medienmitteilungen.msg-id-8421.html, Stand vom 20.04.2018 (aufgerufen am 07.05.2019).

[7] Verordnung über die Vermeidung und die Entsorgung von Abfällen (Abfallverordnung, VVEA) vom 4. Dezember 2015. Online verfügbar unter: https://www.admin.ch/opc/de/official-compilation/2015/5699.pdf (aufgerufen am 08.11.2018).

[8] M. Löschau, Reinigung von Abgasen – unter besonderer Berücksichtigung der thermischen Abfallbehandlung –, TK Verlag Karl Thomé-Kozmiensky, Neuruppin, 2014.

[9] Verband der Betreiber Schweizerischer Abfallverwertungsanlagen, Internetseite http://vbsa.ch/fakten/abfallverwertung/ (aufgerufen am 08.11.2018).

[10] M.J. Quina, E. Bontempi, A. Bogush, S. Schlumberger, G. Weibel, R. Braga, V. Funari, J. Hyks, E. Rasmussen, J. Lederer, Technologies for the management of MSW incineration ashes from gas cleaning: New perspectives on recovery of secondary raw materials and circular economy, Science of the Total Environment, 2018, 635, 526–542.

[11] X. Guo, H. Shi, K. Wu, Z. Ju, W.A. Dick, Performance and risk assessment of alinite cement-based materials from municipal solid waste incineration fly ash (MSWIFA), Materials and Structures, 2016, 49, 2383–2391.
[12] L.J. Belmonte, L.M. Ottosen, G.M. Kirkelund, P.E. Jensen, A.P. Vestbø, Screening of heavy metal containing waste types for use as raw material in Arctic clay-based bricks, Environmental Science and Pollution Research, 2018, 25, 32831–32843.
[13] G. Cappai, S. Cara, A. Muntoni, M. Piredda, Application of accelerated carbonation on MSW combustion APC residues for metal immobilization and CO2 sequestration, Journal of Hazardous materials, 2012, 207, 159–164.
[14] S. Schlumberger, M. Schuster, S. Ringmann, R. Koralewska, Recovery of high purity zinc from filter ash produced during the thermal treatment of waste and inerting of residual materials, Waste Management & Research, 2007, 25, 547–555.
[15] A. Purgar, F. Winter, D. Blasenbauer, S. Hartmann, J. Fellner, J. Lederer, H. Rechberger, Main drivers for integrating zinc recovery from fly ashes into the Viennese waste incineration cluster, Fuel Processing Technology, 2016, 141, 243–248.
[16] J. Fellner, J. Lederer, A. Purgar, A. Winterstetter, H. Rechberger, F. Winter, D. Laner, Evaluation of resource recovery from waste incineration residues–The case of zinc, Waste Management, 2015, 37, 95–103.
[17] H. Lassesson, K. Karlfeldt Fedje, B.-M. Steenari, Leaching for recovery of copper from municipal solid waste incineration fly ash: Influence of ash properties and metal speciation, Waste Management & Research, 2014, 32, 755–762.
[18] K. Karlfeldt Fedje, C. Ekberg, G. Skarnemark, E. Pires, B.-M. Steenari, Initial studies of the recovery of Cu from MSWI fly ash leachates using solvent extraction, Waste Management & Research, 2012, 30, 1072–1080.
[19] Y. Kalmykova, K. Karlfeldt Fedje, Phosphorus recovery from municipal solid waste incineration fly ash, Waste Management, 2013, 33, 1403–1410.
[20] K.J. Thomé-Kozmiensky, H.-W. Borchers, M. Faulstich, Maßnahmen zur Schadstoffreduzierung bei der Abfallverbrennung, in: K.J. Thomé-Kozmiensky (Hrsg.), Müllverbrennung und Umwelt 2, EF-Verlag für Energie- und Umwelttechnik GmbH, Berlin, 2. Ausgabe, 1991.
[21] G. Pfrang-Stotz, J. Schneider, Comparative studies of waste incineration bottom ashes from various grate and firing systems, conducted with respect to mineralogical and geochemical methods of examination, Waste Management & Research, 1995, 13, 273–292.
[22] L. Barniske, Stand der Abfallverbrennung in der Bundesrepublik Deutschland, in: K.J. Thomé-Kozmiensky (Hrsg.), Müllverbrennung und Umwelt 2, EF-Verlag für Energie- und Umwelttechnik GmbH, Berlin, 2. Ausgabe, 1991.

[23] A.J. Chandler, T.T. Eighmy, J. Hartlén, O. Hjelmar, D.S. Kosson, S.E. Sawell, H.A. van der Sloot, J. Vehlow, Municipal Solid Waste Incinerator Residues, The International Ash Working Group, Studies in Environmental Science 67, Elsevier, Amsterdam, Lausanne, New York, Oxford, Shannon, Tokyo, 1997.

[24] N.H. Le, A. Razakamanantsoa, M.-L. Nguyen, P.-L. Dao, D.H. Nguyen, Evaluation of physicochemical and hydromechanical properties of MSWI bottom ash for road construction, Waste Management, 2018, 80, 168–174.

[25] C. Caviglia, G. Confalonieri, I. Corazzari, E. Destefanis, G. Mandrone, L. Pastero, R. Boero, A. Pavese, Effects of particle size on properties and thermal inertization of bottom ashes (MSW of Turin’s incinerator), Waste Management, 2019, 84, 340–354.

[26] S. Bethanis, C. Cheeseman, C. Sollars, Properties and microstructure of sintered incinerator bottom ash, Ceramics International, 2002, 28, 881–886.

[27] J.D. Eusden, T.T. Eighmy, K. Hockert, E. Holland, K. Marsella, Petrogenesis of municipal solid waste combustion bottom ash, Applied Geochemistry, 1999, 14, 1073–1091.

[28] H. Belevi, D. Stämpfli, P. Baccini, Chemical behaviour of municipal solid waste incinerator bottom ash in monofills, Waste Management & Research, 1992, 10, 153–167.

[29] C.A. Johnson, S. Brandenberger, P. Baccini, Acid neutralizing capacity of municipal waste incinerator bottom ash, Environmental Science & Technology, 1995, 29, 142–147.

[30] E. Loginova, D. Volkov, P. van de Wouw, M. Florea, H. Brouwers, Detailed characterization of particle size fractions of municipal solid waste incineration bottom ash, Journal of Cleaner Production, 2019, 207, 866–874.

[31] J.J. Martin, R. Koralewska, A. Wohlleben, Advanced solutions in combustion-based WtE technologies, Waste Management, 2015, 37, 147–156.

[32] V. Funari, R. Braga, S.N.H. Bokhari, E. Dinelli, T. Meisel, Solid residues from Italian municipal solid waste incinerators: a source for “critical” raw materials, Waste Management, 2015, 45, 206–216.

[33] C. Fuchs, M. Schmidt, Aufbereitung und Wiederverwertung von Schlacken aus Abfallverbrennungsanlagen unter Rückgewinnung von Nichteisenmetallen, in: K.J. Thomé-Kozmiensky (Hrsg.), Aschen Schlacken Stäube – aus Abfallverbrennung und Metallurgie –, TK Verlag Karl Thomé-Kozmiensky, Neuruppin, 2013.

[34] W. Li, Z. Ma, Q. Huang, X. Jiang, Distribution and leaching characteristics of heavy metals in a hazardous waste incinerator, Fuel, 2018, 233, 427–441.

[35] L.S. Morf, R. Gloor, O. Haag, M. Haupt, S. Skutan, F. Di Lorenzo, D. Böni, Precious metals and rare earth elements in municipal solid waste–sources and fate in a Swiss incineration plant, Waste Management, 2013, 33, 634–644.

[36] B. Buchholz, S. Landsberger, Leaching dynamics studies of municipal solid waste incinerator ash, Journal of the Air and Waste Management Association, 1995, 45, 579–590.

[37] P. Van Herck, B. Van der Bruggen, G. Vogels, C. Vandecasteele, Application of computer modelling to predict the leaching behaviour of heavy metals from MSWI fly ash and comparison with a sequential extraction method, Waste Management, 2000, 20, 203–210.

[38] T. Mangialardi, A. Paolini, A. Polettini, P. Sirini, Optimization of the solidification/stabilization process of MSW fly ash in cementitious matrices, Journal of Hazardous materials, 1999, 70, 53–70.

[39] H. Belevi, H. Moench, Factors determining the element behavior in municipal solid waste incinerators. 1. Field studies, Environmental Science & Technology, 2000, 34, 2501–2506.

[40] M. Li, J. Xiang, S. Hu, L.-S. Sun, S. Su, P.-S. Li, X.-X. Sun, Characterization of solid residues from municipal solid waste incinerator, Fuel, 2004, 83, 1397–1405.

[41] L.S. Morf, P.H. Brunner, S. Spaun, Effect of operating conditions and input variations on the partitioning of metals in a municipal solid waste incinerator, Waste Management and Research, 2000, 18, 4–15.

[42] P.H. Brunner, H. Mönch, The flux of metals through municipal solid waste incinerators, Waste Management & Research, 1986, 4, 105–119.

[43] E. Allegrini, A. Maresca, M.E. Olsson, M.S. Holtze, A. Boldrin, T.F. Astrup, Quantification of the resource recovery potential of municipal solid waste incineration bottom ashes, Waste Management, 2014, 34, 1627–1636.

[44] Y.-S. Chung, J.-H. Moon, S.-H. Kim, S.-H. Kang, Y.-J. Kim, Determination of the elemental composition of the bottom ash of a municipal incinerator by instrumental neutron activation analysis, Journal of Radioanalytical and Nuclear Chemistry, 2007, 271, 339–344.

[45] A. Kida, Y. Noma, T. Imada, Chemical speciation and leaching properties of elements in municipal incinerator ashes, Waste Management, 1996, 16, 527–536.

[46] G. Weibel, U. Eggenberger, S. Schlumberger, U.K. Mäder, Chemical associations and mobilization of heavy metals in fly ash from municipal solid waste incineration, Waste Management, 2017, 62, 147–159.

[47] S. Abanades, G. Flamant, B. Gagnepain, D. Gauthier, Fate of heavy metals during municipal solid waste incineration, Waste Management & Research, 2002, 20, 55–68.

[48] D. Verhulst, A. Buekens, P.J. Spencer, G. Eriksson, Thermodynamic behavior of metal chlorides and sulfates under the conditions of incineration furnaces, Environmental Science & Technology, 1996, 30, 50–56.

[49] K.-S. Wang, K.-Y. Chiang, S.-M. Lin, C.-C. Tsai, C.-J. Sun, Effects of chlorides on emissions of toxic compounds in waste incineration: study on partitioning characteristics of heavy metal, Chemosphere, 1999, 38, 1833–1849.

[50] A. Jakob, S. Stucki, R.P.W.J. Struis, Complete heavy metal removal from fly ash by heat treatment: influence of chlorides on evaporation rates, Environmental Science & Technology, 1996, 30, 3275–3283.

[51] B. Nowak, A. Pessl, P. Aschenbrenner, P. Szentannai, H. Mattenberger, H. Rechberger, L. Hermann, F. Winter, Heavy metal removal from municipal solid waste fly ash by chlorination and thermal treatment, Journal of Hazardous materials, 2010, 179, 323–331.

[52] B. Nowak, S.F. Rocha, P. Aschenbrenner, H. Rechberger, F. Winter, Heavy metal removal from MSW fly ash by means of chlorination and thermal treatment: influence of the chloride type, Chemical Engineering Journal, 2012, 179, 178–185.

[53] J. Yu, Y. Qiao, L. Jin, C. Ma, N. Paterson, L. Sun, Removal of toxic and alkali/alkaline earth metals during co-thermal treatment of two types of MSWI fly ashes in China, Waste Management, 2015, 46, 287–297.

[54] J. Zhao, X. Wei, T. Li, H. Li, F. Bin, Behavior of Alkali Metals in Fly Ash during Waste Heat Recovery for Municipal Solid Waste Incineration, Energy & Fuels, 2018, 32, 4417–4423.

[55] F. Colangelo, R. Cioffi, F. Montagnaro, L. Santoro, Soluble salt removal from MSWI fly ash and its stabilization for safer disposal and recovery as road basement material, Waste Management, 2012, 32, 1179–1185.

[56] A.P. Bayuseno, W.W. Schmahl, Characterization of MSWI fly ash through mineralogy and water extraction, Resources, Conservation and Recycling, 2011, 55, 524–534.

[57] P. Van Herck, C. Vandecasteele, Evaluation of the use of a sequential extraction procedure for the characterization and treatment of metal containing solid waste, Waste Management, 2001, 21, 685–694.

[58] H. Vogg, M. Metzger, L. Stieglitz, Recent findings on the formation and decomposition of PCDD/PCDF in municipal solid waste incineration, Waste Management & Research, 1987, 5, 285–294.

[59] K. Tuppurainen, I. Halonen, P. Ruokojärvi, J. Tarhanen, J. Ruuskanen, Formation of PCDDs and PCDFs in municipal waste incineration and its inhibition mechanisms: a review, Chemosphere, 1998, 36, 1493–1511.

[60] M. Giugliano, S. Cernuschi, M. Grosso, E. Aloigi, R. Miglio, The flux and mass balance of PCDD/F in a MSW incineration full scale plant, Chemosphere, 2001, 43, 743–750.

[61] G. Zhang, J. Hai, J. Cheng, Characterization and mass balance of dioxin from a large-scale municipal solid waste incinerator in China, Waste Management, 2012, 32, 1156-1162.

[62] V. Funari, S.N.H. Bokhari, L. Vigliotti, T. Meisel, R. Braga, The rare earth elements in municipal solid waste incinerators ash and promising tools for their prospecting, Journal of Hazardous materials, 2016, 301, 471–479.

[63] S. Schlumberger, J. Bühler, Metallrückgewinnung aus Filterstäuben der thermischen Abfallbehandlung nach dem FLUREC-Verfahren, in: K.J. Thomé-Kozmiensky (Hrsg.), Aschen Schlacken Stäube – aus Abfallverbrennung und Metallurgie –, TK Verlag Karl Thomé-Kozmiensky, Neuruppin, 2013.

[64] F. Adam, D. Böni, F. Böni, Technischer Statusbericht Thermo-Recycling Stand Oktober 2011, Stiftung Zentrum für nachhaltige Abfall- und Ressourcennutzung, Hinwil, 2011. Online verfügbar unter: https://zar-ch.ch/fileadmin/user_upload/Contentdokumente/Oeffentliche_Dokumente/zar_technischerzwischenbericht.pdf (aufgerufen am 20.11.2018).
[65] K.J. Thomé-Kozmiensky, Möglichkeiten und Grenzen der Verwertung von Sekundärabfällen aus der Abfallverwertung, in: K.J. Thomé-Kozmiensky (Hrsg.), Aschen Schlacken Stäube – aus Abfallverbrennung und Metallurgie –, TK Verlag Karl Thomé-Kozmiensky, Neuruppin, 2013.
[66] H. Rietz, Erst brennen, dann trennen, Artikel in der Neuen Züricher Zeitung, Forschung & Technik, Ausgabe 5. Januar 2018. Online verfügbar unter: http://www.kezo.ch/fileadmin/user_upload/Medien/Presse/18_01_05_Seite_51_Thermorecycling_NZZpdf.pdf (aufgerufen am 20.11.2018).
[67] G. Doka, Life cycle inventories of municipal waste incineration with residual landfill & FLUWA filter asg treatment, Doka Life Cycle Assessments, Zürich, Schweiz, 2015. Beauftragt vom Bundeamt für Umwelt (BAUF), Bern. Online verfügbar unter: http://www.doka.ch/ecoinventMSWIupdateLCI2015.pdf (aufgerufen am 21.11.2018).
[68] S. Schlumberger, Neue Technologien und Möglichkeiten der Behandlung von Rauchgasreinigungsrückständen im Sinne eines nachhaltigen Ressourcenmanagements, in: Bundesamt für Umwelt BAFU, KVA-Rückstände in der Schweiz. Der Rohstoff mit Mehrwert, Bern, 2010. Online verfügbar unter: https://www.bafu.admin.ch/bafu/de/home/themen/abfall/publikationen-studien/publikationen/kva-rueckstaende-schweiz.html (aufgerufen am 21.03.2019).
[69] Europäische Kommission, Mitteilung der Kommission an das europäische Parlamant, den Rat, den europäischen Wirtschafts- und Sozialausschuss und den Ausschuss der Regionen, Grundstoffmärkte und Rohstoffe: Herausforderungen und Lösungsansätze, Brüssel, den 2.2.2011. Online verfügbar unter: https://eur-lex.europa.eu/legal-content/DE/TXT/PDF/?uri=CELEX:52011DC0025&from=DE (aufgerufen am 22.11.2018).
[70] Europäische Kommission, Mitteilung der Kommission an das europäische Parlamant, den Rat, den europäischen Wirtschafts- und Sozialausschuss und den Ausschuss der Regionen über die Überprüfung der Liste kritischer Rohstoffe für die EU und die Umsetzung der Rohstoffinitiative, Brüssel, den 26.5.2014. Online verfügbar unter: http://ec.europa.eu/transparency/regdoc/rep/1/2014/DE/1-2014-297-DE-F1-1.Pdf (aufgerufen am 08.05.2019).
[71] Europäische Kommission, Mitteilung der Kommission an das europäische Parlamant, den Rat, den europäischen Wirtschafts- und Sozialausschuss und den Ausschuss der Regionen über die Liste kritischer Rohstoffe für die EU 2017, Brüssel, den 13.9.2017. Online

verfügbar unter: https://ec.europa.eu/transparency/regdoc/rep/1/2017/DE/COM-2017-490-F1-DE-MAIN-PART-1.PDF (aufgerufen am 22.11.2018).

[72] M. Hammami, D.J. Ennigrou, K. Horchani-Naifer, M. Ferid, Comparative study of neodymium recovery from aqueous solutions by polyelectrolytes assisted-ultrafiltration, Korean Journal of Chemical Engineering, 2018, 35, 518–525.

[73] J. Llanos, Á. Pérez, P. Cañizares, Copper recovery by polymer enhanced ultrafiltration (PEUF) and electrochemical regeneration, Journal of Membrane Science, 2008, 323, 28–36.

[74] J. Zeng, X. Sun, L. Zheng, Q. He, S. Li, Recovery of Tungsten(VI) from Aqueous Solutions by Complexation-ultrafiltration Process with the Help of Polyquaternium, Chinese Journal of Chemical Engineering, 2012, 20, 831–836.

[75] A. Hirner, Trace element speciation in soils and sediments using sequential chemical extraction methods, International Journal of Environmental Analytical Chemistry, 1992, 46, 77–85.

[76] F.G. Viets Jr, Micronutrient availability, chemistry and availability of micronutrients in soils, Journal of Agricultural and Food Chemistry, 1962, 10, 174–178.

[77] J.R. Bacon, C.M. Davidson, Is there a future for sequential chemical extraction?, Analyst, 2008, 133, 25–46.

[78] C.E. Casalino, M. Malandrino, A. Giacomino, O. Abollino, Total and fractionation metal contents obtained with sequential extraction procedures in a sediment core from Terra Nova Bay, West Antarctica, Antarctic Science, 2013, 25, 83–98.

[79] C. Gleyzes, S. Tellier, M. Astruc, Fractionation studies of trace elements in contaminated soils and sediments: a review of sequential extraction procedures, TRAC Trends in Analytical Chemistry, 2002, 21, 451–467.

[80] G. Rauret, Extraction procedures for the determination of heavy metals in contaminated soil and sediment, Talanta, 1998, 46, 449–455.

[81] V. Kennedy, A. Sanchez, D. Oughton, A. Rowland, Use of single and sequential chemical extractants to assess radionuclide and heavy metal availability from soils for root uptake, Analyst, 1997, 122, 89R–100R.

[82] A. Tessier, P.G.C. Campbell, Partitioning of trace elements in sediments: Relationships with bioavailability, in: R.L. Thomas, R. Evans, A.L. Hamilton, M. Munawar, T.B. Reynoldson, M.H. Sadar (Hrsg.), Ecological Effects of In Situ Sediment Contaminants. Developments in Hydrobiology, Band 39, Springer Verlag, Dordrecht, 1987.

[83] A. Tessier, P.G. Campbell, M. Bisson, Sequential extraction procedure for the speciation of particulate trace metals, Analytical Chemistry, 1979, 51, 844–851.

[84] A. Filgueiras, I. Lavilla, C. Bendicho, Chemical sequential extraction for metal partitioning in environmental solid samples, Journal of Environmental Monitoring, 2002, 4, 823–857.

[85] M. Kersten, C.-D. Garbe-Schönberg, S. Thomsen, C. Anagnostou, A. Sioulas, Source apportionment of Pb pollution in the coastal waters of Elefsis Bay, Greece, Environmental Science & Technology, 1997, 31, 1295–1301.

[86] B. Marin, M. Valladon, M. Polve, A. Monaco, Reproducibility testing of a sequential extraction scheme for the determination of trace metal speciation in a marine reference sediment by inductively coupled plasma-mass spectrometry, Analytica Chimica Acta, 1997, 342, 91–112.

[87] M. Gibson, J. Farmer, Multi-step sequential chemical extraction of heavy metals from urban soils, Environmental Pollution Series B, Chemical and Physical, 1986, 11, 117–135.

[88] D.M. Diks, H.E. Allen, Correlation of copper distribution in a freshwater-sediment system to bioavailability, Bulletin of Environmental Contamination and Toxicology, 1983, 30, 37–43.

[89] C.Y. Chang, H.L. Chiang, Z.J. Su, C.F. Wang, A sequential extraction method measures the toxic metal content in fly ash from a municipal solid waste incinerator, Journal of the Chinese Chemical Society, 2005, 52, 921–926.

[90] A. Ure, P. Quevauviller, H. Muntau, B. Griepink, Speciation of heavy metals in soils and sediments. An account of the improvement and harmonization of extraction techniques undertaken under the auspices of the BCR of the Commission of the European Communities, International Journal of Environmental Analytical Chemistry, 1993, 51, 135–151.

[91] P. Quevauviller, G. Rauret, H. Muntau, A. Ure, R. Rubio, J. López-Sánchez, H. Fiedler, B. Griepink, Evaluation of a sequential extraction procedure for the determination of extractable trace metal contents in sediments, Fresenius' Journal of Analytical Chemistry, 1994, 349, 808–814.

[92] G. Rauret, J. Lopez-Sanchez, A. Sahuquillo, R. Rubio, C. Davidson, A. Ure, P. Quevauviller, Improvement of the BCR three step sequential extraction procedure prior to the certification of new sediment and soil reference materials, Journal of Environmental Monitoring, 1999, 1, 57–61.

[93] Z. Yutong, X. Qing, L. Shenggao, Chemical fraction, leachability, and bioaccessibility of heavy metals in contaminated soils, Northeast China, Environmental Science and Pollution Research, 2016, 23, 24107–24114.

[94] Z. Evans, H. Van Ryswyk, M. Los Huertos, T. Srebotnjak, Robust spatial analysis of sequestered metals in a Southern California Bioswale, Science of the Total Environment, 2019, 650, 155–162.

[95] Y. Liu, J. Zhang, H. He, Assessment of the Tessier and BCR sequential extraction procedures for elemental partitioning of Ca, Fe, Mn, Al, and Ti and their application to surface sediments from Chinese continental shelf, Acta Oceanologica Sinica, 2018, 37, 22–28.

[96] A. Bogusz, P. Oleszczuk, Sequential extraction of nickel and zinc in sewage sludge-or biochar/sewage sludge-amended soil, Science of the Total Environment, 2018, 636, 927–935.

[97] Z.B. Lu, M. Kang, Risk assessment of toxic metals in marine sediments from the Arctic Ocean using a modified BCR sequential extraction procedure, Journal of Environmental Science and Health, Part A, 2018, 53, 278–293.

[98] W. Miller, D. Martens, L. Zelazny, Effect of Sequence in Extraction of Trace Metals from Soils, Soil Science Society of America Journal, 1986, 50, 598–601.

[99] M.K. Schultz, W.C. Burnett, K.G. Inn, Evaluation of a sequential extraction method for determining actinide fractionation in soils and sediments, Journal of Environmental Radioactivity, 1998, 40, 155–174.

[100] A. Bouzidi, A. Ararem, D. Imessaoudene, B. Yabrir, Sequential extraction of Cs and Sr from Ain Oussera soils around Es-Salam research reactor facility, Journal of Environmental Sciences, 2015, 36, 163–172.

[101] S. Akkus, T. Bal, N.M. Karaaslan, E. Yaman, E. Kilinc, M. Yaman, Fractionation of Ni, Cr and Cu from soil by sequential extraction procedure and determination by inductively coupled plasma optical emission spectrometry, CLEAN–Soil, Air, Water, 2013, 41, 1229–1234.

[102] H. Zhu, C. Wang, P. Wang, J. Hou, J. Qian, Y. Ao, C. Liu, Speciation of potentially mobile Si in Yangtze Estuary surface sediments: estimates using a modified sequential extraction technique, Environmental Science and Pollution Research, 2016, 23, 18928–18941.

[103] A.M. Ure, Trace element speciation in soils, soil extracts and solutions, Microchimica Acta, 1991, 104, 49–57.

[104] T.A. Kirpichtchikova, A. Manceau, L. Spadini, F. Panfili, M.A. Marcus, T. Jacquet, Speciation and solubility of heavy metals in contaminated soil using X-ray microfluorescence, EXAFS spectroscopy, chemical extraction, and thermodynamic modeling, Geochimica et Cosmochimica Acta, 2006, 70, 2163–2190.

[105] A. Manceau, M.-C. Boisset, G. Sarret, J.-L. Hazemann, M. Mench, P. Cambier, R. Prost, Direct determination of lead speciation in contaminated soils by EXAFS spectroscopy, Environmental Science & Technology, 1996, 30, 1540–1552.

[106] A. Funatsuki, M. Takaoka, K. Oshita, N. Takeda, Methods of determining lead speciation in fly ash by X-ray absorption fine-structure spectroscopy and a sequential extraction procedure, Analytical Sciences, 2012, 28, 481–490.

[107] M.-C. Hsiao, H.P. Wang, Y.-J. Huang, Y.-W. Yang, EXAFS study of copper in waste incineration fly ashes, Journal of Synchrotron Radiation, 2001, 8, 931–933.

[108] M. Takaoka, T. Yamamoto, T. Tanaka, N. Takeda, K. Oshita, T. Uruga, Direct speciation of lead, zinc and antimony in fly ash from waste treatment facilities by XAFS spectroscopy, Physica Scripta, 2005, 2005, 943.
[109] F. Bordas, A.C. Bourg, A critical evaluation of sample pretreatment for storage of contaminated sediments to be investigated for the potential mobility of their heavy metal load, Water, Air, and Soil Pollution, 1998, 103, 137–149.
[110] G.E. Hall, J.E. Vaive, P. Pelchat, G.F. Bonham-Carter, D.A. Kliza-Petelle, K. Telmer, Effects of sample drying on element forms in lake sediments, Geochemistry: Exploration, Environment, Analysis, 2006, 6, 163–177.
[111] I. Bódog, K. Polyák, Z. Csikós-Hartyányi, J. Hlavay, Sequential extraction procedure for the speciation of elements in fly ash samples, Microchemical Journal, 1996, 54, 320–330.
[112] F. Jiao, L. Zhang, Z. Dong, T. Namioka, N. Yamada, Y. Ninomiya, Study on the species of heavy metals in MSW incineration fly ash and their leaching behavior, Fuel Processing Technology, 2016, 152, 108–115.
[113] S.-J. Huang, C.-Y. Chang, F.-C. Chang, M.-Y. Lee, C.-F. Wang, Sequential extraction for evaluating the leaching behavior of selected elements in municipal solid waste incineration fly ash, Journal of Hazardous materials, 2007, 149, 180–188.
[114] Y. Pan, Z. Wu, J. Zhou, J. Zhao, X. Ruan, J. Liu, G. Qian, Chemical characteristics and risk assessment of typical municipal solid waste incineration (MSWI) fly ash in China, Journal of Hazardous materials, 2013, 261, 269–276.
[115] Y. Xiong, F. Zhu, L. Zhao, H. Jiang, Z. Zhang, Heavy metal speciation in various types of fly ash from municipal solid waste incinerator, Journal of Material Cycles and Waste Management, 2014, 16, 608–615.
[116] V. Bruder-Hubscher, F. Lagarde, M. Leroy, C. Coughanowr, F. Enguehard, Application of a sequential extraction procedure to study the release of elements from municipal solid waste incineration bottom ash, Analytica Chimica Acta, 2002, 451, 285–295.
[117] J. Yao, W.-B. Li, M. Tang, C.-R. Fang, H.-J. Feng, D.-S. Shen, Effect of weathering treatment on the fractionation and leaching behavior of copper in municipal solid waste incinerator bottom ash, Chemosphere, 2010, 81, 571–576.
[118] A. Bogush, J.A. Stegemann, I. Wood, A. Roy, Element composition and mineralogical characterisation of air pollution control residue from UK energy-from-waste facilities, Waste Management, 2015, 36, 119–129.
[119] G. Weibel, U. Eggenberger, D.A. Kulik, W. Hummel, S. Schlumberger, W. Klink, M. Fisch, U.K. Mäder, Extraction of heavy metals from MSWI fly ash using hydrochloric acid and sodium chloride solution, Waste Management, 2018, 76, 457–471.
[120] José A. C. Broekaert, Analytical Atomic Spectroscopy with Flames and Plasmas, WILEY-VCH Verlag, Weinheim, 2. Auflage, 2005.

[121] Joachim Nölte, ICP Emissionsspektrometrie für Praktiker, Grundlagen, Methodenentwicklung, Anwendungsbeispiele, WILEY-VCH Verlag, Weinheim, 2002.
[122] A. Okino, H. Miyahara, T. Iwai, K. Chiba, Plasma Spectroscopy – Principles and Applications, Encyclopedia of Analytical Chemistry: Applications, Theory and Instrumentation, 2016.
[123] Agilent Technologies, Agilent 7800/7900 ICP–MS Hardware Maintenance Manual, Manual Part Number G8400-90005 Revision A Oktober 2018.
[124] R. Thomas, A beginner's guide to ICP-MS, Part V – The Ion Focusing System, Spectroscopy, 2001, 16, 38–44.
[125] R. Thomas, A beginner's guide to ICP-MS, Part XII – A Review of Interferences, Spectroscopy, 2002, 17, 24–31.
[126] Römpp Enzyklopädie Online, Stichwort "ICP-MS", bearbeitet von J.K. Wesener, Stand Mai 2014, Thieme Verlag, Stuttgart, 2019.
[127] R. Thomas, A beginner's guide to ICP-MS, Part IV – Mass Analyzers: Collision/Reaction Cell Technology, Spectroscopy, 2002, 17, 42–48.
[128] D.W. Koppenaal, G.C. Eiden, C.J. Barinaga, Collision and reaction cells in atomic mass spectrometry: development, status, and applications, Journal of Analytical Atomic Spectrometry, 2004, 19, 561–570.
[129] N. Yamada, Kinetic energy discrimination in collision/reaction cell ICP-MS: Theoretical review of principles and limitations, Spectrochimica Acta Part B: Atomic Spectroscopy, 2015, 110, 31–44.
[130] P. Fermo, F. Cariati, A. Pozzi, F. Demartin, M. Tettamanti, E. Collina, M. Lasagni, D. Pitea, O. Puglisi, U. Russo, The analytical characterization of municipal solid waste incinerator fly ash: methods and preliminary results, Fresenius' Journal of Analytical Chemistry, 1999, 365, 666–673.
[131] N. Rodella, A. Bosio, R. Dalipi, A. Zacco, L. Borgese, L. Depero, E. Bontempi, Waste silica sources as heavy metal stabilizers for municipal solid waste incineration fly ash, Arabian Journal of Chemistry, 2017, 10, S3676–S3681.
[132] W. Gerwinski, D. Goetz, Multielement analysis of standard reference materials with total reflection X-ray fluorescence (TXRF), Fresenius' Zeitschrift für analytische Chemie, 1987, 327, 690–693.
[133] M. Guarienti, A. Gianoncelli, E. Bontempi, S.M. Cardozo, L. Borgese, D. Zizioli, S. Mitola, L.E. Depero, M. Presta, Biosafe inertization of municipal solid waste incinerator residues by COSMOS technology, Journal of Hazardous materials, 2014, 279, 311–321.
[134] A.K. Detcheva, S.E. Mitsiev, P.S. Vassileva, J.H. Jordanov, M.G. Karadjov, E. Ivanova, Total reflection X-ray fluorescence analysis of fly ash from Bulgarian coal-fired power plants, Chemical Papers, 2015, 69, 650–654.

[135] K. Cammann (Hrsg.), Instrumentelle Analytische Chemie, Verfahren, Anwendungen, Qualitätssicherung, Spektrum Akademischer Verlag, Heidelberg, 2001.

[136] R. Klockenkämper, A. von Bohlen, Survey of sampling techniques for solids suitable for microanalysis by total-reflection X-ray fluorescence spectrometry, Journal of Analytical Atomic Spectrometry, 1999, 14, 571–576.

[137] R. Klockenkämper, A. von Bohlen, Total-Reflection X-Ray Fluorescence Analysis and Related Methods, John Wiley & Sons, Hoboken, New Jersey, 2. Auflage, 2015.

[138] I. De La Calle, N. Cabaleiro, V. Romero, I. Lavilla, C. Bendicho, Sample pretreatment strategies for total reflection X-ray fluorescence analysis: A tutorial review, Spectrochimica Acta Part B: Atomic Spectroscopy, 2013, 90, 23–54.

[139] F.J. Antosz, Y. Xiang, A.R. Diaz, A.J. Jensen, The use of total reflectance X-ray fluorescence (TXRF) for the determination of metals in the pharmaceutical industry, Journal of Pharmaceutical and Biomedical Analysis, 2012, 62, 17–22.

[140] E. Marguí, I. Queralt, M. Hidalgo, Determination of platinum group metal catalyst residues in active pharmaceutical ingredients by means of total reflection X-ray spectrometry, Spectrochimica Acta Part B: Atomic Spectroscopy, 2013, 86, 50–54.

[141] R. Fernández-Ruiz, J.C. Rodríguez-Ubis, Á. Salvador, E. Brunet, O. Juanes, Eu and Tb quantitation in luminescent γ-ZrP-organometallics compounds by TXRF direct solid procedure, Journal of Analytical Atomic Spectrometry, 2010, 25, 1882–1887.

[142] S. Kunimura, J. Kawai, Application of a portable TXRF spectrometer to determine trace amounts of toxic elements, Advances in X-Ray Analysis, 2010, 53, 180–186.

[143] C. Vázquez, G. Custo, N. Barrio, J. Burucúa, S. Boeykens, F. Marte, Inorganic pigment study of the San Pedro Gonzalez Telmo Sibyls using total reflection X-ray fluorescence, Spectrochimica Acta Part B: Atomic Spectroscopy, 2010, 65, 852–858.

[144] R. Fernández-Ruiz, M. Malki, A.I. Morato, I. Marin, Study of bioaccumulation kinetics of chromium (VI) in Acinetobacter beijerinckii type bacterium by Total Reflection X-Ray Fluorescence Spectrometry, Journal of Analytical Atomic Spectrometry, 2011, 26, 511–516.

[145] A. Khuder, M. Bakir, R. Hasan, A. Mohammad, Determination of nickel, copper, zinc and lead in human scalp hair in Syrian occupationally exposed workers by total reflection X-ray fluorescence, Environmental Monitoring and Assessment, 2008, 143, 67–74.

[146] J. Boman, A. Wagner, M.J. Gatari, Trace elements in PM2. 5 in Gothenburg, Sweden, Spectrochimica Acta Part B: Atomic Spectroscopy, 2010, 65, 478–482.

[147] S. Tejeda, G. Zarazúa, P. Ávila-Pérez, L. Carapia-Morales, T. Martínez, Total reflection X-ray fluorescence spectrometric determination of elements in water hyacinth from the Lerma River, Spectrochimica Acta Part B: Atomic Spectroscopy, 2010, 65, 483–488.

[148] E. Marguí, G. Floor, M. Hidalgo, P. Kregsamer, G. Román-Ross, C. Streli, I. Queralt, Analytical possibilities of total reflection X-ray spectrometry (TXRF) for trace selenium determination in soils, Analytical Chemistry, 2010, 82, 7744–7751.

[149] M.A. Marks, T. Wenzel, M.J. Whitehouse, M. Loose, T. Zack, M. Barth, L. Worgard, V. Krasz, G.N. Eby, H. Stosnach, The volatile inventory (F, Cl, Br, S, C) of magmatic apatite: An integrated analytical approach, Chemical Geology, 2012, 291, 241–255.

[150] L. Bonizzoni, A. Galli, M. Gondola, M. Martini, Comparison between XRF, TXRF, and PXRF analyses for provenance classification of archaeological bricks, X-Ray Spectrometry, 2013, 42, 262–267.

[151] F. Bilo, L. Borgese, D. Cazzago, A. Zacco, E. Bontempi, R. Guarneri, M. Bernardello, S. Attuati, P. Lazo, L.E. Depero, TXRF analysis of soils and sediments to assess environmental contamination, Environmental Science and Pollution Research, 2014, 21, 13208–13214.

[152] R. Fernández-Ruiz, Three empirical cases of the deposition morphology influence in the analytical quality of direct solid suspension measurements by total-reflection X-ray fluorescence, Spectrochimica Acta Part B: Atomic Spectroscopy, 2009, 64, 672–678.

[153] I. De La Calle, M. Costas, N. Cabaleiro, I. Lavilla, C. Bendicho, Use of high-intensity sonication for pre-treatment of biological tissues prior to multielemental analysis by total reflection X-ray fluorescence spectrometry, Spectrochimica Acta Part B: Atomic Spectroscopy, 2012, 67, 43–49.

[154] I. Machado, S. Mondutey, N. Pastorino, V. Arce, M. Pistón, A green analytical method for the determination of Cu, Fe, Mn, and Zn in wheat flour using total reflection X-ray fluorescence, Journal of Analytical Atomic Spectrometry, 2018, 33, 1264–1268.

[155] M.A. Amberger, M. Höltig, J.A. Broekaert, Direct determination of trace elements in boron nitride powders by slurry sampling total reflection X-ray fluorescence spectrometry, Spectrochimica Acta Part B: Atomic Spectroscopy, 2010, 65, 152–157.

[156] A. Meyer, S. Grotefend, A. Gross, H. Wätzig, I. Ott, Total reflection X-ray fluorescence spectrometry as a tool for the quantification of gold and platinum metallodrugs: Determination of recovery rates and precision in the ppb concentration range, Journal of Pharmaceutical and Biomedical Analysis, 2012, 70, 713–717.

[157] J. Haberl, Masterarbeit, Technische Universität München, 2016.

[158] Bruker Nano GmbH, S4 T-Star Broschüre, Benchtop TXRF Spectrometer for Ultra-Trace Element Analysis, Rev. 1.2, 2018. Online verfügbar unter: https://www.bruker.com/fileadmin/user_upload/8-PDF-Docs/X-rayDiffraction_ElementalAnalysis/TXRF/Brochures/bro_S4_TStar_en_8p_rev1_2_lores.pdf (aufgerufen am 09.05.2019).